ADDIS ABABA UNIVERSITY
ADDIS ABABA INSTITUTE OF TECHNOLOGY
SCHOOL OF CIVIL AND ENVIRONMENTAL ENGINEERING

THE PERFORMANCE OF A RECENTLY DEVELOPED TWO-PARAMETER FOUNDATION MODEL FOR THE ANALYSIS OF RAFT FOUNDATION

A Thesis in Geotechnical Engineering

By Frehiwot Belay

Advisor

Asrat Worku Prof. (Dr.-Ing)

Addis Ababa Institute of Technology

June, 2025

Addis Ababa, Ethiopia

Submitted in Partial Fulfillment of the Requirements for the Degree of Master of Science in Geotechnics

The undersigned have examined the thesis proposal entitled '**The performance of a recently developed two-parameter foundation model for the analysis of raft foundation**' presented by **Frehiwot Belay**, a candidate for the degree of **Master of Science** and hereby certify that it is worthy of acceptance.

Prof. Asrat Worku		25/06/25
Advisor	Signature	Date
Dr. Tensay Gebremedhin		25/06/25
Internal Examiner	Signature	Date
Dr. Tesfaye Firew		25/06/25
External Examiner	Signature	Date
Dr. Tensay Gebremedhin		25/06/25
Chairperson	Signature	Date

Tensay Gebremedhin Berhe (Dr.-Ing.)
I/Head, School of Civil &
Environmental Engineering

UNDERTAKING

I certify that the research work titled "The performance of a recently developed two-parameter foundation model for the analysis of raft foundation" is my own work. The work has not been presented elsewhere for assessment. Where material has been used from other sources, it has been properly acknowledged.

Name:	Signature:
Frehiwot Belay:	
Advisor: Prof. (Dr.Eng) Asrat Worku :	

Acknowledgment

First and foremost, my deepest gratitude goes to **Almighty God** for granting me the strength and courage to complete this work.

I would like to express my sincere appreciation to my advisor, **Professor Asrat Worku**, for his unwavering support, insightful guidance, and open-door mentorship throughout the course of this research. Special thanks also goes to **Leamlak Minwuyelet** and **Abraham Mengistu** for their valuable technical support and for generously sharing their expertise in the subject matter. This could not be complete without your help.

I am profoundly grateful to my **family** for their constant encouragement and support during this journey.Lastly, my heartfelt appreciation goes to my husband**, Elias Degefa**, and our two wonderful **children**. Thank you for your patience, understanding, and support through this long journey.

ABSTRACT

Different viewpoints on modeling the Soil-Structure interaction (SSI) in mat foundation design exist in engineering practice. Some believe that modeling the SSI using a few mechanical elements during design is sufficient, while others contend that modeling the soil as a continuum model is necessary to produce an adequate analysis.

Commonly, the analysis and design of mat foundations is done by performing static analysis of a plate resting on vertically uncoupled Winkler springs. Despite being a somewhat simplified idealization of reality and the emergence of more accurate techniques, the Winkler spring methodology continues to be the state-of-the-practice because it is simple to implement in most commercial structural analysis computer programs.

This and related shortcomings have meanwhile been addressed by a number of improved models including Worku's two-parameter subgrade model (2014). Worku's model is a mechanical equivalent of an originally elastic continuum idealization of the soil under the foundation, whereby all components of the continuum deformation and the stress and strain tensors are retained. This is unlike a number of previous similar attempts by other authors, who proposed simplified versions of such a continuum representation. The implementation of this analytically rigorous model into applications such as beams and plates on elastic foundations and laterally loaded plates has been under investigation showing promising results.

This thesis deals with a comparative study of the performance of the model to rectangular raft foundations against existing methods of analysis. To this effect, a recently adjusted version of the model under an on-going PhD research is employed.

A finite element algorithm developed under this project and written in MATLAB to solve the resulting partial differential equation of the plate along with a calibration chart for different loading conditions was used and compared with a rigorous continuum based finite element model of the plate-soil system (cFEM). The findings show that the model adequately represents the behavior of rectangular plates on elastic foundations showing remarkable agreement with the cFEM outputs.

TABLE OF CONTENTS

LIST OF FIGURES

LIST OF TABLES

LIST OF SYMBOLS AND ABBREVIATION

AdJ : adjusted

B: Plate width

cFEM: Continuum Finite element method

D: Flexural rigidity of a plate

DE: Differential equation

E_p : Modulus of elasticity of a plate

E_s : Modulus of elasticity of a soil

FDM: Finite difference method

FE: Finite element

FEM: Finite element method

G_p : Pasternak's shear layer constant with units of kN/m

H: Thickness of a stratum

h : Plate thickness

L: Plate length

C_1 : Spring coefficient in Pasternak's model with units of kN/m3

k_s: Modulus of subgrade reaction with units of kN/m3

SSI: Soil Structure Interaction

CHAPTER ONE

1. INTRODUCTION

1.1 Background

The response of a concrete slab (plate) supported directly by a soil medium when loaded externally is influenced by the behavior of the soil and the interaction of the two media. A rational approach to the design of foundations resting on soils should thus take into account both the foundation's flexibility and the soil medium's deformational characteristics. This has led to a wide range of analytical and experimental studies on the topic of the typical soil-structure interaction (SSI) problem at hand.

In engineering practice, various points of view exist on modeling SSI analysis and mat foundation design. For the purpose of producing an effective SSI analysis, some think that modeling the subgrade using idealized mechanical elements during design is sufficient, while others argue that modeling the soil as a continuum is required. As can be observed from previous studies, figuring out the contact pressure is the fundamental difficulty in analyzing the interaction between soil and foundation. For this reason, highly simplified models are still in wide use among practicing engineers.

Despite the remarkable advances made in numerical modelling of both structural and geotechnical media, the rather rudimentary single-parameter Winkler spring methodology continues to be part and parcel of the state of practice.

Noting this inconsistency, Worku A. (2009, 2010, 2013, and 2014) has developed an improved methodology having a potential for use in routine analysis of beam-like and plate–like shallow foundations. As part of this ongoing project Minwuyelet and Worku (2022) developed a calibration chart for use in the analysis of square and rectangular plates on an elastic foundation.

In light of this, the current work aims to verify the calibrated model for analysis of square and rectangular raft foundations resting on elastic soils.

1.2 Statement of the Problem (Significance)

Though, the problem of beams and plates on deformable foundation soils is a complicated soil-structure interaction (SSI) problem, most structural analysis software currently in the market still employ the rather rudimentary Winkler's foundation model to account for SSI effects. Hence, practicing engineers often use software which are capable of modelling the structure in detail, while the subgrade is represented by a single spring bed, which poorly describe the behavior of the soil.

Thus, a model that takes into account the inherent soil-structure interaction (SSI) and is still simple enough for implementation to the analysis of raft foundations is considered necessary.

1.3 Objectives of the Study

1.3.1 Main Objectives

The main objective of this study is to verify the effectiveness of the newly calibrated Worku's Kerr Equivalent Pasternak model in the analysis of rafts through comparison with rigorous FE models and other simplified methods in practical use.

1.3.2 Specific Objectives

1) Verify the performance of the newly calibrated Worku's Kerr Equivalent Pasternak model in the analysis of thin square and rectangular rafts using continuum finite element software, Plaxis 3D.

2) Compare the performance of the model with selected commonly used subgrade models for the analysis of rafts based on single and two parameter subgrade models.

1.4 Scope of Work

The scope of the study is limited to:

- Vertically loaded thin plate-like structures specifically raft of square and rectangular geometry having constant cross-section.
- Linear elastic plate and foundation soil response.
- Common load configuration cases that are as many as one may anticipate in practice.

1.5 Methodology

In the present study six different types of SSI analysis methods:

- Single parameter Subgrade Model (Winkler)
- Pseudo Coupled Method of Analysis (ACI, 2002)
- Vlasov's two Parameter Model
- Worku's original Model
- Worku's Adjusted model, and
- Continuum Finite Element Method (cFEM)) are employed

For thus, six models with various load geometry, aspect ratio, load pattern, and stiffness are studied; and the models are presented here to demonstrate the effectiveness of the recently developed two-parameter foundation model for the analysis of raft foundation.

CHAPTER TWO

2. LITERATURE REVIEW

2.1 Plates on Elastic Foundations

A large number of structural components of considerable practical importance in engineering like foundation slabs can be analyzed as plates whose bending properties depend greatly on its thickness as compared with its other dimensions. On the base of the ratio of the thickness to the smaller span length, plates may be classified into two groups: thin plates, and thick plates.

For a thin plate, Kirchhoff assumed that plane cross-sections normal to the un-deformed mid-surface would remain normal to the deformed mid-surface. Therefore, the deflection (*w*) of a plate subjected to the applied load $q(x,y)$ and reaction $p(x,y)$, neglecting friction and cohesion between it and the soil medium, can be given by

$$D\nabla^4 w(x,y) = D\nabla^2\nabla^2 w(x,y) = q(x,y) - p(x,y) \quad (1)$$

where $D = \dfrac{E_p h^3}{12\left(1-\nu_p^2\right)}$ is the flexural rigidity of the plate

∇^4, denotes the Bi-harmonic operator and ∇^2 is the Laplace operator

$w(x,y) =$ Vertical displacements of the plate surface,

$E_p =$ Modulus of elasticity of plate material

$\nu_p =$ Poisson's ratio of plate material and $h =$ Thickness of the plate

In expanded form

$$D\nabla^4 w(x,y) = D\left(\frac{\partial^4 w}{\partial x^4} + 2\frac{\partial^4 w}{\partial x^2 \partial y^2} + \frac{\partial^4 w}{\partial y^4}\right) = q(x,y) - p(x,y) \quad (2)$$

To solve the final form of soil–structure interaction Equation (1) and (2), the soil reaction, $p(x)$, has to be incorporated in these equations which are dependent on the plate and soil characteristics and the bond at the interface. Assuming frictionless contact, and complete bond at the interface between the plate and the soil, $p(x)$ can be expressed in terms of soil displacements (mainly vertical displacement for vertical loads) using different foundation

models usually by replacing the soil with material that behaves under applied loads like the given real soil.

The models created to address issues with foundation-soil interaction, however, are numerous because of the intrinsic complexity in the behavior of soil mass. Generally, the response of these models is represented by the surface deflection caused by an external system of forces. Assuming a linear, elastic, homogeneous and isotropic behavior of the soil, subgrade models can be broadly categorized as mechanical and continuum approach.

2.2 MECHANICAL MODELS

2.2.1 Single parameter models

A number of mechanical models have been proposed in the past having varying degrees of mathematical complexity and different numbers of model parameters. The simplest representation of a foundation subgrade is in the form of the classical Winkler model, which replaces the subgrade by a mechanical analogy consisting of a single bed of closely spaced vertical springs acting independently of each other (Worku, 2009).

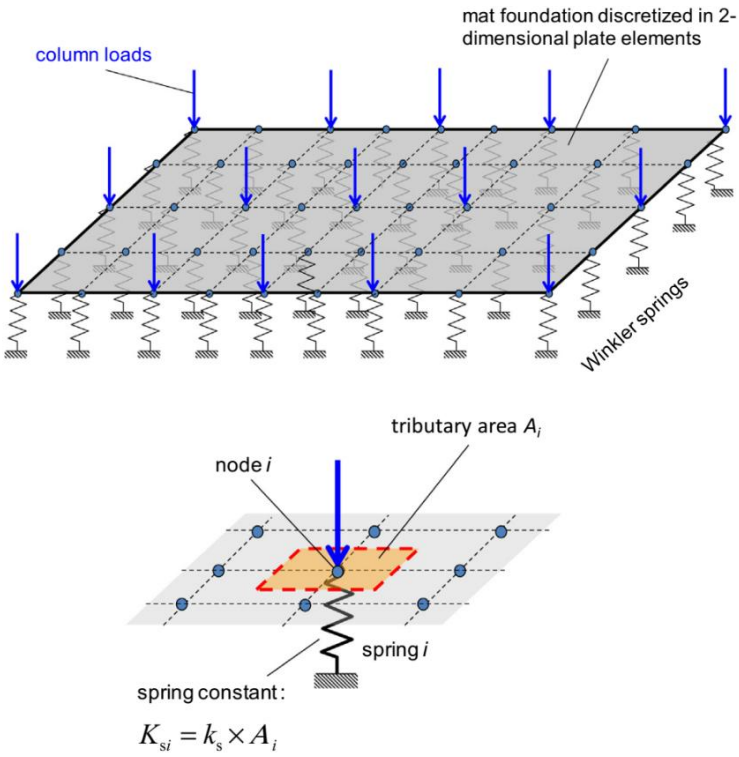

Figure 1. Winkler spring model idealization

In this model, the plate is treated either as several strips (beams) or as a thin plate and the soil is represented by discrete springs (linear elastic) located at arbitrarily selected nodes along the

strips or plate (Winkler spring model). The stiffness coefficient of a Winkler spring K_s is expressed as the product of the area A_s of the portion of the slab influenced by the spring (the tributary area) and the parameter known as modulus of subgrade reaction k_s. Mathematically the governing equation when the mat is a thin plate is

$$D\left(\frac{\partial^4 w}{\partial x^4}+2\frac{\partial^4 w}{\partial x^2\partial y^2}+\frac{\partial^4 w}{\partial y^4}\right)+k_s w(x,y)=q(x,y) \quad (3)$$

in which $w(x,y)$ is the vertical deformation; and k_s is a proportionality constant representing contact pressure per unit deformation - commonly referred to as the coefficient of subgrade reaction or simply as the subgrade modulus. Thus, k_s is the only quantity characterizing the subgrade material (Worku, 2009).

The analytical solutions of these differential equations are laborious and computationally intensive, and are limited to homogeneous plates of relatively simple geometry, loading and boundary conditions. Even when solved, they are often too difficult and cumbersome to use in everyday engineering practice. Hence numerical methods such as the finite difference method (FDM) or the finite element method (FEM) are used for such problems which can handle the practical situations of various parameters of the problems easily.

Owing to the absence of interaction between adjacent springs, the model has the following notable shortcomings as many studies have pointed out:

- Neglects the vertical shearing stress that occurs within subgrade materials.
- In addition, a displacement discontinuity appears between the loaded and the unloaded part of the foundation surface contrary to reality.

Pseudo-coupled approach

To overcome the shortcomings of the Winkler's approach, a lot of alternatives have been proposed. One of these alternatives is the pseudo coupled approach, in which the plate still rests on vertical springs, but with spring constants that vary across the mat depending on the location of a given spring. The pseudo-coupled approach is meant to improve the accuracy of the original Winkler spring method while retaining its simplicity (D. Loukidis, 2017).

To date, the suitable spatial distribution of k_s has not been firmly established and the existing variations of the pseudo coupled method differ significantly between each other. The most basic form of pseudo-coupling is to simply use for the springs connected to the edge of the

foundation twice as much k_s as for the springs at rest of the foundation (Bowles, 1995). A more elaborate version proposed by ACI (2002) and Bowles (1995) dictates that k_s should decrease progressively from the edge to the center of the mat.

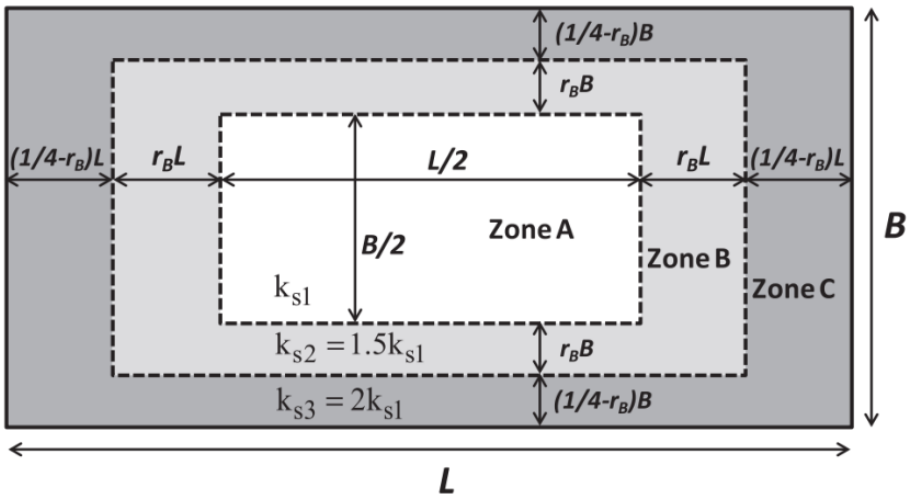

Figure 2: Plate with different $\boldsymbol{k_s}$ values for pseudo-coupled analysis (Couduto D. P., 2001)

Coduto (2001) proposed a simpler version of the pseudo-coupled method, which does not require a trial analysis or iterations. According to this version, the plate is divided in N (two or more) concentric zones, with the central zone having half the width and the length of the mat. Each zone i is assigned a different value of $k_{s,i}$ in such a way that k_s increases from the inner to the outer zones and the outmost zone has twice as much k_s as the central zone (i.e. $k_{sN} = 2k_{s1}$), with the additional condition that the weighted (based on the zone areas) average of all $k_{s,i}$ ($k_{s,ave}$) is equal to the k_s obtained from using settlement w calculations that treat the plate as a large rigid one. Applying this concept to a mat divided in three zones as shown in figure (6), with areas A1 (central), A2 (intermediate), A3 (outer), and assuming that for the intermediate zone $k_{s2} = 1.5k_{s1}$, one obtains

$$k_{s1} = k_{s,ave} \times \frac{A_1 + A_2 + A_3}{A_1 + 1.5A_2 + 2A_3} \tag{4}$$

2.2.2 Two parameter models

In essence, there have been two different approaches taken in the development of these two parameter models. They relied on the Winkler model and managed to get rid of its discontinuous behavior by introducing a mechanical connection between the various spring

components. Such physical representations of the behavior of the ground have been put forth by different studies.

Filonenko-Borodich (1940), proposed a model which represent the continuous behavior of the soil by introducing a thin elastic membrane under constant tension which connects the winkler spring elements. In this model, the subgrade reaction is given by;

$$p(x,y) = k_p w(x,y) - T\nabla^2 w(x,y) \quad (5)$$

Filonenko-Borodich model is characterized by two elastic constant k and T.

Where ∇^2 is Laplace operator in x and y-direction.

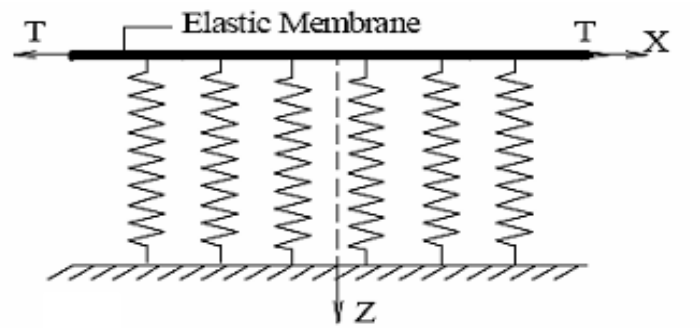

Figure 3 : Basic model of Filonenko-Borodich model (1940**)**

Hetenyi (1946), in this model, interaction between independent spring elements is accomplished by incorporating a pure flexural elastic plate in three-dimensional problems, or an elastic beam in the case of two-dimensional problems.

$$p(x,y) = k_p w(x,y) - D\bar{\nabla}^4 w(x,y) \quad (6)$$

Where D is the flexural rigidity of the elastic plate

Pasternak (1954), proposed ground behavior model by assuming the existence of shear interaction between the spring elements. This is achieved by connecting the spring elements to a layer of incompressible vertical elements that deform in transverse shear.

$$p(x,y) = k_p w(x,y) - G_p\nabla^2 w(x,y) \quad (7)$$

Where G_p is a shear parameter layer.

Improved versions of higher order models have been proposed and developed by including arbitrary combinations of mechanical elements such as axial springs, tensioned membranes, shear layers, and flexural layers. For example, Kerr and Rhines (1967) proposed that increasing

the number of spring beds and shear components in various combinations could lead to a more accurate solution. However, due to their mathematical complexity and the fact that higher order models are not required to provide superior results, they are frequently used only in academic arena.

The inherent deficiency of the Winkler model in depicting the continuous behavior of real soil masses and the mathematical complexities of the higher order mechanical models has led to the development of the elastic continuum model (Worku, 2009).

2.3 Elastic continuum models

In contrast to the mechanical models, continuum-based subgrade models proposed in the past are relatively few in number. The common models that take into consideration such simplifications are those proposed by Reissner which is regarded as the pioneer.

Reissner (1958), idealized the soil medium as an elastic layer of thickness, H, overlying a perfectly rigid medium as shown.

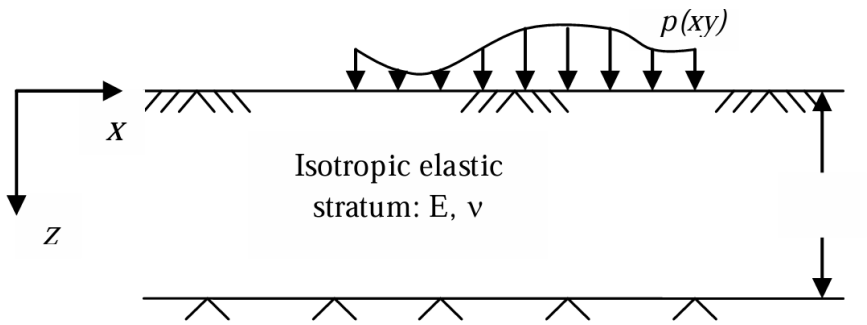

Figure 4: Elastic soil layer overlying a rigid stratum

Assuming the in-plane stresses in the x-y plane throughout a soil layer of thickness H are negligibly small and the remaining stress components satisfy the well-known equilibrium differential equations, Reissner proposed the following second order differential equations.

$$p-\frac{H^2 G_s}{12E_s}\nabla^2 p=\frac{E_s}{H}w-\frac{G_s H}{3}\nabla^2 w \qquad (8)$$

Where G_s is the shear modulus of the elastic continuum, E_s is Young's modulus of the sub-grade, p is the load intensity at the interface, and H is the subgrade thickness.

Based on a simplified set of assumptions regarding the distribution of stresses and displacements which is based on the elastic continuum model, Reissner (1958) and Vlazov and Leontiev (1966) proposed models that account for the use of synthesis.

The model proposed by Vlazov (1956a, b) is an example of such type of two-parameter elastic model, derived by introducing displacement constraints that simplify the basic equations of the linear theory of elasticity for an isotropic continuum and using the variational approach. Vlazov (1956a, b) obtained a response function similar in character to Pasternak (1954) and Filonenko-Borodich (1940) by imposing certain restrictions on the possible distribution of displacements in an elastic layer of thickness, H, modulus of elasticity, E_s, and Poisson's ratio, ν_s, subjected to an arbitrary plane strain load, q(x), on the surface.

The final form of the model developed by Vlazov and Leontiev (1966), which considers the variation of displacements with depth using linear and exponential variation functions for thin and thick deposits takes the following form.

$$C_1.w - C_2.\Delta w = f_z \qquad (9)$$

where: C_1 - foundation compression modulus of the Winkler type, expressing resistance to the vertical displacement of the subsoil surface

C_2 - foundation shear modulus expressing resistance to the shear components

w - deflection in the vertical direction

f_z - vertical load acting on a layer

$$C_1 = \frac{E_o}{H\left(1-2\nu_s^2\right)}; \quad C_2 = \frac{E_o.H}{6\left(1+\nu_s\right)} \quad \textit{For thin Layers}$$

$$C_1 = \frac{E_o}{H\left(1-2\nu_s^2\right)}\psi_{c_1}; \quad C_2 = \frac{E_o.H}{6\left(1+\nu_s\right)}\psi_{c_2} \quad \textit{For thick Layers}$$

where

$$\psi_{c_1} = \left(\gamma H / 2L\right)\frac{\left[\sinh(\gamma H / L)\cosh(\gamma H / L) \pm (\gamma H / L)\right]}{\sinh^2(\gamma H / L)}$$

$$\psi_{c_2} = \left(3L / 2\gamma H\right)\frac{\left[\sinh(\gamma H / L)\cosh(\gamma H / L) \pm (\gamma H / L)\right]}{\sinh^2(\gamma H / L)}$$

$$E_o = \frac{E_s}{\left(1-\nu_s^2\right)} \text{ and } \nu_o = \frac{\nu_s}{\left(1-\nu_s\right)}$$

The parameters, C_1 and C_2, illustrate the relationship of this model to the Winkler model described previously. When C_2 equals zero, Winkler representation is recovered (C_1 is the Winkler foundation spring stiffness). The Vlazov model is identical to the Pasternak model with the additional advantage that the parameters, C_1 and C_2, can be derived from the elastic deformation properties of the ground (Madhav M., Abhishek S.V. and Rajyalakshmi K., 2006).

Available software programs in the market calculate the parameters C_1, C_2 from deformation parameters of soils, or from geological profile. In the case of Geo5 Slab software package, the constants C_1 and C_2 are calculated from the condition of equal compliance matrices of infinitely stiff infinite strip footing resting on the Winkler - Pasternak and elastic subsoil. This condition is represented by the following equalities:

$$[C] = \begin{bmatrix} \frac{1}{2\left[\sqrt{C_{1WP}C_{2WP}} + bC_{1WP}\right]} & 0 \\ 0 & \frac{1}{2\left[b^2\sqrt{C_{1WP}C_{2WP}} + bC_{2WP} + \frac{b^3}{3}C_{1WP}\right]} \end{bmatrix}$$

$$= \begin{bmatrix} \sum_{n=0}^{\infty} \frac{1}{2\sqrt{H}\left[(2n+1)\sqrt{C_{1W}C_{2W}} + (2n+1)^2 bC_{1W}\right]} & 0 \\ 0 & \sum_{n=0}^{\infty} \frac{1}{2\sqrt{H}\left[(2n+1)b^2\sqrt{C_{1W}C_{2W}} + bC_{2W} + (2n+1)^2\frac{b^3}{3}C_{1W}\right]} \end{bmatrix}$$

where: $[C]$ - matrix of constants C_1 and C_2

b - half width of foundation

C_{1w}, C_{2w} - Winkler's constants

H - depth of the deformation zone

It is obvious that this approach produces results that are far reasonable than those produced by the Winkler model, however calculating the C_2 parameters is not an easy task and is very sensitive to the depth of deformation value.

2.3.1 The generalized continuum model

Worku has proposed a generalized continuum model without neglecting any stress, strain and displacement components that addresses the major shortcomings in the two approaches, and most continuum models available in the literature could be regarded as special cases of this generalized model (worku, 2010).

Generally, continuum models have the advantage that the elastic constants can be established from tests but suffer from a common shortcoming that they are difficult to apply directly. On the other hand, mechanical models suffer in general from a major common drawback of not suggesting ways of estimating the model parameters. Hence synthesis of the two approaches has the benefit of using the strengths of both methods and provides a means of quantifying the mechanical model parameters in terms of the known parameters of the continuum model (Worku 2010).

With the understanding that a two-parameter mechanical model like that of Pasternak (1954) is much easier for analysis than the three-parameter Kerr (1964) model, and taking the advantages of model synthesis, Worku (2013) proposed calibrated closed-form relations for two parameter mechanical model with a calibration factor being introduced in place of the layer thickness.

Thus, this study uses the recently developed Kerr equivalent Pasternak model by Worku (2014). The relationship between the contact pressure, $p(x,y)$, and the surface deflection, $w(x,y)$,using the model is given by the following form:

$$D\nabla^4 w(x,y) = D\nabla^2\nabla^2 w(x,y) = q(x,y) - p(x,y) \tag{10}$$

$$P(x,y) = k_p\, w(x,y) - G_p\nabla^2 w(x,y) \tag{11}$$

Combining equation (10) & (11) and rearranging, one obtains:

$$D\nabla^4 w(x,y) - G_p\nabla^2 w(x,y) + k_p w(x,y) = q(x,y) \tag{12}$$

Where;

$$k_p = \frac{(0.4\nu_s + 0.67)E_s}{\chi B}; \qquad G_p = (1.36\nu_s + 2.28)G_s B\chi \tag{13}$$

A calibration factor chart was proposed using comparative study of numerical analysis in a recent ongoing work using plates on elastic foundations by Minwuyelet and Worku (2022).

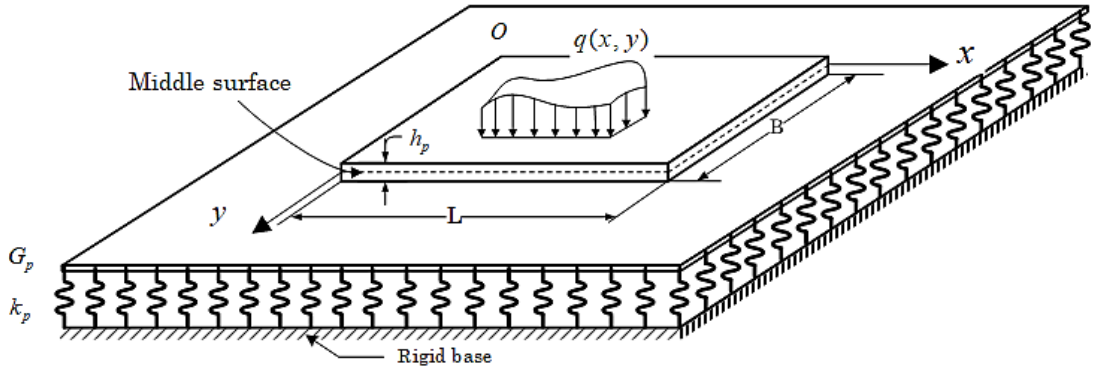

Figure 5: Plate on Pasternak's foundation

Thus, due to the increase in computing power numerical methods like the finite element method (FEM) are used for such kind of analysis. The FEM is currently the most powerful and versatile numerical technique for the solution of structural-mechanics problems. The FEM applies a physical discretization in which the actual continuum is replaced by an assembly of discrete elements, referred to as finite elements, connected together to form the given two- or three-dimensional structure. The method assumes that if the load deformation characteristics of each element can be defined, then by assembling the elements the load deflection behavior of the plate can be approximated. Mathematically, the FEM is based on the Ritz variational approach.

2.4 Continuum Finite Element Method (cFEM)

In this analysis, the mat is treated as a structural element-a thin plate (thickness small compared with the other dimensions) - and the soil by appropriate constitutive model. The governing equation is

$$D\left(\frac{\partial^4 w}{\partial x^4}+2\frac{\partial^4 w}{\partial x^2\partial y^2}+\frac{\partial^4 w}{\partial y^4}\right)=\left(q(x,y)+\frac{q_z}{\partial x\partial y}\right)-p(x,y) \tag{14}$$

Where q , is the uniformly distributed vertical load (including the self-weight of the mat), q_z is the column loads and p is reaction of the ground. The settlement of the mat is assumed to be small in comparison with its thickness.

The solution of the governing equation is found using FDM or FEM. This type of analysis can simulate complex soil conditions such as soil layering, groundwater conditions, and construction sequencing and it is often used for sensitive, high valued structures. The accuracy

of the solution depends on the experience of the analyst, the accuracy of the soil parameters, the accuracy of the material model representing the soil, and the boundary conditions imposed (Budhu, 2008). Computer programs, such as ABAQUS, ANSYS, MIDAS GTS NX and PLAXIS are some of the commercially available FE software to solve mat problems treating soil as a continuum.

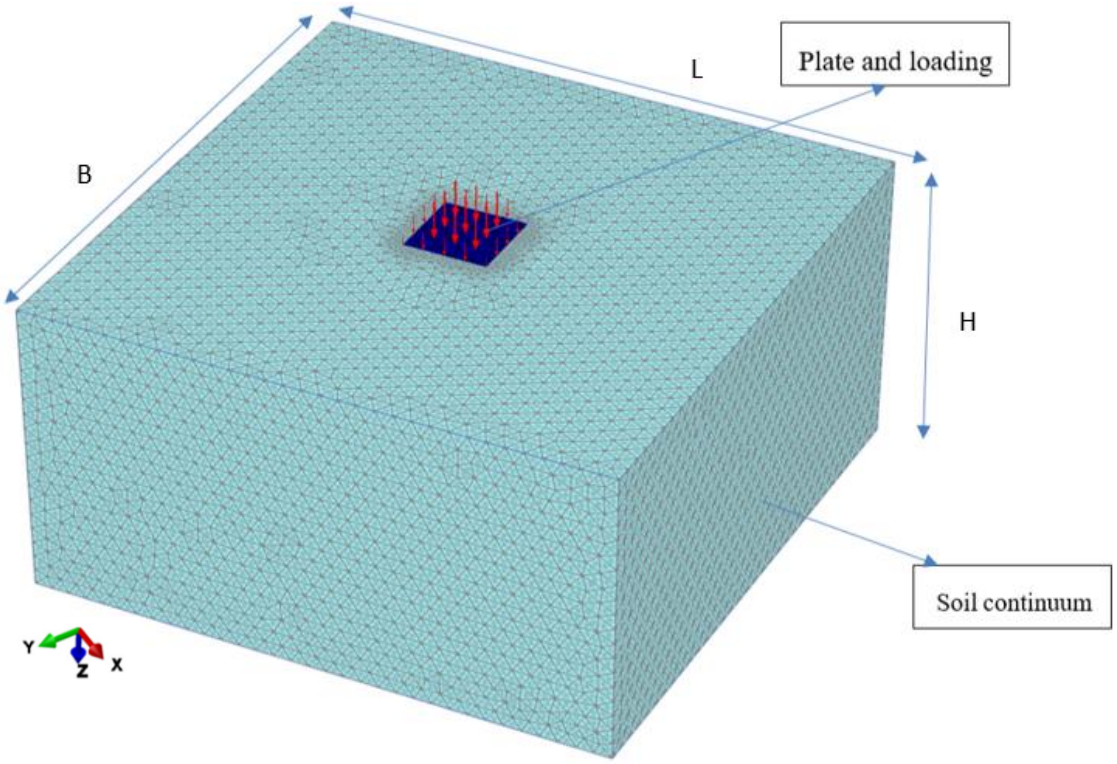

Figure 6: Raft Modeling using PLAXIS 3D

FEM provides a powerful numerical method for the analysis of complex problems of soil–foundation interaction. The usual way of conducting FEM analysis of plates resting on the Winkler subgrade model involves the use of rectangular and/or triangular plate bending/shell finite elements connected to the ground through a series of "springs," which are defined using the modulus of subgrade reaction K_s. Normally, each element has one spring at each corner. Generally, finite element models require gridding that produces large number of elements, nodes, and equations. For this reason, the FEM is computationally intensive (Baban, 2016).

Finite element programs use displacement functions to produce conforming inter-element compatibility at nodes and along element boundaries. The displacement function for a plate finite element is

$$u = a_1 + a_2x + a_3y + a_4x^2 + a_5xy + a_6y^2 + a_7x^3 + a_8x^2y + a_9xy^2 + a_{10}y^3 + a_{11}x^4 + a_{12}x^3y + a_{13}x^2y^2 + a_{14}xy^3 + a_{15}y^4 \quad (15)$$

There are 15 unknown terms in this generic displacement equation. For bending, the vertical displacement and slopes (rotations) in the X- and Y-directions are required at each node. This means that, using a rectangular plate element and these three general displacements (three degrees of freedom) at each corner node, only 12 unknowns (four translations and eight rotations) are needed. For this reason, one must either add a node and apply the 15-term displacement function or reduce its term count from 15 to 12 instead. There are computer programs which delete terms, combine terms and add nodes. The computed output from both programs will be comparable, thus the user's most familiar software should be chosen.

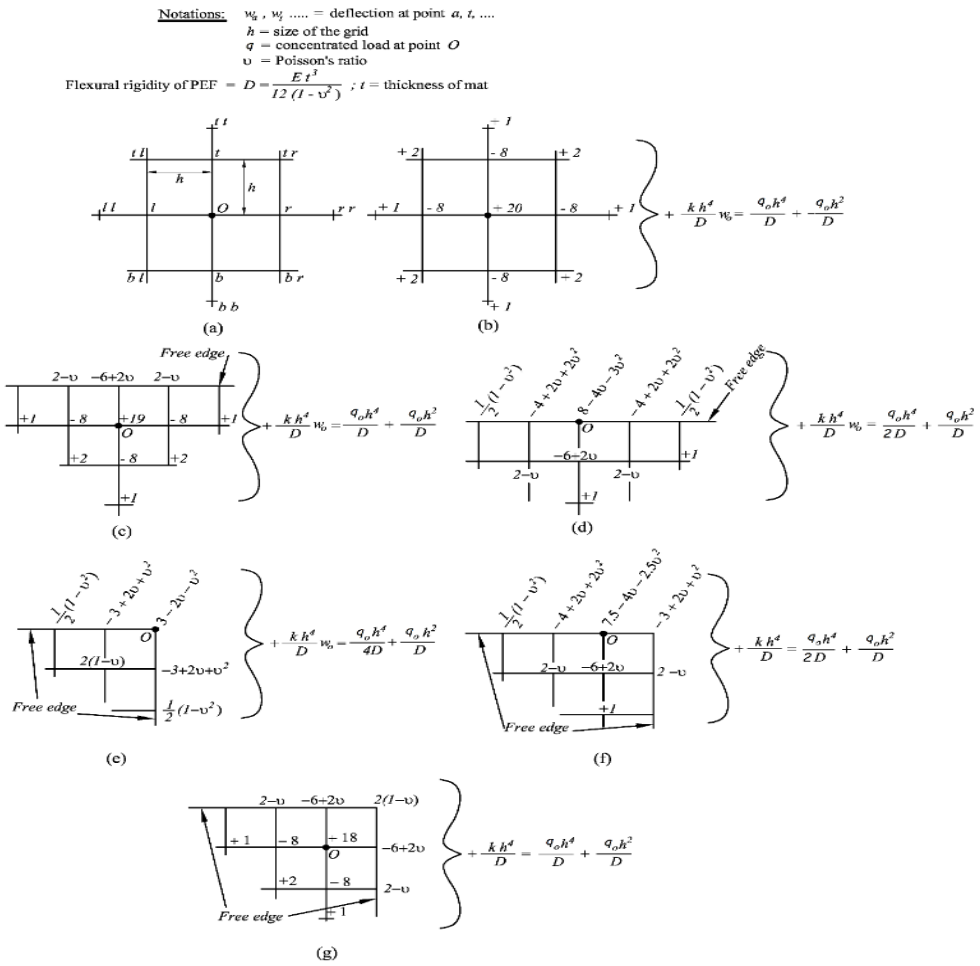

Figure 7: Finite difference equations for analysis of Plates on Elastic Foundation (Rao, 2011)

The FEM technique is mathematically efficient, can model boundary condition displacements effectively and utilize an iso-parametric approach (the same function is used to describe both shape and displacement). Commercial computerized finite element programs, such as CSi-SAP/SAFE/ETABS, PLAXIS 3D, Midas-Gen/nGen, NASTRAN, ANSYS, STAAD FOUNDATION, and ADAPT MAT may be used to run a mat on spring analysis and design.

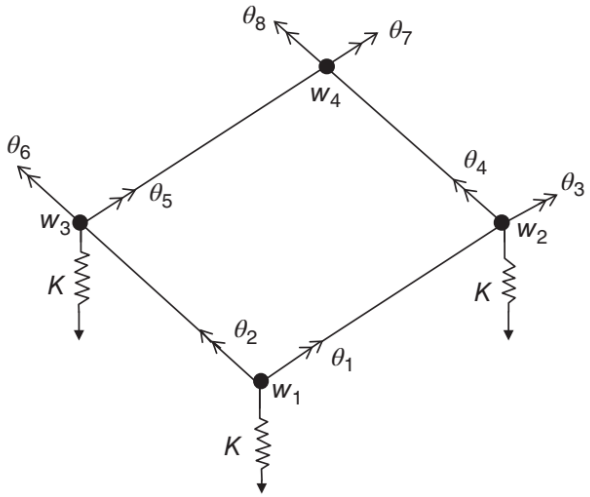

Figure 8: Displacements at the corner nodes of a rectangular plate finite element (Baban, 2016)**.**

For the application of FDM, the plate is divided into a two-dimensional lattice preferably with equal intervals for efficient computation (though not essential) of say $rh \times h$ along both x and y directions. Equation (3) can now be discretized using Finite difference operators, thus converting a continuous partial differential equation (PDE) into algebraic equation at any node j, k in terms of the deflections at the neighboring nodes. The FDM is explained below for a plate on elastic foundations (Figure 8) with all the four edges free (i.e., along $x = 0, a$ and $y = 0, b$).

$$\left(\frac{6}{r^4}+\frac{8}{r^2}+6\right)w_0+\left(-\frac{4}{r^4}-\frac{4}{r^2}\right)(w_L+w_R)+\left(-\frac{4}{r^2}-4\right)(w_T+w_B)+\frac{2}{r^2}(w_{TL}+w_{TR}+w_{BL}+w_{BR})+w_{TT}+w_{BB}$$
$$+\frac{1}{r^4}(w_{LL}+w_{RR})+\frac{k_s h^4}{D}w_o=\frac{q_o h^4}{D}+\frac{q_o h^2}{rD} \qquad (16)$$

When r = 1, that is using a grid of square elements, Equation (16) becomes

$$20w_0-8(w_L+w_R+w_T+w_B)+2(w_{TL}+w_{TR}+w_{BL}+w_{BR})+(w_{TT}+w_{BB}+w_{LL}+w_{RR})=\frac{q_o h^4}{D}+\frac{q_o h^2}{D}$$

where $q_o(x, y)$ is the distributed load and q_o is the concentrated load at node 0. The notations w_L, w_T, w_R, …, represent deflection at points O, T, R, …. Suffixes L, T, R and B respectively stand for left, top, right and bottom, as shown in figure (9).

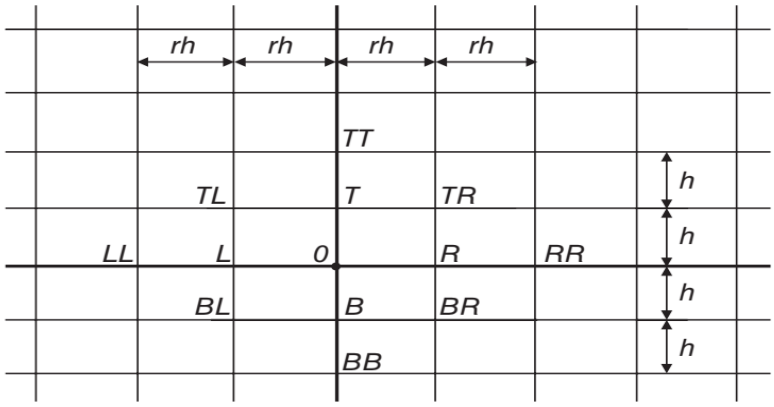

Figure 9: A finite-difference grid of elements of *rh* × *h* dimension (Baban, 2016)

For points at or near free edges, the difference equations are modified to account for boundary conditions. By solving these simultaneous equations, the deflections at all points are computed and the contact pressure (soil reaction) at any node (i, j) is computed by multiplying deflection with k_s, that is, $q_{i,j}(x, y) = k_{i,j} w_{i,j}$.

In view of the increasing complexity of these expressions, these are to be carried out using computers (with customized or commercial software packages) for general application.

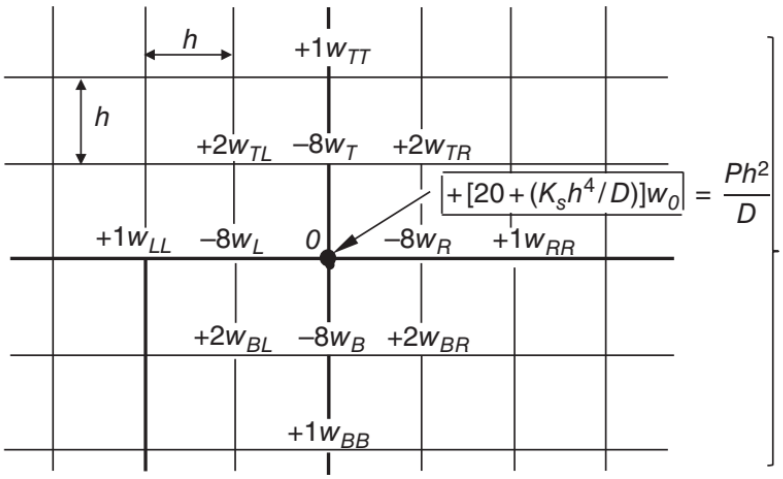

Figure 10: Diagrammatical representation of the finite-difference equation, for deflection at an interior node, using a grid of square elements (Baban, 2016).

The finite-difference method was extensively used in the past, but is sometimes used as a check on alternative methods where it is practical. It is reliable if the mat can be modeled using a finite-difference grid. It does not require massive computer resources, since the input data are minimal compared with any other discrete method.

However, it is very difficult for the method to model boundary conditions for column fixity, to allow for holes, notches, or re-entrant corners. Also, it is difficult to account for moments applied at nodes (such as column moments) since the difference model uses moment per unit of width. These manipulations have been carried out by Rijhsinghani (Teng, 1964) for PEF with free edges (Rao, 2011). There are FDM computer programs, such as program FADMATFD, B19, which can be used to illustrate the procedure (Bowles, 1995).

CHAPTER THREE

3. METHODOLOGY

3.1 Introduction

In order to investigate the performance of Worku's calibrated Kerr equivalent Pasternak model, this research focuses on the deflection of surface raft foundations on elastic foundations subjected to vertical load.

The selected plate dimensions (squares and rectangles with various aspect ratios) were chosen to satisfy the thin plate theory, and the majority of the layouts were taken from D. Loukidis's (D. Loukidis, 2017) most recent work. In addition, the load configurations were chosen to avoid tension in the contact pressure while realistically depicting a plate subjected to no eccentricity, one side eccentricity, and both side eccentricity.

In all analyses, the Young's modulus of the plate E_P was set to 32 GPa, and the Poisson's ratio to 0.2. In contrasts, an effort was made to encompass soils with Young's modulus ranging from 20 MPa (soft clay or loose sand) to 70 MPa (medium stiff clay or medium dense sand).

For the present study six different types of SSI analysis methods (Single parameter Subgrade Model (Winkler), Pseudo Coupled Method of Analysis (ACI, 2002), Vlasov's two Parameter Model, Worku's Model, Worku's Adjusted model, and Continuum Finite Element Method (cFEM)) are employed. The original form of Winkler's model and the pseudo coupled version as proposed by ACI are included in this study, mainly due to the simplicity of Winkler's model in practical applications and its long-standing familiarity among practicing engineers.

Therefore, different analysis will be performed for various square and rectangular thin plates (having various aspect ratio) having different load configurations (i.e., number, location, and relative magnitude of column loads) as proposed by Loukidis (D. Loukidis, 2017).

The following section deals with description of the proposed methodology for the present study.

3.2 Single parameter Subgrade Model (Winkler)

In this type of analysis, the raft is modeled as a plate or flat shell element while the subgrade is represented by a single spring bed calculated based on modulus of subgrade reaction. For this thesis, CSi product SAFE is used to idealize and model the raft on single parameter subgrade model. CSi is recognized globally as the pioneering leader in software tools for structural and earthquake engineering. SAFE is a finite element-based software tailored for the engineering of elevated floor and foundation slab systems. Interoperability with SAP2000 and ETABS allows users to import models, loading, and displacement fields into SAFE for more advanced local assessment of slab systems within larger structures.

Spring supports are utilized to define soil supports for raft foundation analysis using SAFE, and thus the subgrade modulus parameter is used as input calculated from geotechnical reports. On the basis of the node's effective area as shown in figure 11, the software will then automatically compute and assign each node its unique spring properties. These springs can be defined as either points, lines, or areas and as tension-only or compression-only.

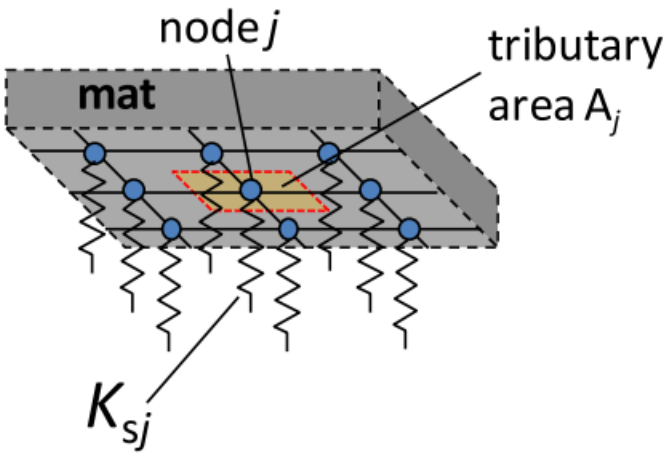

Figure 11: Spring Tributary Area

Even though several empirical formulae have been given in the past for computing subgrade reactions, the Meyrhof's method of subgrade modulus, as described in Equation (10), is adopted in the current study since it is bearing capacity independent, widely accepted and used in practice.

$$K_s = \frac{E_s}{B\left(1-v_s^2\right)} \quad (17)$$

Where E_s is the Elastic modulus of the soil

v_s is the poison's ratio of the soil

and B is the width (shorter dimension) of the raft

For instance, as per Meyrhof's suggestion, a square mat with a length of 24 meters undelaying on soil with a Young's modulus of 50 MPa and a poison's ratio value of 0.28 would have a subgrade reaction value of roughly 2,260.56 KN/m3.

Engineers usually run into a convergence issue with single parameter Winkler type of analysis since the spring supports assigned are only vertical. This issue is commonly addressed by giving lateral supports for in-plane reactions along the lateral axes. Most practitioners advise employing springs with stiff properties in the lateral directions to offer lateral support; these springs can then be placed around the mat's borders or corners. Hence for this study this approach is adopted to overcome the singularity problem.

3.3 Pseudo Coupled Method of Analysis (ACI 336.2R-88)

The "pseudo-coupling" approach uses edge springs that are stiffer than the center springs to achieve the desired theoretical dished effect of a flexible mat foundation while keeping the usage of a single parameter to represent the soil.

ACI 336.2R-88 (2002) recommends subdividing a mat area into distinct parts and giving various subgrade reaction values, ranging from softer (lower values of spring stiffness) in the middle to stiffer (higher values of spring stiffness) at the edges. Coduto (2001) states that the initially determined modulus of subgrade reaction should be distributed in such a way that each zone gets a value proportional to the area of the zone. Figure 12 shows an example of such zoning as illustrated in Coduto (2001).

It is important to note that Coduto (2001) only recommended zoning, and the distribution in figure 12 is presented merely for the purpose of illustration. The book does not state how many zones should be used or by how much their area should vary. For this, the current study utilized a zoning made up of three subdivisions, and the distribution of

$$k_{s1} = k_{s,ave} \times \frac{A_1 + A_2 + A_3}{A_1 + 1.5A_2 + 2A_3}$$

the subgrade reaction is as shown in Equation (18) as proposed by Coduto (2001).

(18)

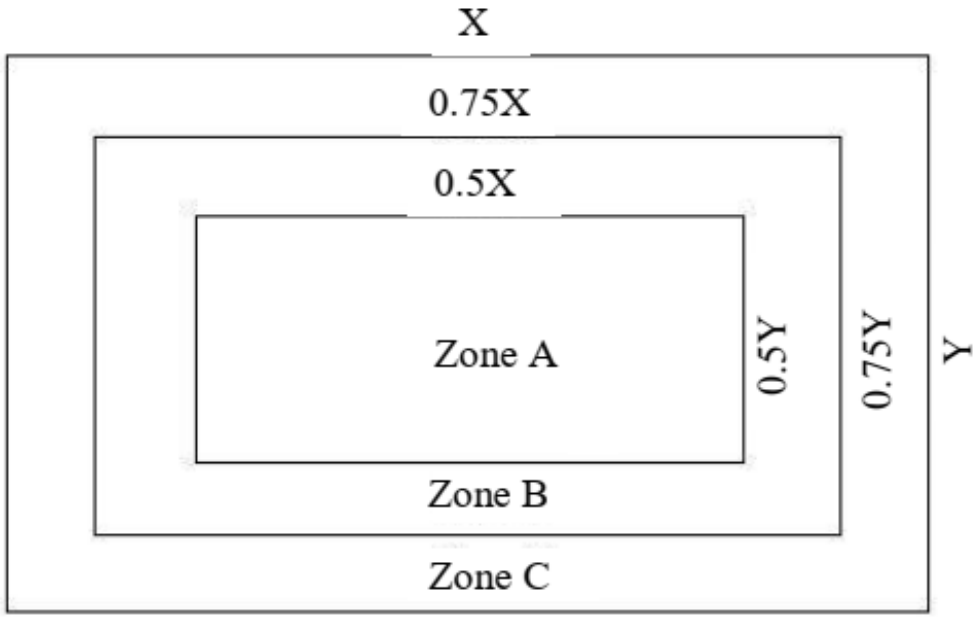

Figure 12: Sample zoning recommendation by Coduto (2001)

The CSi product SAFE is used to represent the pseudo-coupled approach, with subgrade reaction values for each division of the mat being carefully defined and assigned.

As an illustration, a square mat with a length of 24 meters resting on a soil with given subgrade reaction value of 2,260.56 KN/m^3 will have subgrade reaction values of 1,418.39 KN/m^3, 2,127.59 KN/m^3, and 2,836.78 KN/m^3 for the inner, middle, and outer divisions of the mat, respectively.

3.4 Vlasov's two Parameter Model

As stated in the literature review section, the parameters C1 and C2 are utilized in GEO5's Slab program to idealize the soil, following the suggestion made by Vlazov and Leontiev (1966) using the variational technique. Winkler representation restores when C_2 is set to zero (C_1 is the Winkler foundation spring stiffness). The advantage of the Vlazov model over the Pasternak model is that the parameters, C_1 and C_2, may be obtained from the elastic deformation characteristics of the ground.

GEO5 Slab is an intuitive program used for the analysis of raft foundations and slabs of any shape on elastic subsoil, using the Finite Element Method. The software automatically calculates the parameters C_1 and C_2 from the condition of equal compliance matrices of infinitely stiff infinite strip footing resting on the Winkler - Pasternak and elastic subsoil using deformation parameters of soils, or from geological profile. Hence a user is expected to inset the elastic properties of the soil (Young's modulus and poison's ratio) and the depth of influence zone which is not straight forward.

It is obvious that this approach produces results that are far reasonable than those produced by the Winkler model, however calculating the C_2 parameters is not an easy task and is very sensitive to the depth of deformation value. Therefore, the back-calculated depth of deformation value obtained from the calibration value of Worku's calibrated Kerr equivalent Pasternak model is used in this thesis for the study of raft foundation utilizing the GEO5's two parameter model.

For example, a square mat with a length of 24 meters undelaying on a soil with a Young's modulus of 50 MPa and a poison's ratio value of 0.28 would have a calibration value of 1.25 (see figure 13), hence the depth of influence zone will be equal to 30 meters.

3.5 Worku's Model

This model uses the recently developed Kerr equivalent Pasternak model by Worku (2014) and a calibration factor chart that was produced in a recent ongoing work by Minwuyelet and Worku (2022). With the help of this model, plates on elastic foundations can be analytically analyzed under various loading and boundary conditions. However, the available analytical solutions of these differential equations are limited to simple cases such as homogeneous plates of relatively simple geometry, loading and boundary conditions. Ultimately the solution of these type of engineering problems, which involve equilibrium equations together with constitutive relations, compatibility considerations, and complex boundary conditions, would require such an effort that a purely analytical approach would be complex for practicing engineers.

Thus, as the primary goal of this study is to show the effectiveness of the newly calibrated Worku's Kerr equivalent Pasternak model for the analysis of mat on an elastic foundation, numerical solution technique such as FEM is more appropriate. For this, the MATLAB algorithm developed by Minwuyelet and Worku (2022) is used.

The algorithm is developed based on thin plate theory and uses the linear elastic constitutive model to represent the stress strain relationship of the raft and soil. Hence as an input it receives plate dimension (length, width, and thickness), plate stiffness property (Young's modulus and poisson's ratio), soil property (Young's modulus, poisson's ratio, and calibration factor) and load.

More than 250 models of square, symmetrically loaded plates were used to develop the calibration chart for their research at first. In this case they used square thin plates (concrete, wood, steel, etc.) having different sizes and resting on soils with Young's modulus ranging from 20 MPa (soft clay or loose sand) to 200 MPa (Soft rock). In order to extract the calibration value from the calibration chart for this model, the relative rigidity (or stiffness) of a foundation is employed in conjunction with the soil stiffness, which frequently plays a significant role in determining how the foundation responds to loads.

The formula recommended by the ACI committee 336 report, DIN 4018 code, Meyerhof, and IS 2950-1 code can be used to calculate the relative rigidity of a raft foundation (R_s), which in turn can be used to determine foundation rigidity. The rigidity formulation shown in equation (12), as proposed by Gorbunov-Possadov and Serebrjanyi (1961), which takes into account the impact of variations in the soil and foundation stiffness as well as Poisson's ratios and plate dimension, was chosen for this study despite the abundance of rigidity formulations that are currently available in the literature.

$$R_s = \frac{8D\left(1-v_s^2\right)}{\pi L^2 B E_s} \qquad where \qquad D = \frac{E_p h^3}{12\left(1-v_p^2\right)} \tag{19}$$

For the combinations of problem studied herein, R_s ranges from 0.010 to 0.160. A foundation is characterized as rigid if $R_s > 0.5$.

They claimed that the chart could be used to examine any type of symmetrically loaded, square, thin plate (concrete, wood, steel, etc.), resting on an elastic foundation. However, they witnessed that it could lead to an error of up to 25% for rectangular plates and asymmetrical loading.

In this thesis this model is referred to as Worku's model and one can obtain the calibration value from figure13 by directly entering with the relative rigidity Equation and soil stiffness.

For example, a square mat (having Young's modulus of 32GPa and Poisson's ratio of 0.2) with a length of 24 meters and thickness of 2.2 meters underlying on a soil with a Young's modulus of 50 MPa and a Poisson's ratio value of 0.28 would have a calibration value of 1.25 (see figure 13).

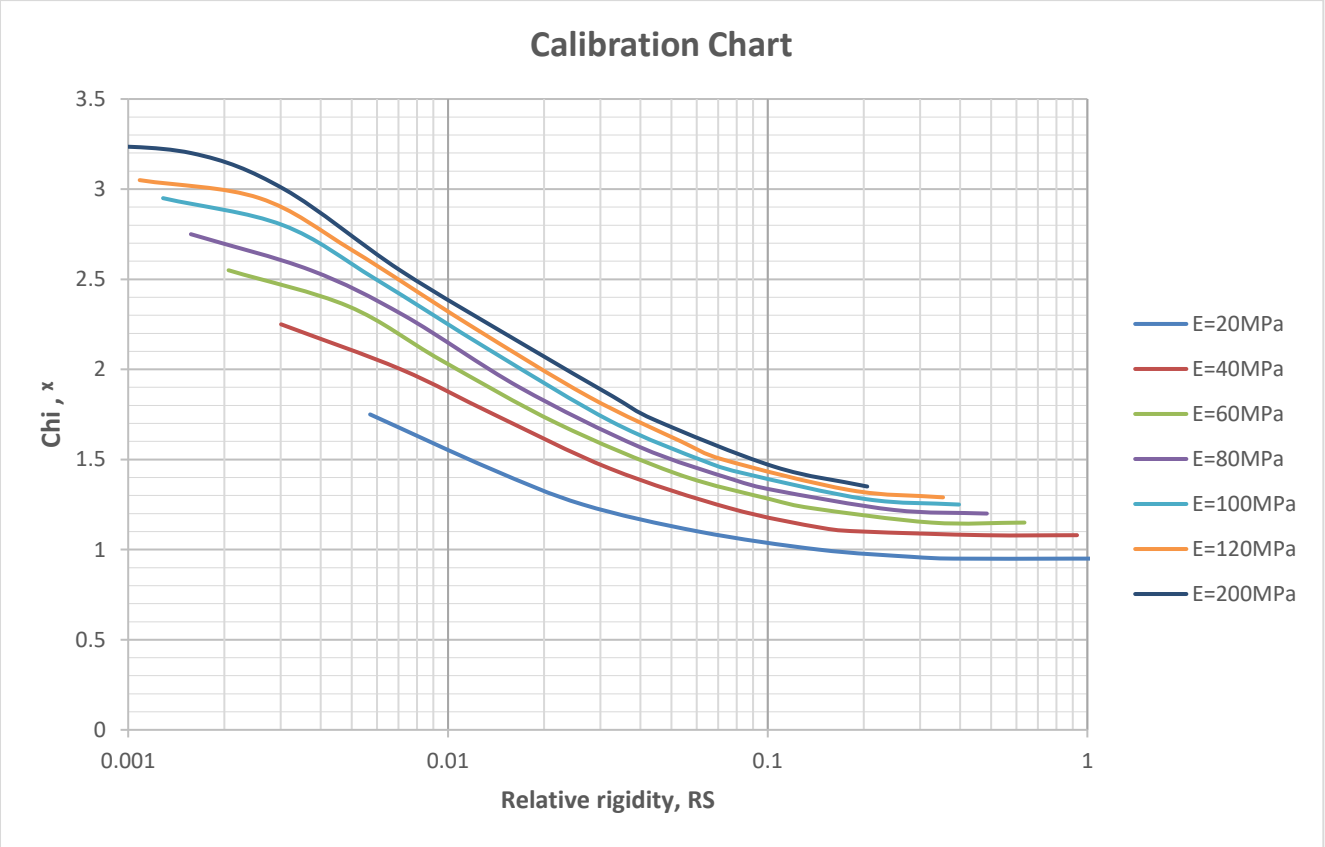

Figure 13: Calibration chart

3.6 Worku's Adjusted Model

The calibration value retrieved from the calibration chart was modified by Minwuyelet and Worku (2022) using a function of aspect ratio, while an adjustment to the edge stiffness was made to account for the effects of both asymmetric loading and aspect ratio. This effort aimed to extend the applicability of the calibration chart for rectangular plates loaded asymmetrically. They asserted that any form of vertically loaded, rectangular, thin plate (concrete, wood, steel, etc.), resting on an elastic foundation, could be fully analyzed with the help of the chart. In the result discussion phase, this is referred to as the Worku's adjusted model (Worku's AdJ).

For instance, a rectangular mat with a Young's modulus of 32GPa and a Poisson's ratio of 0.2 and dimensions of 24 meters long, 8 meters wide, and 0.8 meters thick resting on a soil with a Young's modulus of 60 MPa and a Poisson's ratio of 0.26 would have an initial calibration value of 1.9 (Figure 13) and a modified calibration value of 3.0.

3.7 Continuum Finite Element Method (cFEM)

In this analysis, the mat is treated as a structural element-a thin plate (thickness small compared with the other dimensions) - and the soil by appropriate constitutive model. Three-dimensional continuum-based FEM (cFEM) of PLAXIS 3D was used to verify the performance of the newly calibrated Kerr equivalent Pasternak model. Plaxis 3D is a geotechnical Finite Element Analysis simulation program developed for the evaluation of soil-structure interaction problems based on the finite element method in both 2D and 3D.

Although there are many constitutive models in PLAXIS 3D package, the raft and the soil are both modeled using an elastic constitutive model in order to maintain consistency with the aforementioned models.

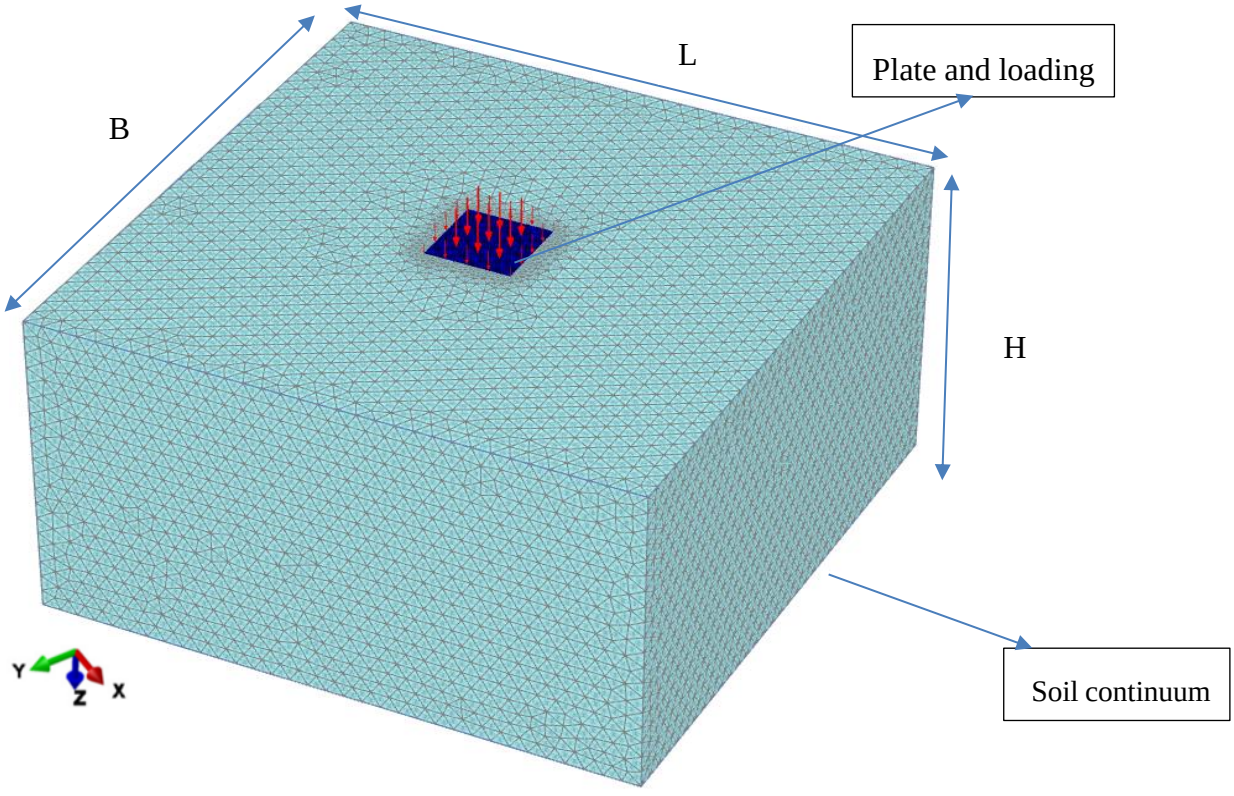

Figure 14: cFEM (continuum finite element)

To make sure that the solutions in this study are stable and reliable enough, the potential effects of the discrete mesh, the model extent, and the boundary conditions were clarified. The lateral and vertical extents used are, respectively, seven and four times the plate's width. For example, a model of a square mat with a length of 24 meters would have a soil model extent of 168 meter in the lateral and 96 meters in the vertical direction having more than 80,000 elements (see figure 14).

CHAPTER FOUR

4. ANALYSIS RESULTS AND DISCUSSIONS

The present study uses carefully chosen foundation dimensions, elastic parameters (plate and soil), and load combinations that one may encounter in real-world projects to meet the research objective.

In all cases the column spacing S range from 4 m to 6 m, resulting in foundation dimensions of 8 m to 24 m, the thickness ranges from 0.75 m to 2.2 m (typical thin plate dimensions).

For this study, the vertical load magnitude is calculated using a central load value (Q) of magnitude 5400KN at the location of the interior columns. This was predicated on the assumption that a 15-storey, frame building with a workable load of 10 KN/m^2 per story and a grid pattern (column center to center spacing) of 6 meters would result in 150 KN/m^2 of load pressure and the equivalent amount of 5,400 KN load at the interior columns. The other load magnitudes, indeed, will be multiplied by the factors that were applied to them. For instance, the load magnitude value for a load defined as 2/3Q will be 3,600 KN.

1) Model_Case_1: Symetrically loaded square raft

This load configuration, designated M1, represents the typical situation in which loads are distributed according to the tributary areas around the columns, with corner and edge columns carrying lighter loads than interior columns. The relevant data are given in table 1. The relative rigidity (R_s) determined according to equation (12) is also included in the eighth column.

The value of the calibration is obtained from Figure 13 by entering with the relative rigidity and soil stiffness.

Table 1: Dimension and Parameters used for plate of size 24mx24mx2.2m loaded symmetrically

L(m)	B(m)	h(m)	E_P(GPa)	ν_p	Es(MPa)	ν_s	R_s	Load Case	e_x(m)	e_y(m)	χ, c_{hart}
24	24	2.2	32	0.2	50	0.28	0.1004	M1	0	0	1.25

Figure 15 Shows a symetrically loaded raft having a similar grid pattern (center to center of the load location) in both directions.

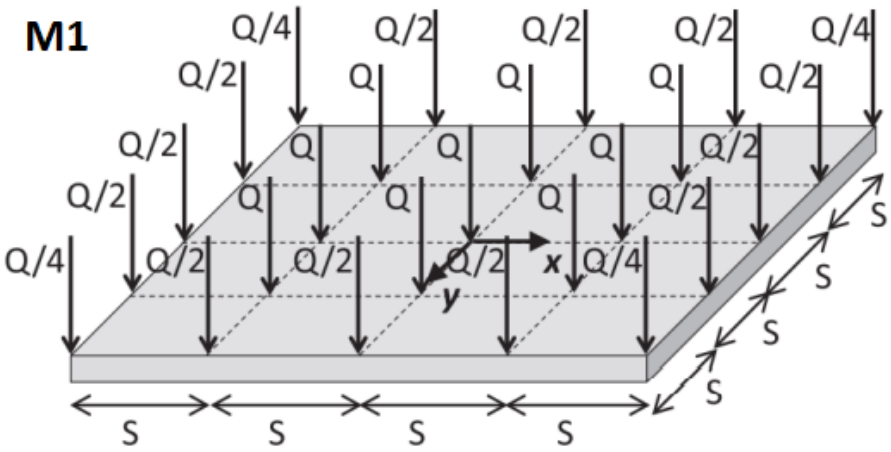

Figure 15: Load configuration used for plate of size 24mx24mx2.2m

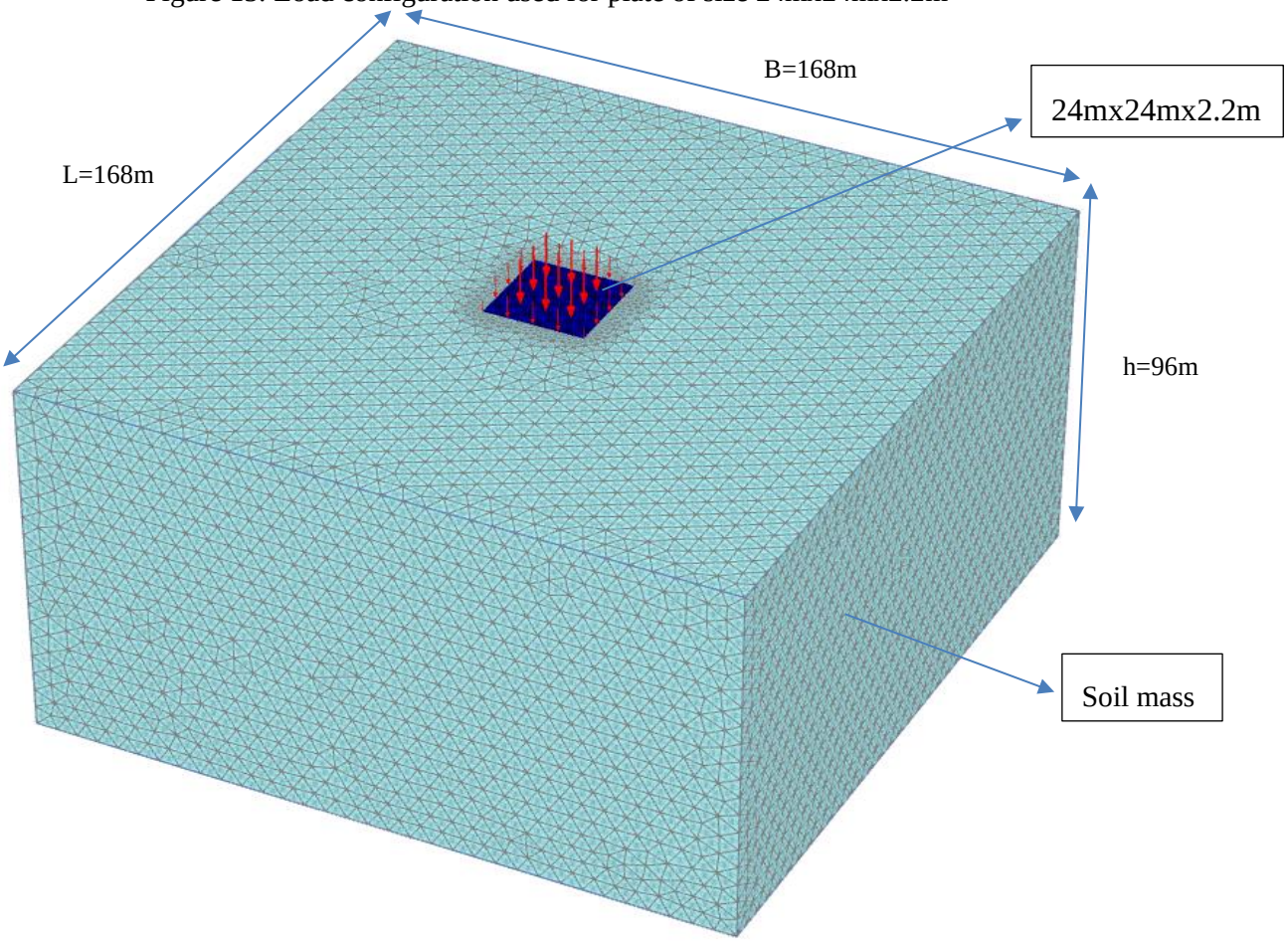

Figure 16: cFEM Model of size 168mx168mx96m

Figure 16 shows the continuum finite element model (cFEM) of the current model as modeled by PLAXIS 3D. The model extent of the soil is 168 meter in the lateral and 96 meters in the vertical direction. A mesh size starting from 0.5 meter around the plate and going to 5 meters at the edge boundary of the soil model is employed. A total of 80,016 elements are generated. 3D solid section with 10-noded tetrahedral elements is used for the soil while the mat is modelled as a two-dimensional plate element with 6-noded triangles.

Figure 17 and figure18 shows the Single parameter Subgrade Model (Winkler) and the Pseudo Coupled analysis model vertical deformation output respectively. Both are modeled and analyzed using the commercial CSi SAFE software.

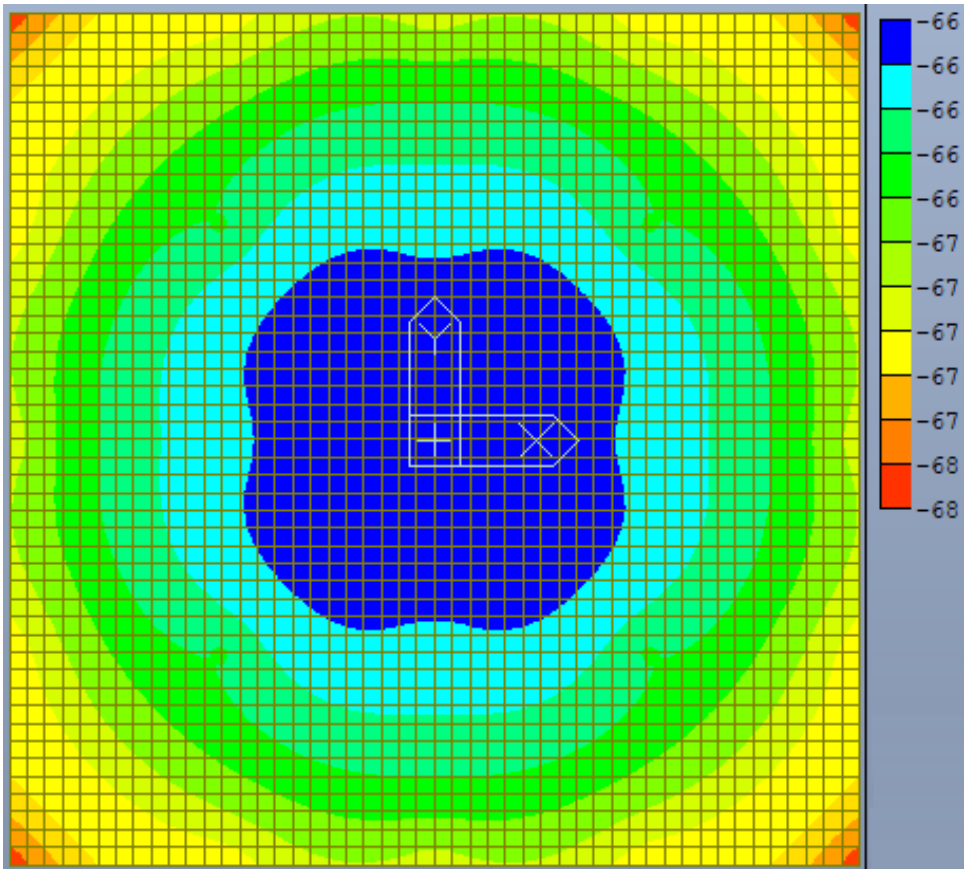

Figure 17: Winkler Model Output for a symmetrically loaded plate of size 24mx24mx2.2m

As is apparent from the above figures, even though the deflection value is somewhat comparable, the two one parameter models have different deflection result indications. In the case of the Winkler model, the maximum deflection is located at the plate's edges, whereas in the case of the pseudo coupled model, it is in the center. This is attributed to the fact that,

compared to the typical Winkler type, the pseudo couple analysis does employ a larger edge spring value.

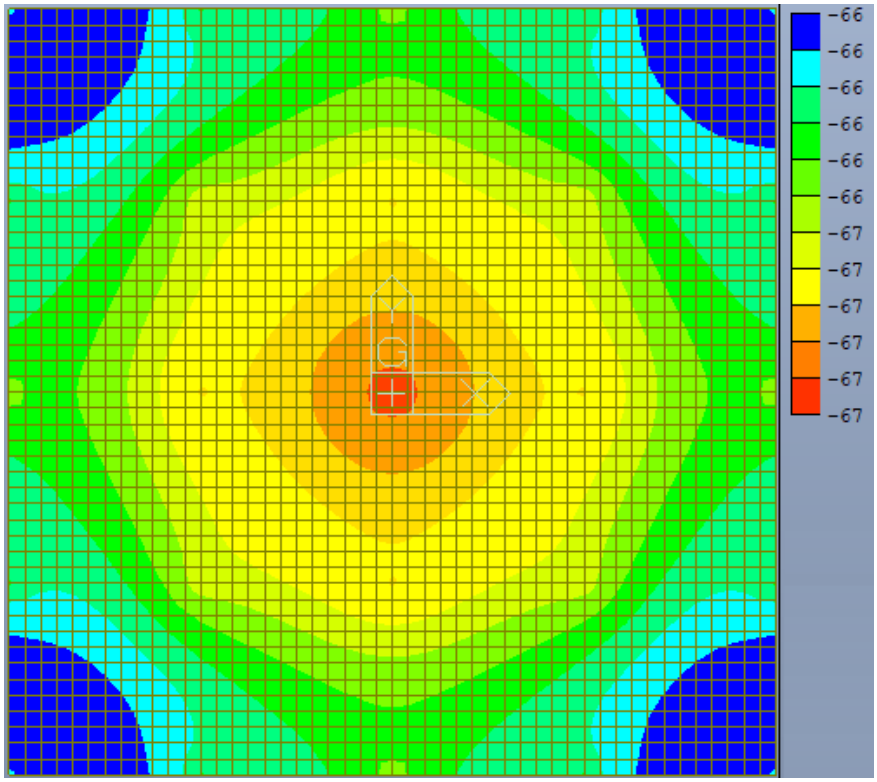

Figure 18: Pseudo Coupled Model Output for a symmetrically loaded plate of size 24mx24mx2.2m

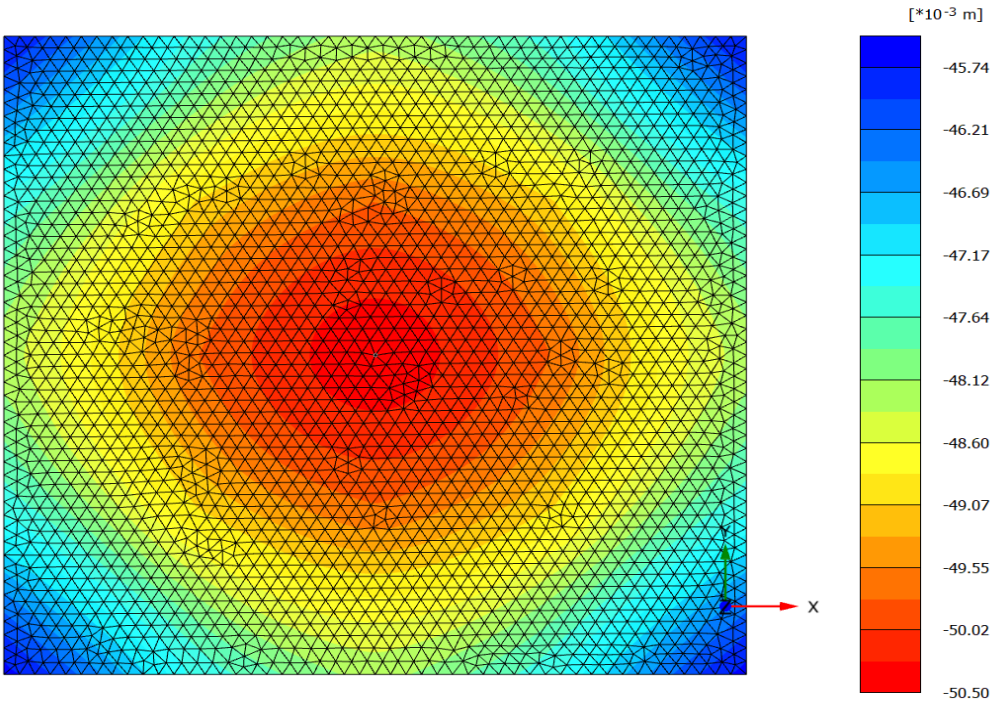

Figure 19: cFEM Model Output for a symmetrically loaded plate of size 24mx24mx2.2m

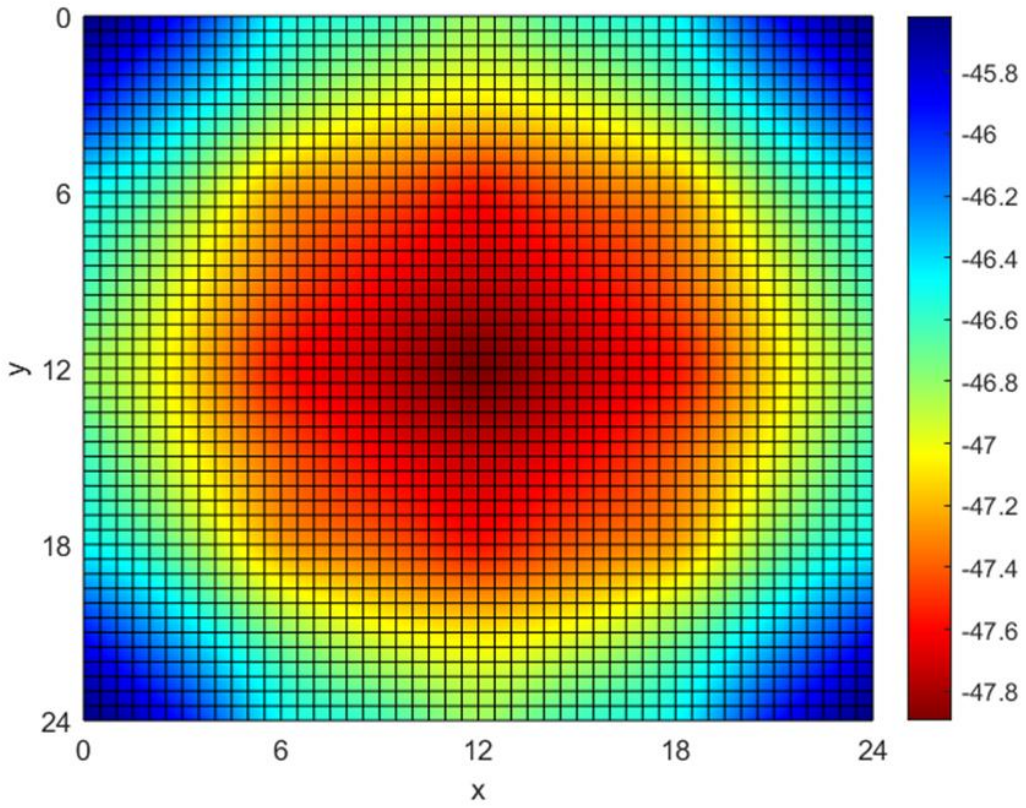

Figure 20: Worku's Model Output for a symmetrically loaded plate of size 24mx24mx2.2m

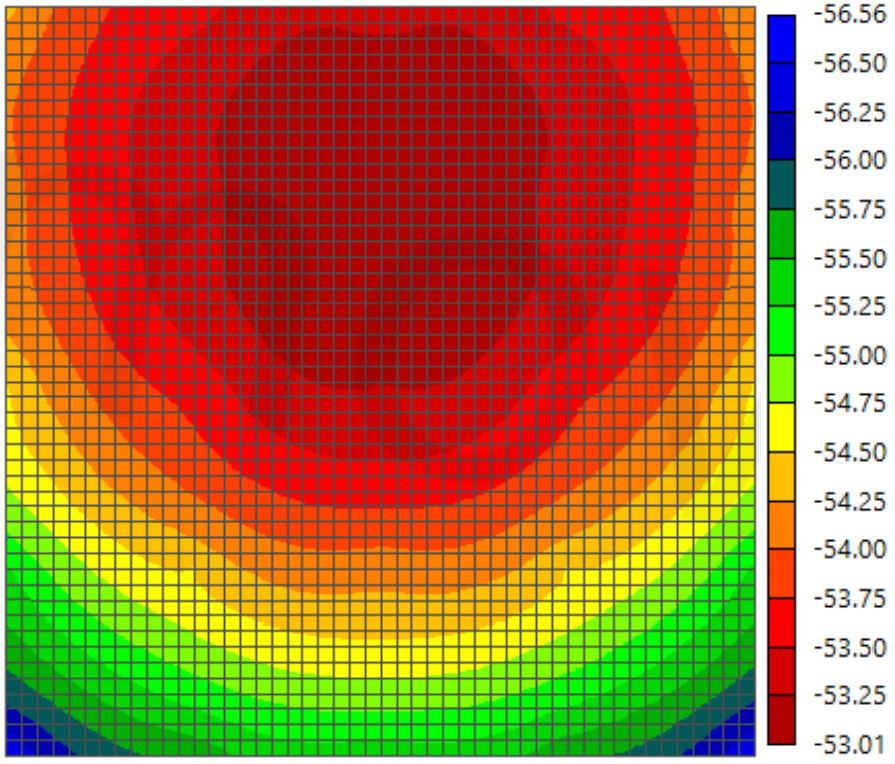

Figure 21: Geo5 Output for a symmetrically loaded plate of size 24mx24mx2.2m

Remarkably, as demonstrated by the deflection chart in Figure 22 and based on the results from the cFEM and Worku Model, there is a comparable deflection pattern.

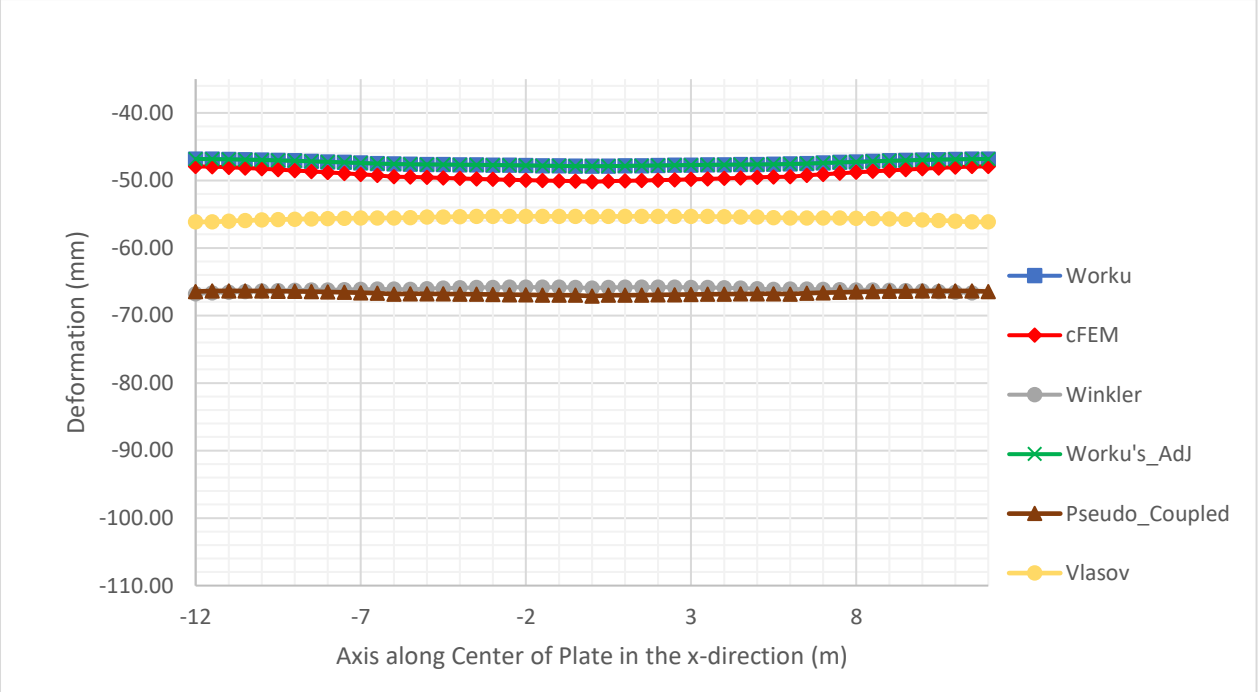

Figure 22: Vertical deformation along the center of the plate in the Length direction

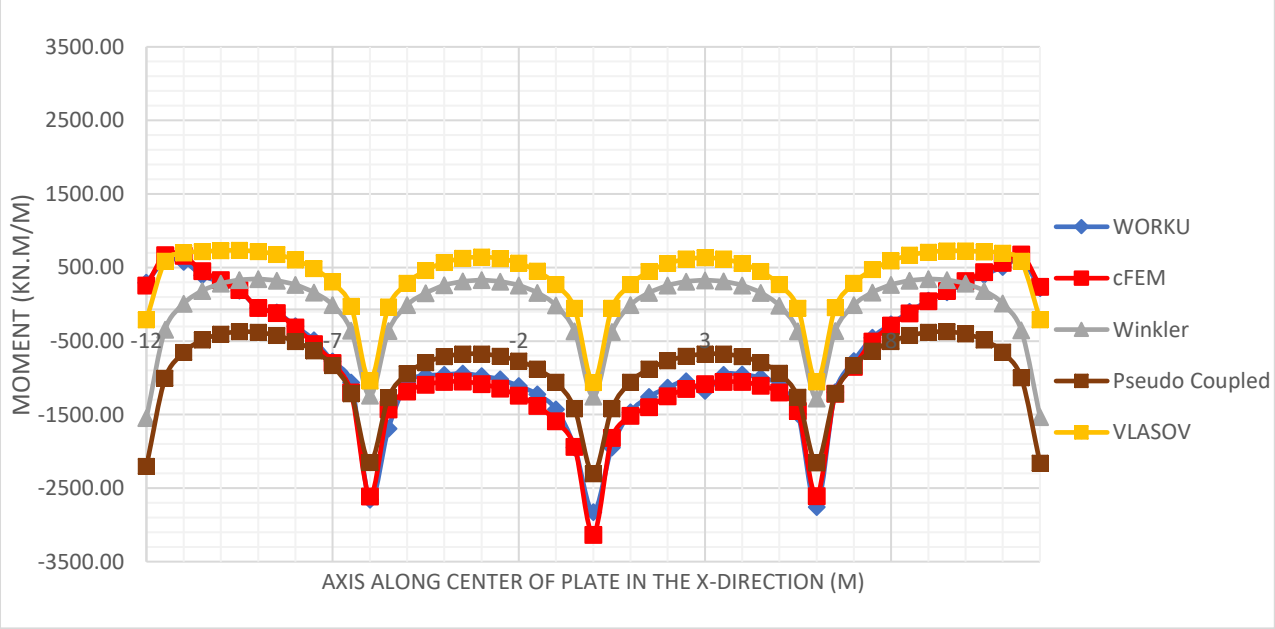

Figure 23: moment values along the center of the plate

The calibration value is read from the calibration chart and utilized without modification because the problem is a symmetrically loaded (no eccentricity in both directions) square

(aspect ratio of 1) plate. As a result, both the Worku's model and the Worku's_AdJ model produced the same deflection output. The overlap of the two curves illustrates this. The two one parameter models—Winkler and Pseudo coupled—produce a closer deflection value. The two parameter Vlasov model, which was modeled and analyzed using GEO5, provides a result that falls between the one parameter models and the rest (Worku, Worku_AdJ, and cFEM).

In conclusion, the tabular data and deflection chart shows that the Worku (calibrated Kerr equivalent Pasternak) model offers superior agreement (only an error of less than 5%) with that of cFEM (PLAXIS 3D), whereas the long-standing one parameter -Winkler model and its variant the Pseudo Coupled method provide an error of 40%.

The bending moment results obtained using Worku's newly calibrated Kerr-equivalent Pasternak model demonstrate excellent agreement with the continuum finite element analysis performed in PLAXIS 3D. The pick moment that occur at the center of the plate will require bottom reinforcement and the top tension area in the mid-span will require a top reinforcement. The other models specially Winkler and Vlasov highly underestimate the positive moment and substantially overestimate the negative moment. The pseudo-coupled model improved this but still underperformed compared to Worku and cFEM by producing up to 40% error at the mid span but produces significantly unrealistic error at the edge. The Vlasov model moderately approximated the correct distribution but underestimated central moments which yield error more than 130% in most of the plate span. But Worku's model follow the cFEM (the benchmark) in close range only producing small error of less than 5 % in most of the mid span and a maximum error of 11% at the edge and center , indicating that Worku's two-parameter foundation model reliably captures both the magnitude and distribution of bending moments in square and rectangular raft foundations.

Table 2: Deformation output for plate of size 24mx24mx2.2m loaded symmetrically

Coordinate	Worku	CFEM	Winkler	Pseudo Coupled	GEO-5	Worku Error (%)
-12	-46.83	-47.94	-66.81	-66.46	-56.13	-2.37
-11.5	-46.85	-47.96	-66.64	-66.38	-56.14	-2.37
-11	-46.88	-48.05	-66.54	-66.36	-56.02	-2.50
-10.5	-46.92	-48.15	-66.46	-66.36	-55.93	-2.64
-10	-46.97	-48.27	-66.38	-66.38	-55.86	-2.77
-9.5	-47.03	-48.40	-66.31	-66.40	-55.79	-2.91
-9	-47.10	-48.53	-66.26	-66.43	-55.73	-3.04
-8.5	-47.17	-48.67	-66.20	-66.47	-55.68	-3.17
-8	-47.25	-48.81	-66.20	-66.52	-55.64	-3.29
-7.5	-47.33	-48.95	-66.16	-66.57	-55.61	-3.41
-7	-47.42	-49.10	-66.13	-66.63	-55.58	-3.53
-6.5	-47.50	-49.25	-66.10	-66.70	-55.56	-3.67
-6	-47.57	-49.45	-66.09	-66.83	-55.55	-3.94
-5.5	-47.61	-49.47	-66.14	-66.78	-55.49	-3.92
-5	-47.63	-49.55	-66.02	-66.80	-55.44	-4.03
-4.5	-47.65	-49.63	-65.96	-66.81	-55.40	-4.15
-4	-47.67	-49.70	-65.91	-66.84	-55.37	-4.27
-3.5	-47.69	-49.78	-65.85	-66.86	-55.34	-4.37
-3	-47.72	-49.84	-65.82	-66.89	-55.32	-4.45
-2.5	-47.75	-49.90	-65.81	-66.91	-55.31	-4.52
-2	-47.78	-49.96	-65.80	-66.94	-55.31	-4.57
-1.5	-47.81	-50.01	-65.81	-66.97	-55.31	-4.60
-1	-47.85	-50.06	-65.82	-67.00	-55.32	-4.62
-0.5	-47.88	-50.10	-65.84	-67.00	-55.34	-4.64
0	-47.89	-50.19	-65.92	-67.12	-55.39	-4.79
0.5	-47.88	-50.10	-65.84	-67.00	-55.34	-4.64
1	-47.85	-50.06	-65.82	-67.00	-55.32	-4.62
1.5	-47.81	-50.01	-65.81	-66.97	-55.31	-4.60
2	-47.78	-49.96	-65.80	-66.94	-55.31	-4.56
2.5	-47.75	-49.90	-65.81	-66.91	-55.31	-4.51
3	-47.72	-49.84	-65.82	-66.89	-55.32	-4.45
3.5	-47.69	-49.77	-65.85	-66.86	-55.34	-4.36
4	-47.67	-49.70	-65.91	-66.84	-55.37	-4.26
4.5	-47.65	-49.63	-65.96	-66.81	-55.40	-4.14
5	-47.63	-49.55	-66.02	-66.80	-55.44	-4.02
5.5	-47.61	-49.47	-66.14	-66.78	-55.49	-3.91
6	-47.57	-49.44	-66.09	-66.83	-55.57	-3.93
6.5	-47.50	-49.24	-66.10	-66.70	-55.55	-3.66
7	-47.42	-49.09	-66.13	-66.63	-55.56	-3.52
7.5	-47.33	-48.95	-66.16	-66.57	-55.58	-3.40
8	-47.25	-48.80	-66.20	-66.52	-55.61	-3.28
8.5	-47.17	-48.66	-66.20	-66.47	-55.64	-3.16
9	-47.10	-48.52	-66.26	-66.43	-55.68	-3.03
9.5	-47.03	-48.39	-66.31	-66.40	-55.73	-2.90
10	-46.97	-48.27	-66.38	-66.38	-55.86	-2.76
10.5	-46.92	-48.15	-66.46	-66.36	-55.93	-2.62
11	-46.88	-48.04	-66.54	-66.36	-56.02	-2.49
11.5	-46.85	-47.95	-66.64	-66.38	-56.14	-2.36
12	-46.83	-47.93	-66.81	-66.46	-56.13	-2.36

Model Parameters		
L=	24	m
B=	24	m
h=	2.2	m
A_R=	1	Aspect Ratio
e_x=	0	m
e_y=	0	m
E_p=	32	GPa
v_p=	0.2	
E_S=	50	MPa
v_s=	0.28	
Flexural Rigidity		
$D = \frac{E_p h^3{}_s}{12(1-{v_p}^2)}$		
D=	29,577.78	MNm
Relative Rigidity		
$R_s = \frac{8D(1-{v_s}^2)}{\pi L^2 B E_s}$		
Rs	0.100	Relative rigidity
Load Type=	C6	
Q=	5400	KN
Calibration Factor		
chi, χ =	1.25	From Chart
chi_M, χ_M =	1.25	Modefied
Modulus of subgrade Reaction, K_s		
$k_s = \frac{E_s}{B(1-{v_s}^2)}$		
Ks=	2,260.56	KN/m^3
Pseudo Coupled		
Ks,ave=	2,260.56	KN/m^3
A_1=	144	m^2
A_2=	180	m^2
A_3=	252	m^2
$k_{s1} = k_{s,ave} \times \frac{A_1 + A_2 + A_3}{A_1 + 1.5A_2 + 2A_3}$		
Ks_1=	1,418.39	KN/m^3
Ks_2=	2,127.59	KN/m^3
Ks_3=	2,836.78	KN/m^3

2) **Model_Case_2: Asymmetrically loaded (in one direction) square raft**

This load configuration, designated M2, is adopted to test the performance of the Worku (Calibrated Kerr equivalent Pasternak) model effectiveness in a square plate loaded unsymmetrically in one direction.

In this case, the aspect ratio of the plate taken is one, thus the calibration factor doesn't need to be modified. However, the MATLAB algorithm was adjusted to account for the asymmetry of the load. Hence the adjusted version of Worku's model is best suit for this scenario.

Table 3: Dimension and Parameters used for plate of size 12mx12mx1.1m loaded asymmetrically

L(m)	B(m)	h(m)	E_P(GPa)	ν_p	Es(MPa)	ν_s	R_s	Load Case	e_x(m)	e_y(m)	χ_{chart}
12	12	1.1	32	0.2	30	0.35	0.1594	M2	1	0	1.05

Figure 24 shows a asymetrically loaded raft having a similar grid pattern (center to center of the load location) in both directions. The eccentricity which is due to the load magnitude is only in one direction (in the x axis). Since the tensile strength of soil is zero an effert was made so as to avoid negative contact pressure. This was made by limiting the eccentricity and proportioning the foundation in such that:

$$e_x \le \frac{L}{6} \text{ or } e_y \le \frac{B}{6} \text{ where } e_x \text{ and } e_y \text{ are eccentricity in the length}(L) \text{ and width}(B) \text{ direction respectivelly}$$

In the current model the eccentricity in the length direction (e_x) is 1 meter while there is no eccentricity in the width direction ($e_y = 0$).

Figure 25 shows the three dimenssional continuum finite element model (cFEM) of the current model as modeled and analysed by PLAXIS 3D. The model extent of the soil is 84 meter in the lateral and 48 meters in the vertical direction. A mesh size starting from 0.5 meter around the plate and going to 5 meters at the edge boundary of the soil model is employed. A total of

60,807 elements are generated. 3D solid section with 10-noded tetrahedral elements is used for the soil while the mat is modelled as a two-dimensional plate element with 6-noded triangles..

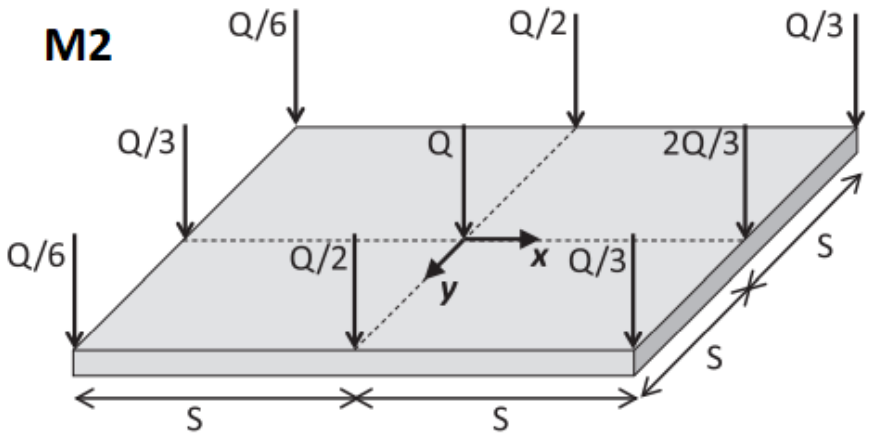

Figure 24: Load configuration used for a plate of size 12mx12mx1.1m

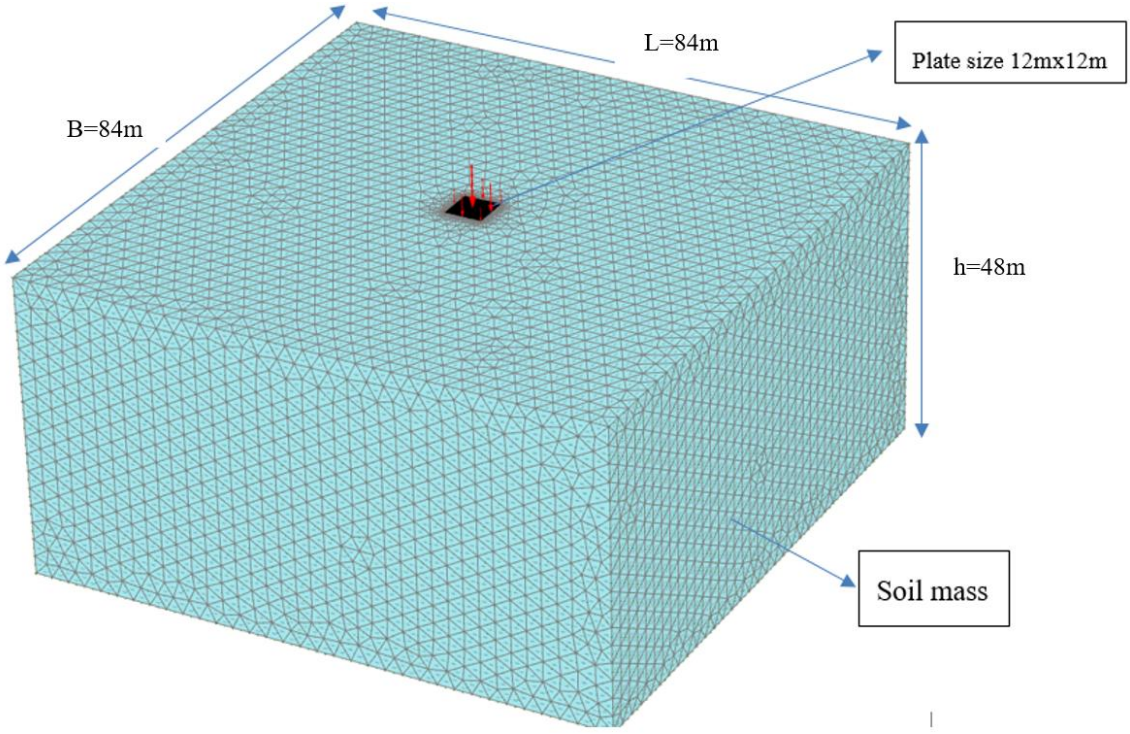

Figure 25: cFEM Model of size 168mx168mx96m

Figure 26 and 27 shows the Single parameter Subgrade Model (Winkler) and the Pseudo Coupled analysis model vertical deformation output respectively. Both are modeled and analyzed using the commercial CSi SAFE software. The Winkler model gave a vertical

deformation ranging from 27.29 mm to 80.24 mm whereas the Pseudo coupled technique produced a vertical deformation output that ranged from 30.14 mm to 76.79 mm.

The maximum error at the side of the eccentrically loaded area for the two single parameter subgrade models (Winkler and the Pseudo Coupled) was 70% and 75%, respectively, with the Winkler model giving the largest error.

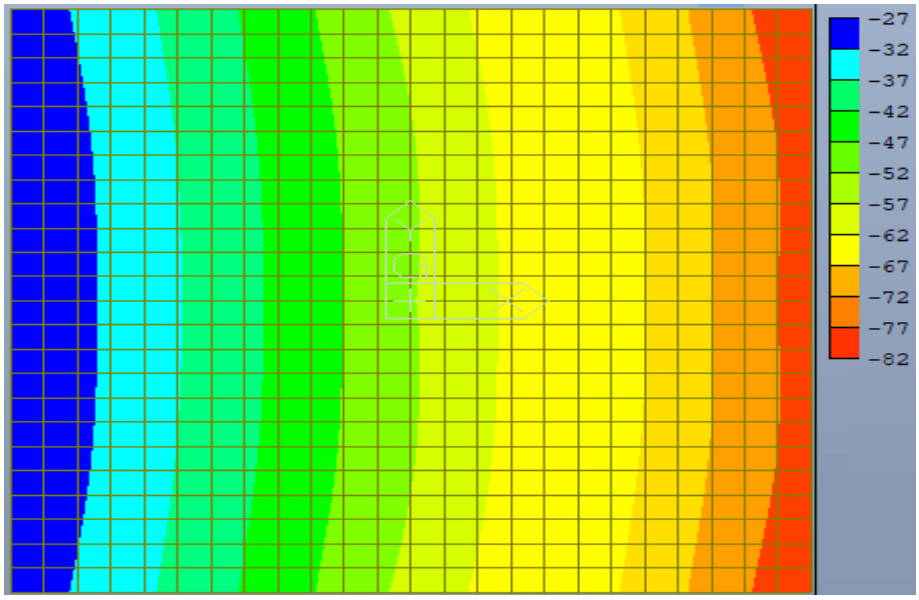

Figure 26: Winkler Model Output for asymmetrically loaded plate of size 12mx12mx1.1

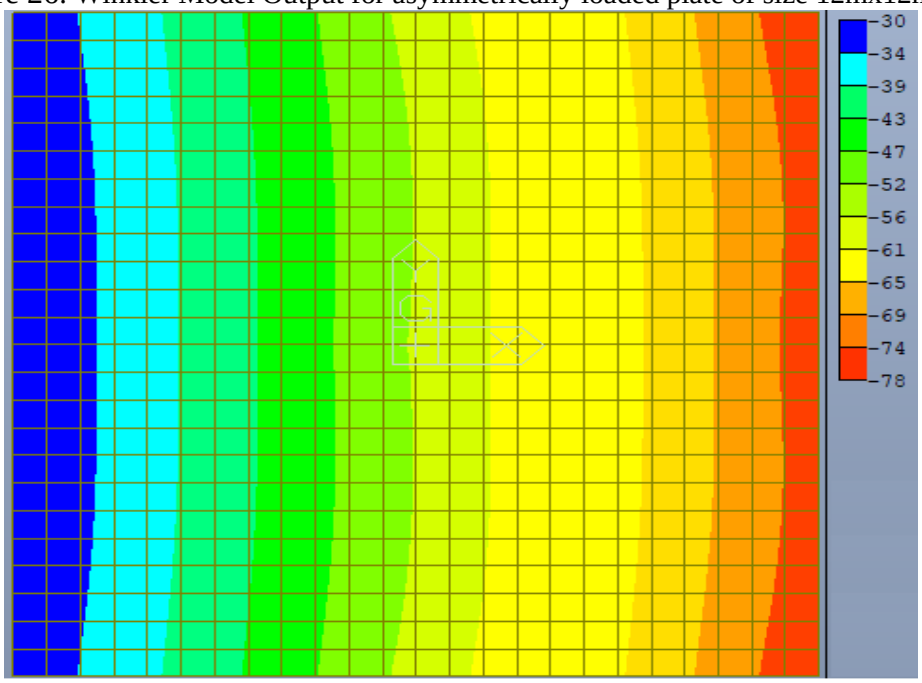

Figure 27: Pseudo Coupled Model Output for asymmetrically loaded plate of size 12mx12mx1.1m

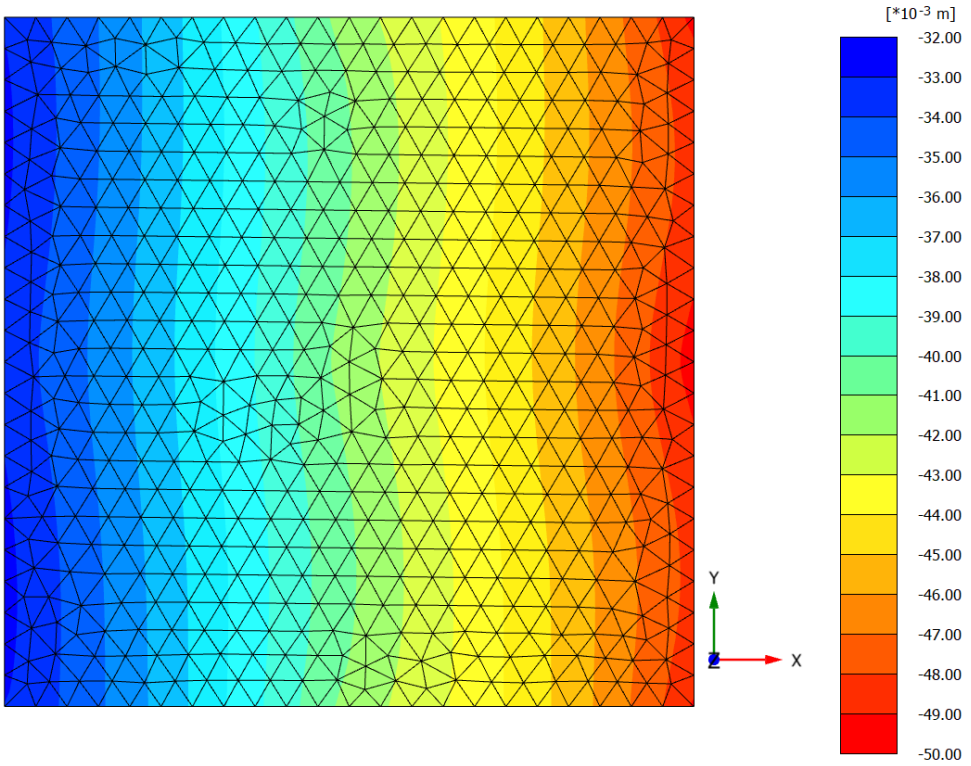

Figure 28: cFEM Model Output for asymmetrically loaded plate of size 12mx12mx1.1m

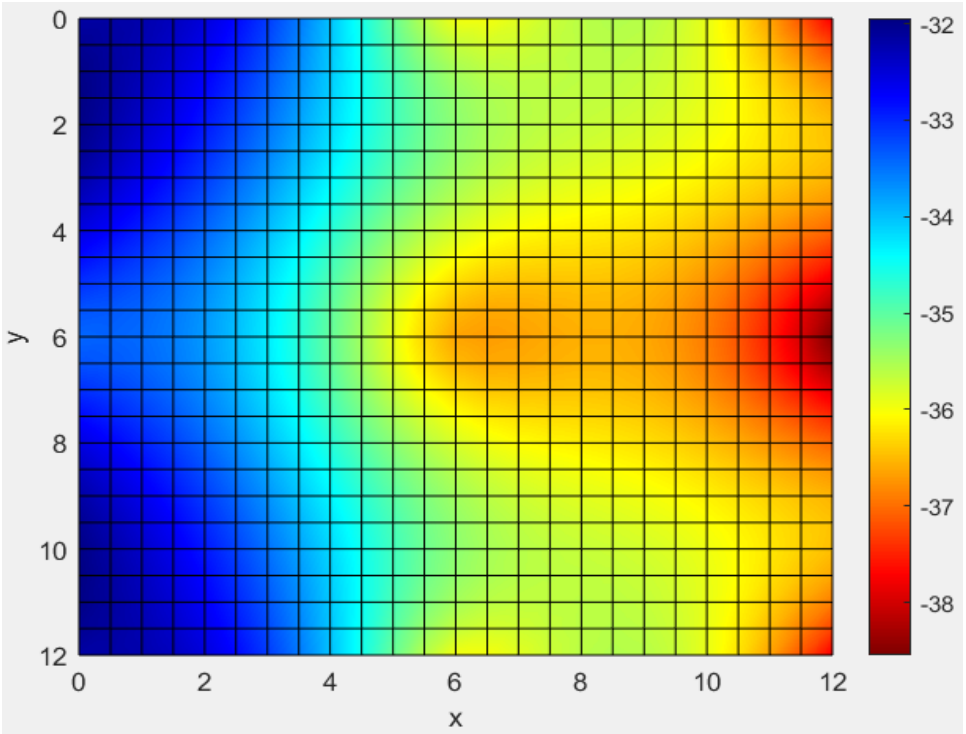

Figure 29: Worku's Model Output for asymmetrically loaded plate of size 12mx12mx1.1m

The maximum error in the deformation value produced by the original Worku's model and the adjusted Worku's model is 15% and 4%, respectively. As was stated before, one should employ

the Worku's_AdJ model rather than Worku's model for problems that are asymmetrically loaded. Matter of fact, when compared to the other models (Winkler-resulted in maximum error of 75%, Pseudo coupled- resulted in maximum error of 70%, and Vlasov- resulted in maximum error of 55%), the Worku's model (without adjustment) produced an acceptable result (maximum error of 15%).

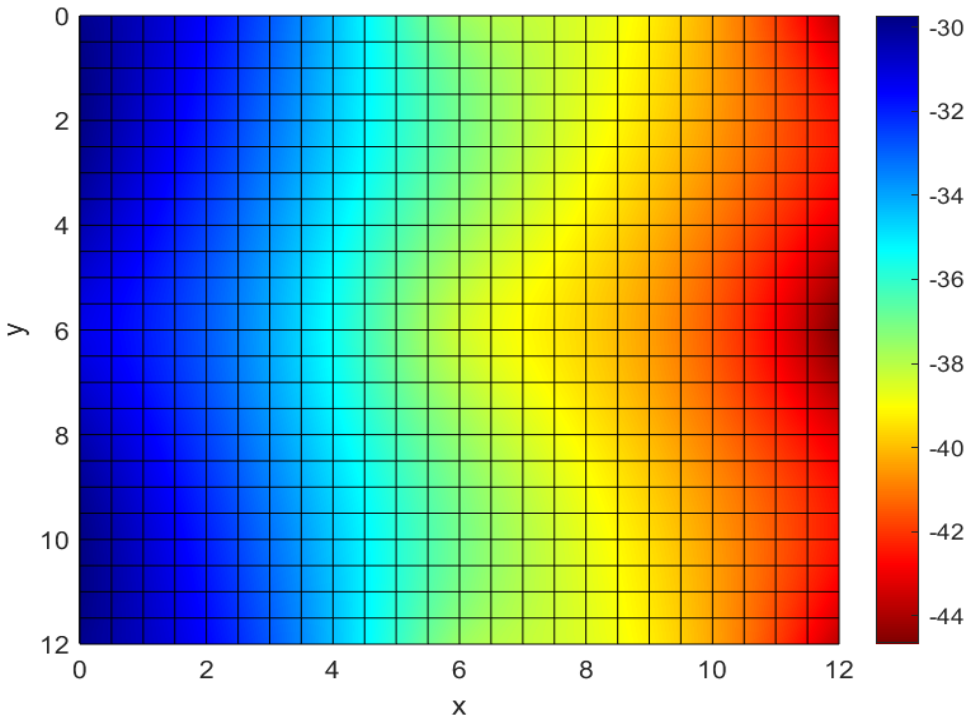

Figure 30: Worku's_AdJ Model Output for asymmetrically loaded plate of size 12mx12mx1.1m

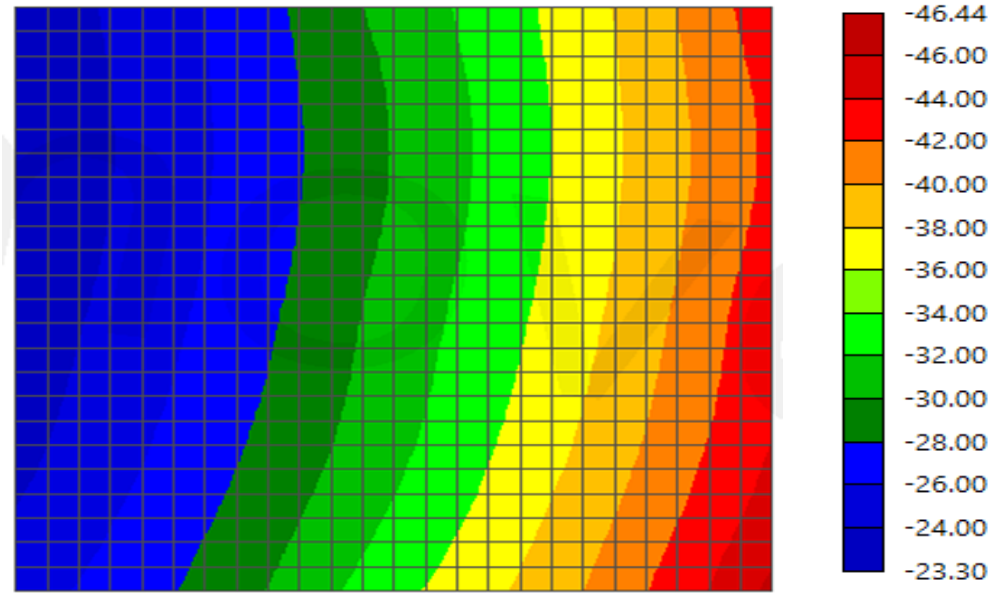

Figure 31: Geo5 Output for a symmetrically loaded plate of size 12mx12mx1.1m

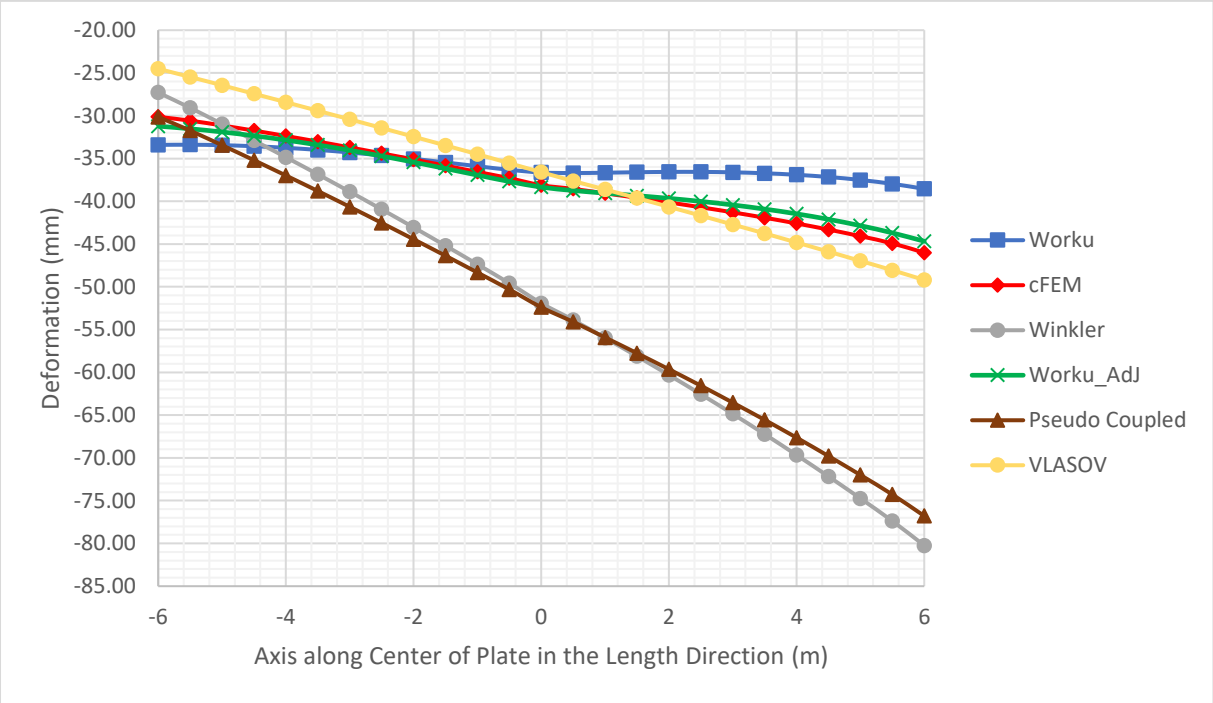

Figure 32: Vertical deformation along asymmetrically loaded side (Length direction)

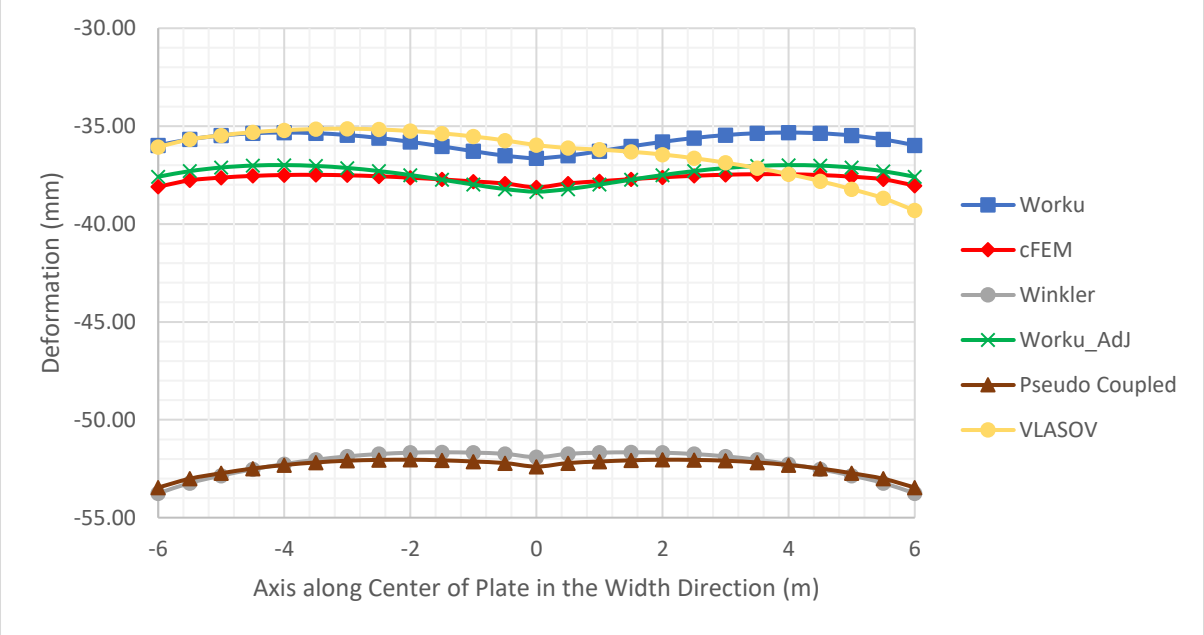

Figure 33: Vertical deformation along the symmetrically loaded (Width direction)

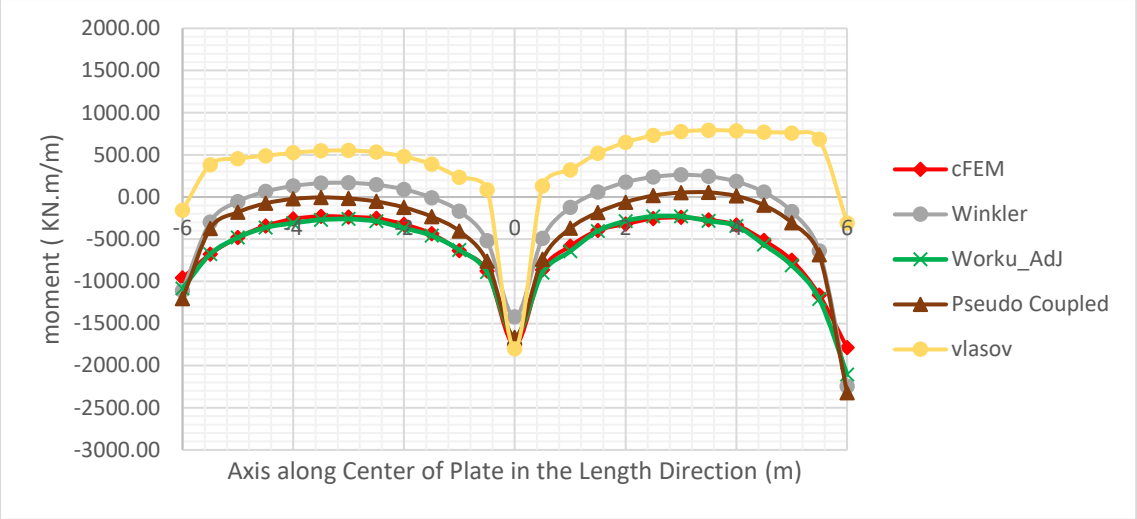

Figure 34: moment value along the center of the plate

The two-parameter subgrade model, which was studied using the GEO5's Slab module, produced a comparably satisfactory deformation result (maximum error of 20%), particularly in the eccentrically loaded side of the raft where the maximum contact pressure is observed.

However, the GEO5 software slab is not stable, giving varying deformation results for the same problem and occasionally generating an improbable deformation result and pattern as seen in figure 30.

As one could anticipate given the presence of eccentricity in the width direction ($e_y = 0$) in this model example, the deformation pattern is symmetrical. However, the Vlasov model (GEO5 Slab), which the researcher attempted to justify but failed to do so, directly contradicts this. Therefore, the researcher thinks that the facts in the paragraph above may provide a more comprehensive explanation.

With eccentricity introduced in the x-direction, the Worku's_AdJ model better captured moment redistribution across the plate, highlighting increased negative moments along the eccentric load path and corresponding positive moments toward the lightly loaded edge.This necessitates asymmetric top and bottom reinforcement design. Pseudo-coupled model, falling between the winkler and cFEM although better, showed a major deviation in the edge. Vlasov model substantially underestimate the maximum positive moment and again highly overestimate the negative moment (top fiber in tension). Only the Worku's_AdJ model followed the cFEM pattern closely, ensuring proper structural detailing.

Table 4: Deformation output for plate of size 12mx12mx1.1m loaded asymmetrically

Coordinate	Worku	Worku Modified	cFEM	Winkler	Pseudo Coupled	GEO-5	Worku Error (%)	Worku Modified Error (%)
-6	-33.41	-31.22	-30.13	-27.29	-30.14	-24.51	10.88	3.62
-5.5	-33.39	-31.53	-30.57	-29.08	-31.74	-25.47	9.21	3.11
-5	-33.44	-31.90	-31.14	-30.97	-33.45	-26.44	7.41	2.45
-4.5	-33.57	-32.34	-31.74	-32.89	-35.20	-27.43	5.76	1.91
-4	-33.75	-32.85	-32.37	-34.85	-36.99	-28.42	4.27	1.49
-3.5	-34.00	-33.42	-33.03	-36.85	-38.80	-29.42	2.94	1.19
-3	-34.30	-34.04	-33.70	-38.88	-40.65	-30.42	1.76	0.99
-2.5	-34.65	-34.71	-34.40	-40.95	-42.53	-31.43	0.71	0.90
-2	-35.04	-35.43	-35.11	-43.05	-44.44	-32.45	0.21	0.89
-1.5	-35.46	-36.18	-35.84	-45.19	-46.37	-33.47	1.05	0.95
-1	-35.90	-36.94	-36.57	-47.37	-48.33	-34.50	1.83	1.02
-0.5	-36.32	-37.69	-37.30	-49.58	-50.31	-35.55	2.64	1.04
0	-36.64	-38.35	-38.12	-51.91	-52.39	-36.60	3.89	0.59
0.5	-36.70	-38.74	-38.55	-53.89	-54.10	-37.63	4.81	0.50
1	-36.66	-39.05	-39.07	-55.98	-55.92	-38.62	6.17	0.06
1.5	-36.61	-39.34	-39.60	-58.12	-57.76	-39.63	7.55	0.64
2	-36.57	-39.66	-40.14	-60.31	-59.64	-40.65	8.89	1.19
2.5	-36.57	-40.02	-40.70	-62.56	-61.56	-41.68	10.16	1.68
3	-36.62	-40.43	-41.30	-64.86	-63.54	-42.72	11.33	2.09
3.5	-36.73	-40.91	-41.92	-67.23	-65.56	-43.76	12.40	2.41
4	-36.91	-41.47	-42.59	-69.67	-67.64	-44.82	13.35	2.64
4.5	-37.16	-42.11	-43.31	-72.17	-69.79	-45.89	14.19	2.77
5	-37.51	-42.85	-44.08	-74.74	-72.00	-46.97	14.91	2.80
5.5	-37.96	-43.70	-44.93	-77.38	-74.28	-48.06	15.50	2.73
6	-38.54	-44.68	-46.01	-80.24	-76.79	-49.20	16.22	2.90

Model Parameters		
L=	12	m
B=	12	m
h=	1.1	m
A_R=	1	Aspect Ratio
e_x=	1	m
e_Y=	0	m
E_p=	32	GPa
ν_p=	0.2	
E_S=	30	MPa
ν_s=	0.35	

Flexural Rigidity

$$D = \frac{E_p h^3{}_s}{12(1-{v_p}^2)}$$

D= 3,697.22 MNm

Relative Rigidity

$$R_s = \frac{8D(1-{v_s}^2)}{\pi L^2 B E_s}$$

Rs 0.159 Relative rigidity

Load Type= C3

Q= 5400 KN

Coordinate	Worku	Worku Modified	cFEM	Winkler	Pseudo Coupled	GEO-5	Worku Error (%)	Worku modified Error (%)
-6	-35.98	-37.58	-38.09	-53.76	-53.46	-36.06	5.56	1.34
-5.5	-35.68	-37.30	-37.77	-53.23	-53.01	-35.68	5.55	1.25
-5	-35.48	-37.11	-37.63	-52.85	-52.73	-35.47	5.72	1.37
-4.5	-35.36	-37.01	-37.54	-52.53	-52.49	-35.31	5.80	1.41
-4	-35.33	-36.99	-37.50	-52.26	-52.31	-35.21	5.78	1.35
-3.5	-35.36	-37.03	-37.49	-52.04	-52.18	-35.15	5.67	1.21
-3	-35.46	-37.14	-37.51	-51.87	-52.09	-35.13	5.48	1.00
-2.5	-35.61	-37.30	-37.56	-51.75	-52.05	-35.17	5.20	0.71
-2	-35.80	-37.50	-37.63	-51.68	-52.04	-35.25	4.86	0.36
-1.5	-36.03	-37.73	-37.72	-51.66	-52.07	-35.37	4.48	0.03
-1	-36.28	-37.98	-37.82	-51.68	-52.13	-35.53	4.08	0.42
-0.5	-36.51	-38.22	-37.93	-51.74	-52.21	-35.73	3.75	0.75
0	-36.64	-38.35	-38.12	-51.91	-52.39	-35.97	3.89	0.59
0.5	-36.51	-38.22	-37.93	-51.74	-52.21	-36.12	3.74	0.76
1	-36.28	-37.99	-37.82	-51.68	-52.13	-36.2	4.06	0.45
1.5	-36.03	-37.74	-37.71	-51.66	-52.07	-36.31	4.44	0.07
2	-35.80	-37.50	-37.62	-51.68	-52.04	-36.45	4.82	0.31
2.5	-35.61	-37.30	-37.54	-51.75	-52.05	-36.64	5.14	0.64
3	-35.46	-37.14	-37.48	-51.87	-52.09	-36.87	5.41	0.92
3.5	-35.36	-37.04	-37.46	-52.04	-52.18	-37.14	5.59	1.12
4	-35.33	-36.99	-37.46	-52.26	-52.31	-37.45	5.69	1.25
4.5	-35.37	-37.02	-37.50	-52.53	-52.49	-37.81	5.69	1.29
5	-35.48	-37.12	-37.58	-52.85	-52.73	-38.22	5.60	1.24
5.5	-35.68	-37.30	-37.72	-53.23	-53.01	-38.68	5.41	1.10
6	-35.98	-37.59	-38.03	-53.76	-53.46	-39.31	5.41	1.18

Calibration Factor		
chi, χ =	1.05	From Chart
chi_M, χ_M =	1.05	Modefied

Modulus of subgrade Reaction, K_s

$$k_s = \frac{E_s}{B(1-{v_s}^2)}$$

Ks= 2,849.00 KN/m^3

Pseudo Coupled

Ks,ave= 2,849.00 KN/m^3

A_1= 36 m^2

A_2= 45 m^2

A_3= 63 m^2

$$k_{s1} = k_{s,ave} \times \frac{A_1 + A_2 + A_3}{A_1 + 1.5A_2 + 2A_3}$$

Ks_1= 1,787.61 KN/m^3

Ks_2= 2,681.41 KN/m^3

Ks_3= 3,575.22 KN/m^3

3) Model_Case_3: Asymmetrically loaded (in both directions) square plate

This model uses a grid pattern and plate geometry identical to the previous one (except for plate thickness), but a different load configuration. This model was chosen because it most closely depicts a thin square plate loaded asymmetrically (with eccentricity in both directions) and resting on a soil that is moderately stiff/dense.

As with the prior model, the calibration factor doesn't need to be modified because the aspect ratio is 1. The MATLAB algorithm was tweaked, however, to take the asymmetry of the load in both directions into consideration.

Table 5: Dimension and Parameters used for plate of size 12mx12mx1.2m loaded asymmetrically

L(m)	B(m)	h(m)	E_P(GPa)	ν_p	Es(MPa)	ν_s	R_s	Load Case	e_x(m)	e_y(m)	χ_{chart}
12	12	1.2	32	0.2	40	0.31	0.1598	M3	17/95	17/95	1.1

Figure 35 shows a asymetrically loaded raft having a similar grid pattern (center to center of the load location) in both directions. The eccentricity which is due to the load magnitude is in both directions (in the x and y axis). Since the tensile strength of soil is zero an effert was made so as to avoid negative contact pressure. This was made by limiting the eccentricity and proportioning the foundation in such that:

$$e_x \le \frac{L}{6} \text{ or } e_y \le \frac{B}{6} \text{ where } e_x \text{ and } e_y \text{ are eccentricity in the length}(L) \text{ and width}(B) \text{ direction respectivelly}$$

Both the eccentricity in the length (e_x) and width direction (e_y) are 17/95 meters in the current model. This was designed to comply with the contact pressure requirements mentioned above.

Figure 36 shows the three dimenssional continuum finite element model (cFEM) of the current model as modeled and analysed by PLAXIS 3D. The model extent of the soil is 84 meter in the lateral and 48 meters in the vertical direction. A mesh size starting from 0.5 meter around

the plate and going to 5 meters at the edge boundary of the soil model is employed. A total of 60807 elements are generated. 3D solid section with 10-noded tetrahedral elements is used for the soil while the mat is modelled as a two-dimensional plate element with 6-noded triangles.

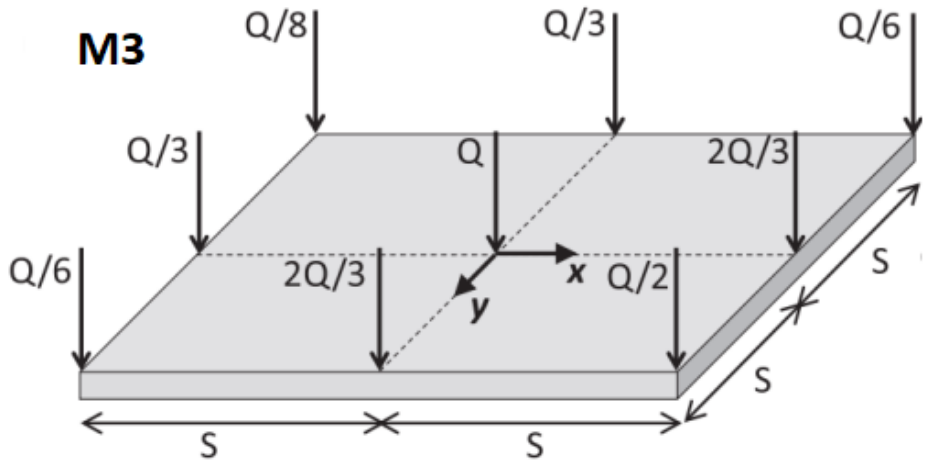

Figure 35: Load configuration used for a plate of size 12mx12mx1.2m

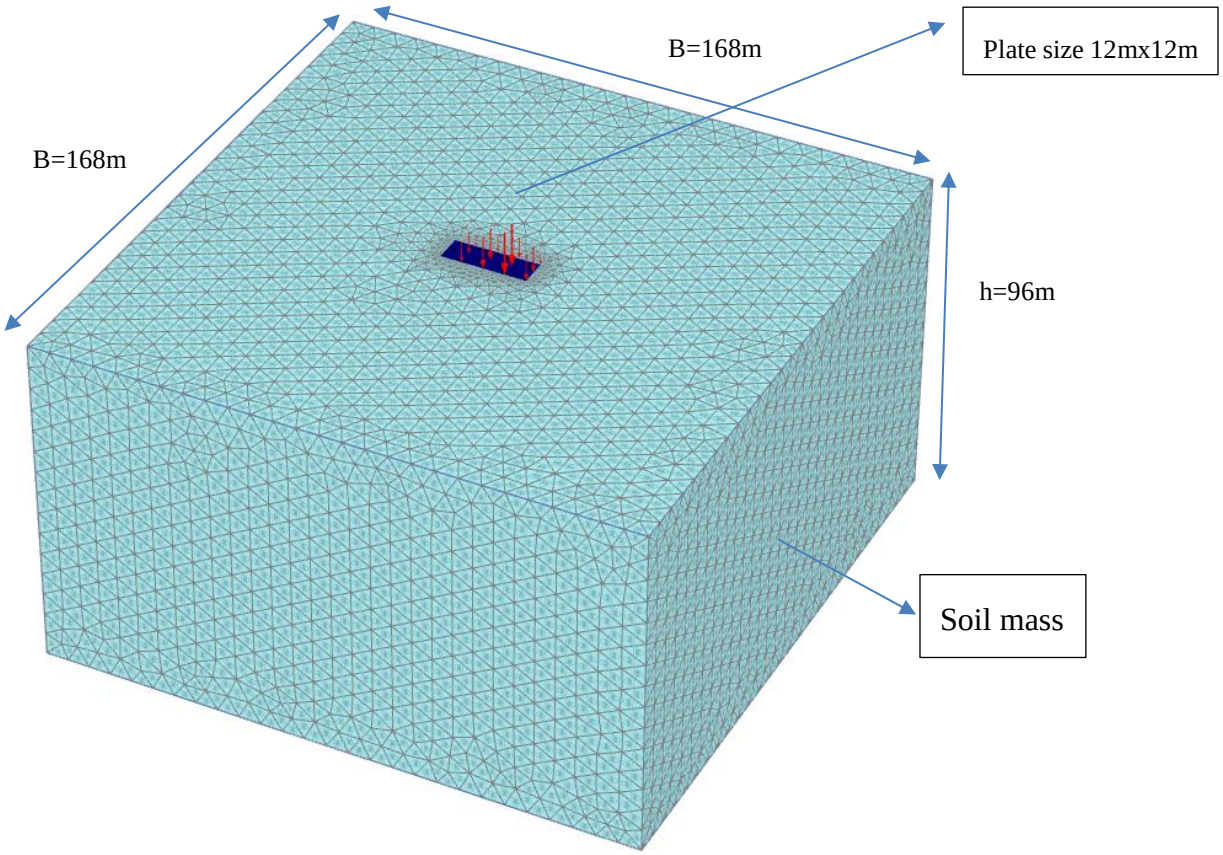

Figure 36: cFEM Model of size 84mx84mx48m

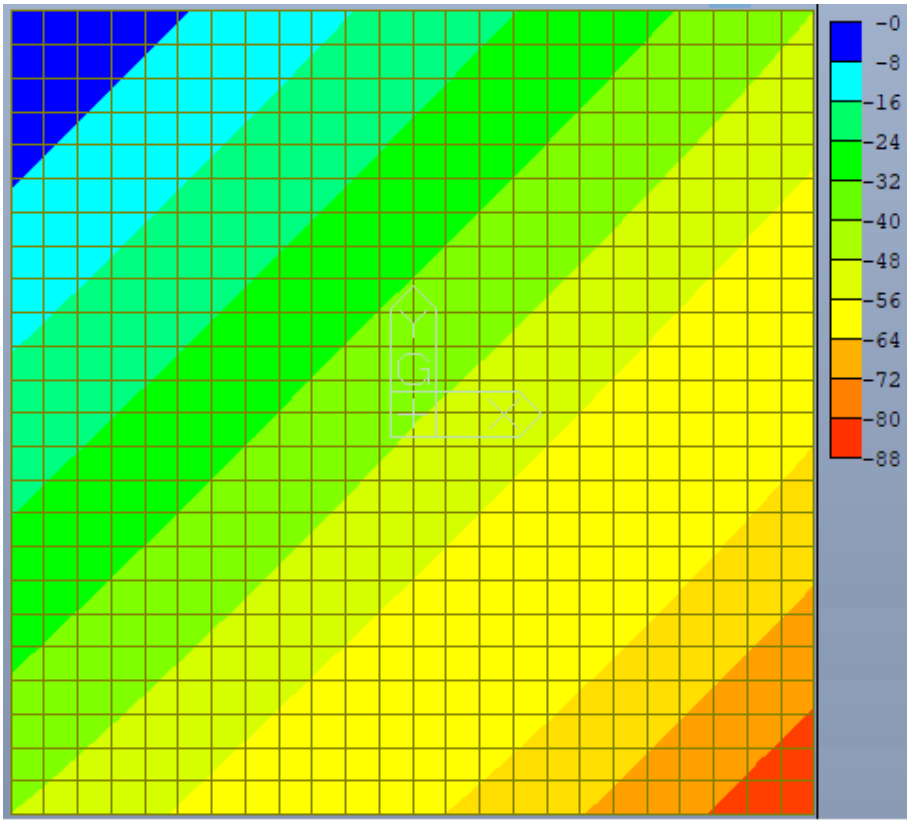

Figure 37: Winkler Model Output for asymmetrically loaded plate of size 12mx12mx1.2m

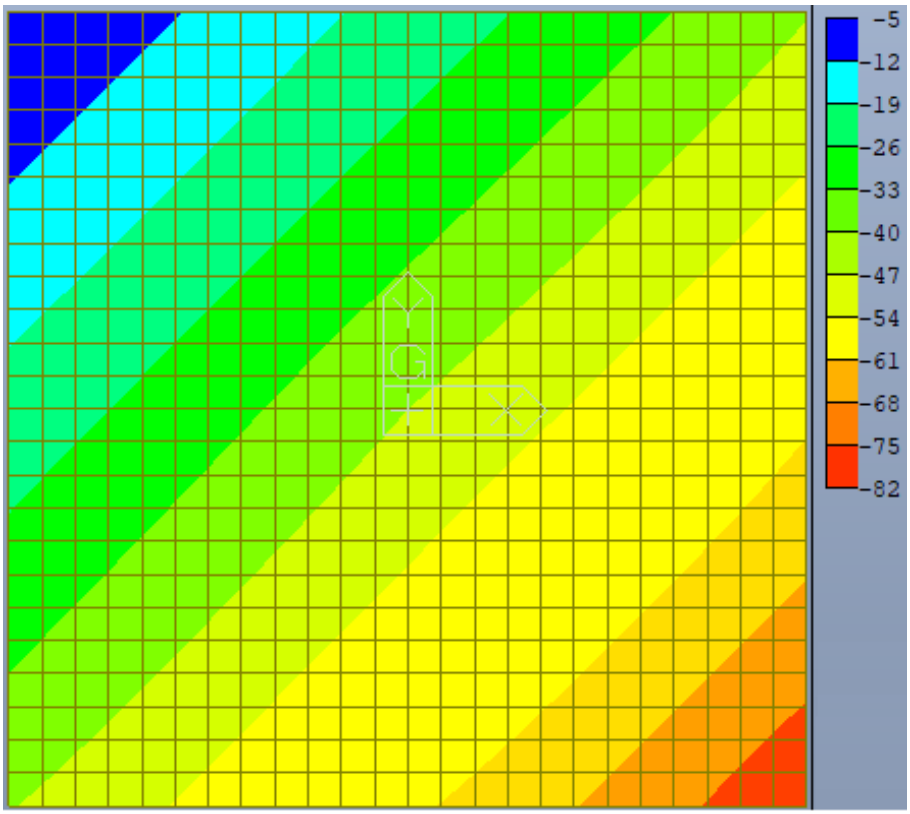

Figure 38: Pseudo Coupled Model Output for asymmetrically loaded plate of size 12mx12mx1.2m

Figure 37 and figure 38 respectively, display the vertical deformation produced by the Single Parameter Subgrade Model (Winkler) and the Pseudo Coupled Analysis Model. The commercial CSi SAFE software is used to simulate and analyze both. The Winkler model produced a vertical deformation output that ranged from 19.44 mm to 62.84 mm, whereas the Pseudo coupled technique produced a vertical deformation output that ranged from 21.80 mm to 60.03 mm.

The maximum error at the side of the eccentrically loaded area for the two single parameter subgrade models (Winkler and the Pseudo Coupled) was 43% and 41%, respectively, with the Winkler model giving the largest error.

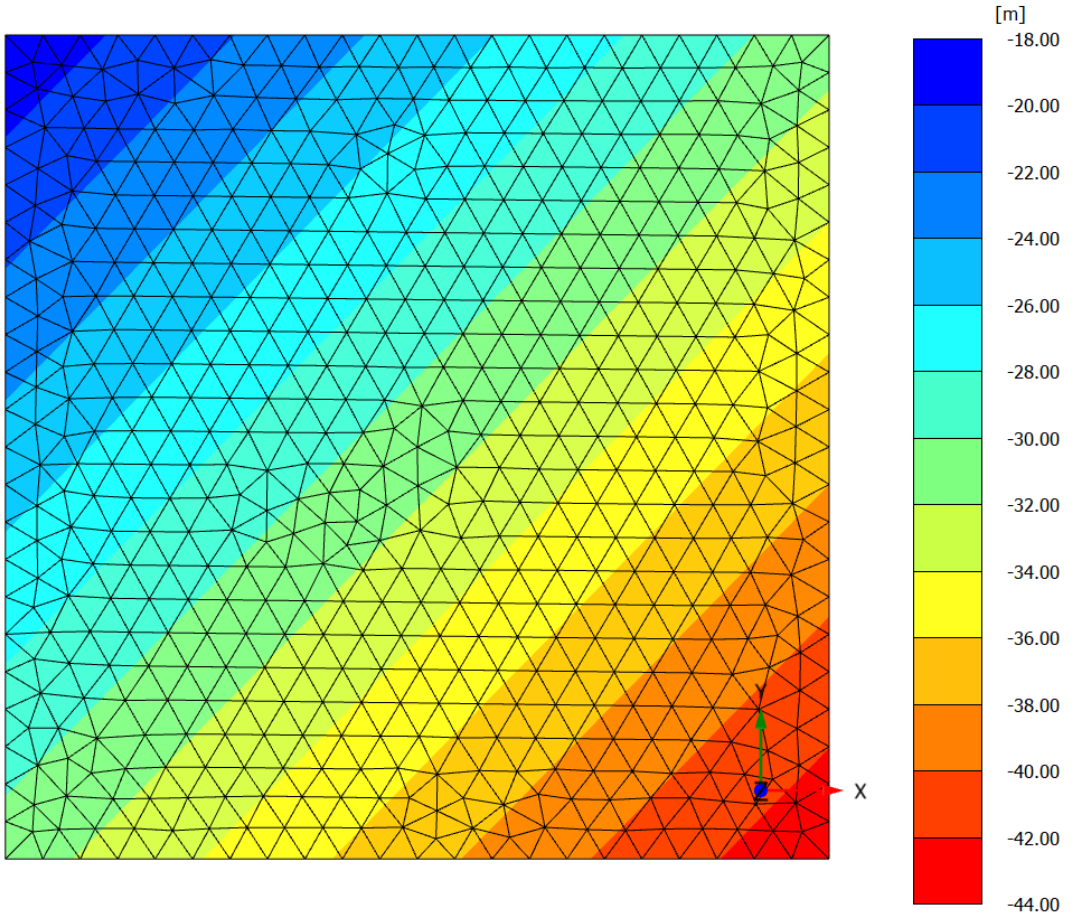

Figure 39: cFEM Model Output for asymmetrically loaded plate of size 12mx12mx1.2m

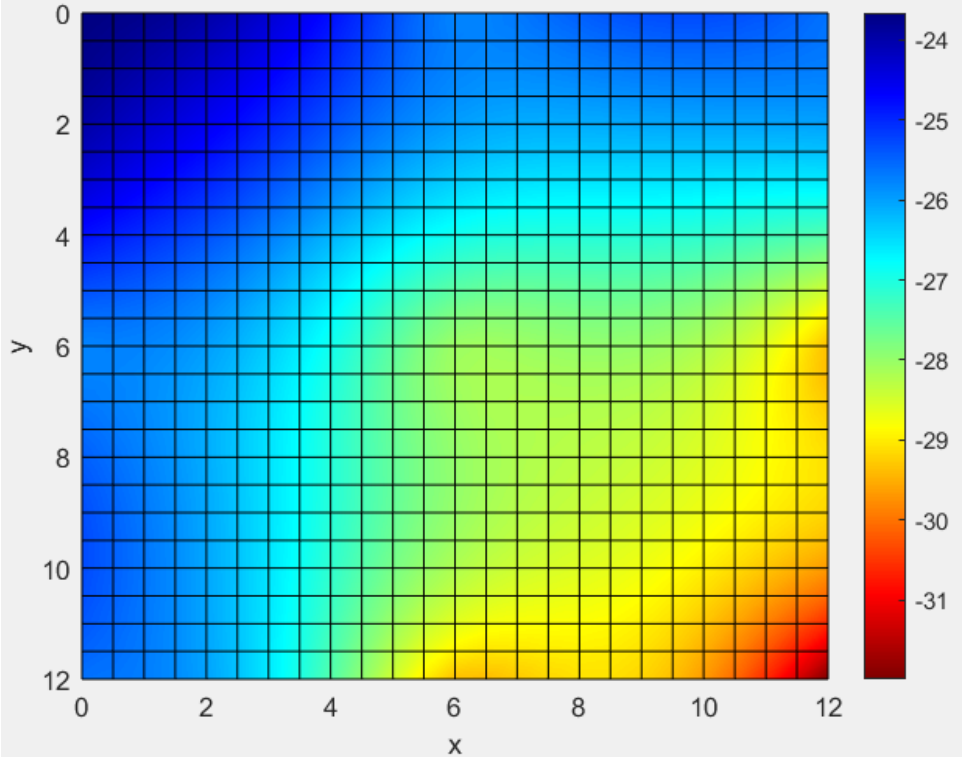

Figure 40: Worku's Model Output for asymmetrically loaded plate of size 12mx1mx1.2m

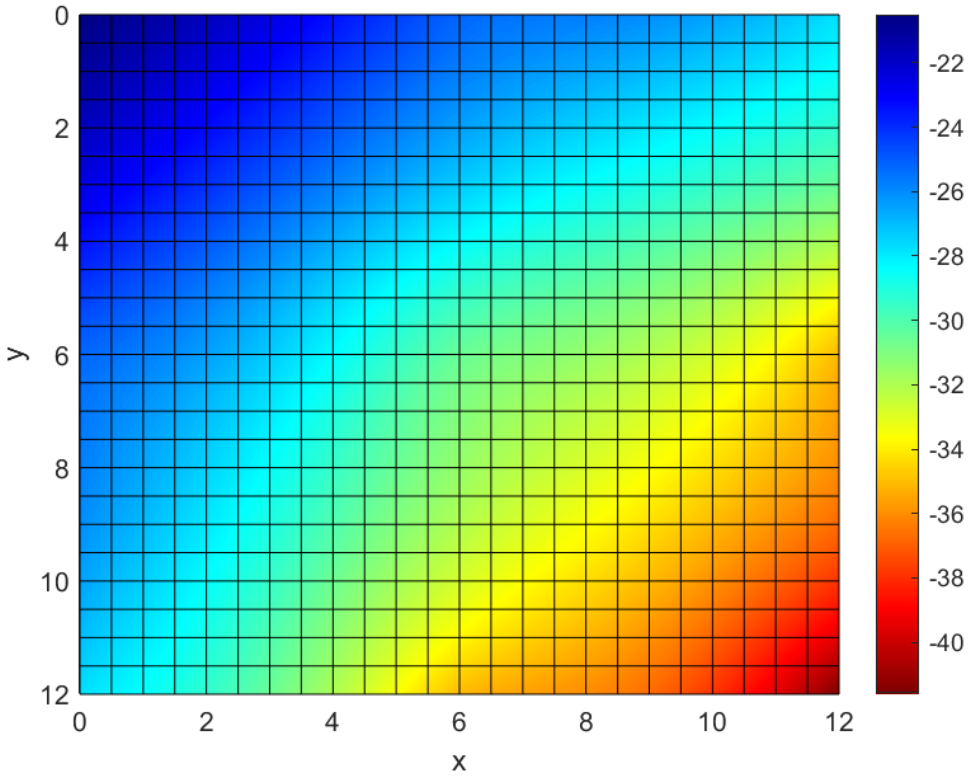

Figure 41: Worku's_AdJ Model Output for asymmetrically loaded plate of size 12mx12mx1.2m

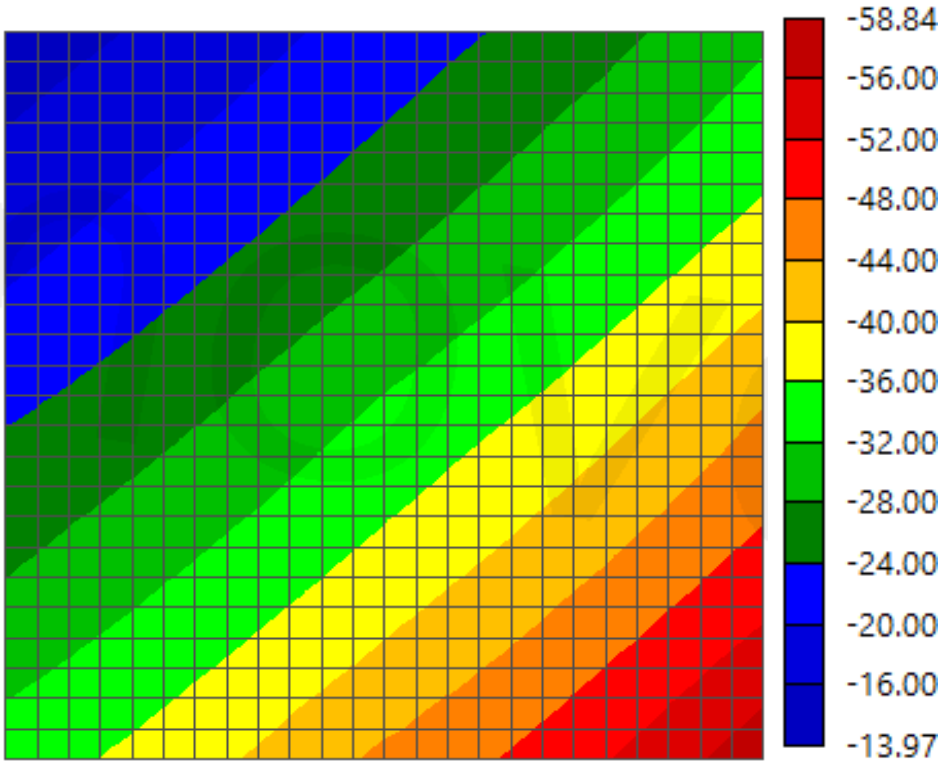

Figure 42: Geo5 Output for Asymmetrically loaded plate of size 12mx12mx1.2m

The maximum error in the deformation value produced by the original Worku's model and the adjusted Worku's model is 18% and 10%, respectively. As was stated before, one should employ the adjusted Worku's model rather than the original Worku model for problems that are asymmetrically loaded. Matter of fact, when compared to the other models (Winkler- resulted in maximum error of 43%, Pseudo coupled- resulted in maximum error of 41%, and Vlasov- resulted in maximum error of 35%), the Worku model (without modification) produced an acceptable result (maximum error of 18%).

The two-parameter subgrade model, which was studied using the GEO5's Slab module, produced a comparably satisfactory deformation result (maximum error of 25%) as seen in figure 40. Given the presence of eccentricity in both directions ($e_x = e_y = {}^{17}\!/_{95}\, meters$), it is expected that the deformation pattern shown by all models is satisfactory regardless of the values reported.

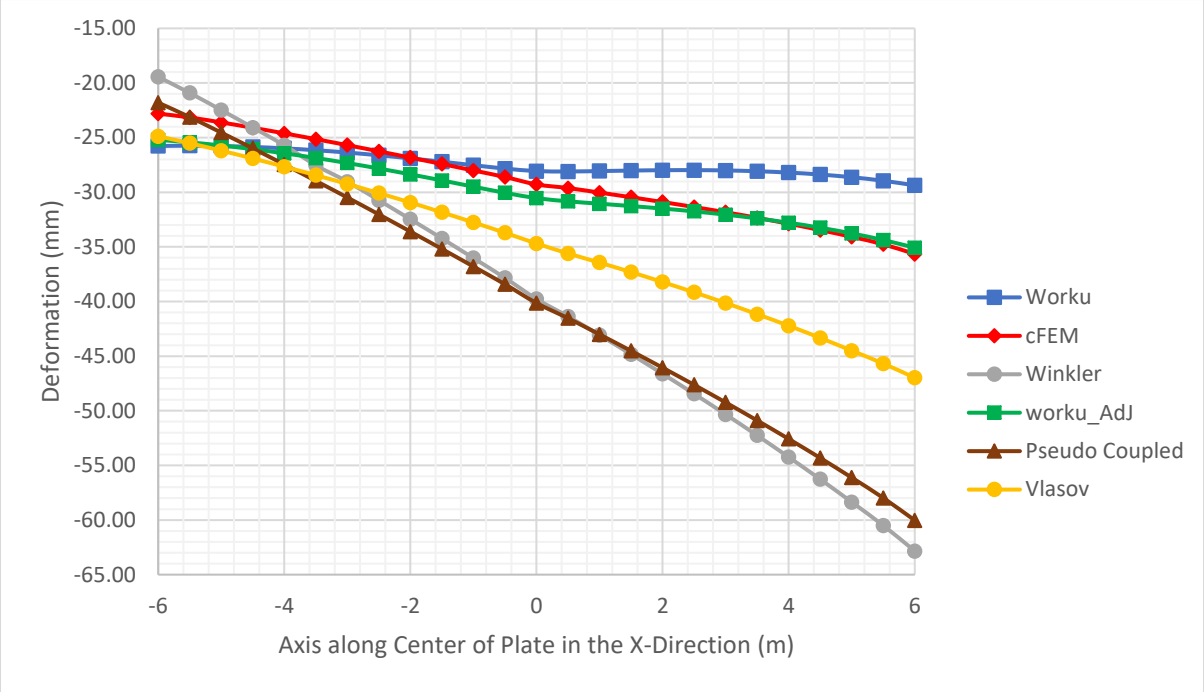

Figure 43: Vertical deformation along the center of the plate in the X- direction

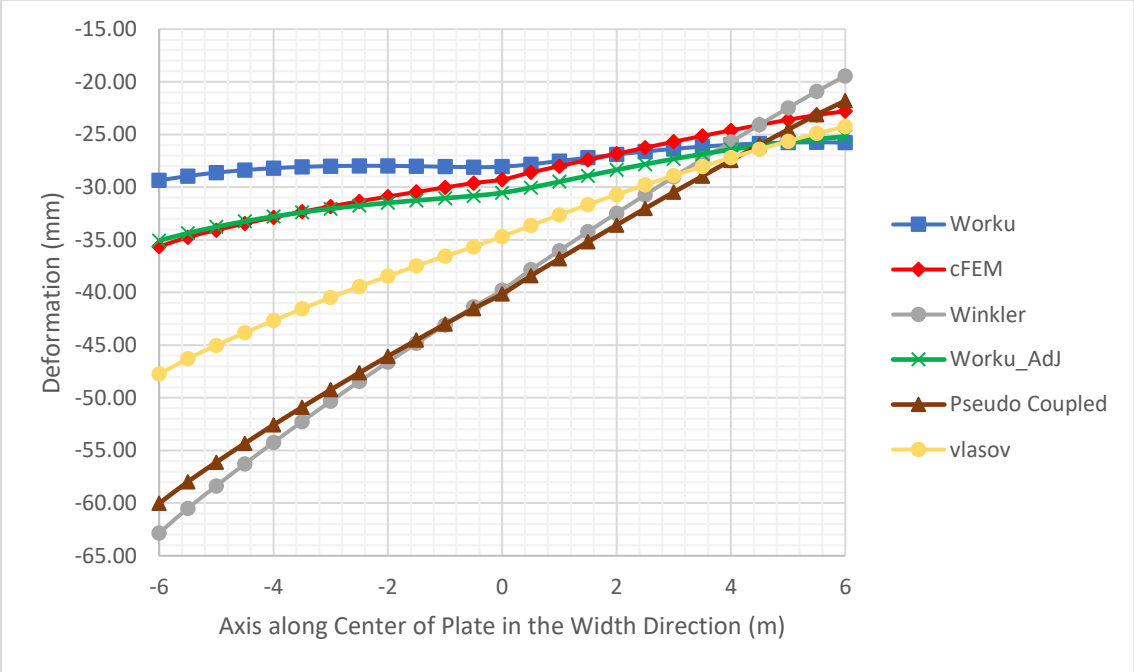

Figure 44: Vertical deformation along the center of the plate in the Y-direction

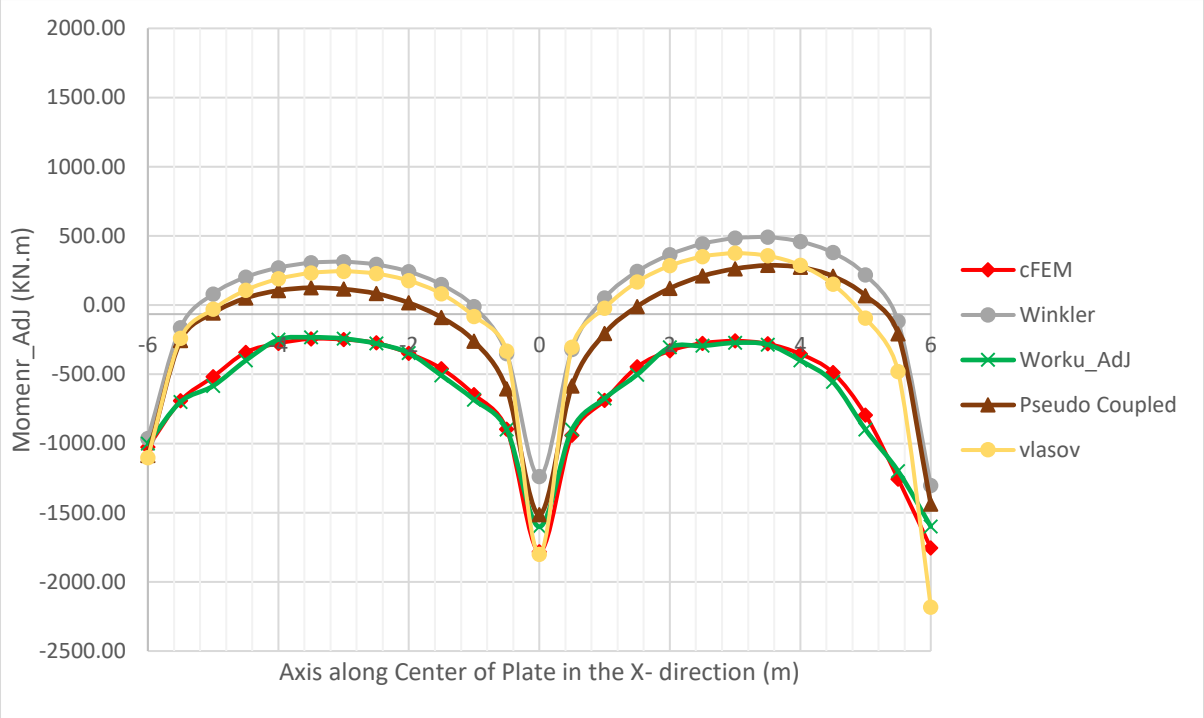

Figure 45: moment values along the center of the plate

This case involved asymmetry in both directions, and this was one of the most challenging configurations. Here too, the modified Worku's_AdJ model gave the best result in terms of moment distribution. The bottom tension was well captured at the center of the plate on the side where load was concentrated, and top tension appeared correctly on the opposite side, requiring reinforcement accordingly. cFEM results matched Worku's_AdJ model very closely, with less than 9% variation in the maximum moment. Winkler and Pseudo coupled tried to capture the bottom positive moment at the center but showed significant error when it comes to top negative moment. Vlasov exhibited inconsistencies near the corners and around the eccentric areas, with errors reaching up to 200%. However, it demonstrated a good correlation with the overall shape of the cFEM output. This suggests that with further calibration, the accuracy of the results could potentially be improved.

Table 6: Deformation output for plate of size 12mx12mx1.2m loaded asymmetrically

Coordinate	Worku	Worku Modefied	cFEM	Winkler	Pseudo Coupled	GEO-5	Worku Error (%)	Worku Modified Error (%)
-6	-25.76	-25.20	-22.80	-19.44	-21.80	-24.87	12.99	10.53
-5.5	-25.74	-25.43	-23.15	-20.91	-23.12	-25.51	11.18	9.86
-5	-25.77	-25.72	-23.61	-22.48	-24.54	-26.19	9.16	8.94
-4.5	-25.85	-26.05	-24.10	-24.08	-25.98	-26.91	7.29	8.13
-4	-25.98	-26.44	-24.61	-25.70	-27.46	-27.66	5.58	7.43
-3.5	-26.15	-26.86	-25.14	-27.53	-28.96	-28.44	4.04	6.85
-3	-26.37	-27.33	-25.69	-29.03	-30.48	-29.24	2.64	6.37
-2.5	-26.62	-27.83	-26.25	-30.74	-32.03	-30.08	1.39	6.00
-2	-26.90	-28.36	-26.83	-32.47	-33.60	-30.94	0.26	5.71
-1.5	-27.21	-28.92	-27.42	-34.23	-35.19	-31.84	0.76	5.49
-1	-27.52	-29.49	-28.01	-36.03	-36.80	-32.76	1.73	5.29
-0.5	-27.83	-30.05	-28.60	-37.84	-38.42	-33.71	2.71	5.05
0	-28.06	-30.54	-29.28	-39.77	-40.14	-34.69	4.17	4.28
0.5	-28.10	-30.83	-29.62	-41.37	-41.53	-35.60	5.12	4.10
1	-28.06	-31.05	-30.03	-43.08	-43.01	-36.44	6.56	3.39
1.5	-28.01	-31.26	-30.46	-44.83	-44.52	-37.31	8.02	2.65
2	-27.98	-31.49	-30.90	-46.62	-46.06	-38.22	9.43	1.94
2.5	-27.97	-31.75	-31.35	-48.45	-47.63	-39.16	10.77	1.28
3	-28.00	-32.05	-31.83	-50.33	-49.24	-40.14	12.03	0.68
3.5	-28.08	-32.39	-32.34	-52.26	-50.89	-41.16	13.18	0.16
4	-28.20	-32.79	-32.88	-54.24	-52.58	-42.22	14.24	0.28
4.5	-28.38	-33.25	-33.46	-56.27	-54.32	-43.33	15.18	0.64
5	-28.62	-33.77	-34.08	-58.36	-56.12	-44.50	16.01	0.92
5.5	-28.95	-34.37	-34.76	-60.50	-57.98	-45.68	16.73	1.12
6	-29.37	-35.07	-35.65	-62.84	-60.03	-46.98	17.63	1.63

Model Parameters

L=	12	m
B=	12	m
h=	1.2	m
A_R=	1	Aspect Ratio
e_x=	1.07	m
e_y=	1.07	m
E_p=	32	GPa
ν_p=	0.2	
E_S=	40	MPa
ν_s=	0.31	

Flexural Rigidity

$$D = \frac{E_p h^3{}_s}{12(1-\nu_p{}^2)}$$

D= 4,800.00 MNm

Relative Rigidity

$$R_s = \frac{8D(1-\nu_s{}^2)}{\pi L^2 B E_s}$$

Rs 0.160 Relative rigidity

Load Type= C7

Q= 5400 KN

Coordinate	Worku	Worku Modefied	cFEM	Winkler	Pseudo Coupled	GEO-5	Worku Error (%)	Worku Modified Error (%)
-6	-29.37	-35.07	-35.65	-62.84	-60.03	-47.75	17.63	1.62
-5.5	-28.95	-34.37	-34.76	-60.50	-57.98	-46.29	16.72	1.11
-5	-28.62	-33.77	-34.08	-58.36	-56.12	-45.03	16.01	0.91
-4.5	-28.38	-33.25	-33.46	-56.27	-54.32	-43.82	15.17	0.63
-4	-28.20	-32.79	-32.88	-54.24	-52.58	-42.67	14.23	0.27
-3.5	-28.08	-32.39	-32.34	-52.26	-50.89	-41.55	13.18	0.17
-3	-28.00	-32.05	-31.83	-50.33	-49.24	-40.48	12.02	0.69
-2.5	-27.97	-31.75	-31.35	-48.45	-47.63	-39.44	10.77	1.28
-2	-27.98	-31.49	-30.89	-46.62	-46.06	-38.45	9.43	1.94
-1.5	-28.01	-31.26	-30.46	-44.83	-44.52	-37.48	8.02	2.65
-1	-28.06	-31.05	-30.03	-43.08	-43.01	-36.55	6.56	3.39
-0.5	-28.10	-30.83	-29.62	-41.37	-41.53	-35.66	5.12	4.10
0	-28.06	-30.54	-29.28	-39.77	-40.14	-34.69	4.17	4.28
0.5	-27.83	-30.05	-28.60	-37.84	-38.42	-33.65	2.71	5.05
1	-27.52	-29.49	-28.01	-36.03	-36.80	-32.64	1.73	5.29
1.5	-27.21	-28.92	-27.42	-34.23	-35.19	-31.66	0.76	5.49
2	-26.90	-28.36	-26.83	-32.47	-33.60	-30.71	0.26	5.71
2.5	-26.62	-27.83	-26.25	-30.74	-32.03	-29.79	1.39	6.00
3	-26.37	-27.33	-25.69	-29.03	-30.48	-28.90	2.64	6.37
3.5	-26.15	-26.86	-25.14	-27.35	-28.96	-28.04	4.04	6.85
4	-25.98	-26.44	-24.61	-25.70	-27.46	-27.21	5.58	7.43
4.5	-25.85	-26.05	-24.10	-24.08	-25.98	-26.41	7.29	8.13
5	-25.77	-25.72	-23.61	-22.48	-24.54	-25.64	9.16	8.94
5.5	-25.74	-25.43	-23.15	-20.91	-23.12	-24.90	11.18	9.86
6	-25.76	-25.20	-22.80	-19.44	-21.80	-24.26	12.99	10.54

Calibration Factor

chi, χ =	1.1	From Chart
chi_M, χ_M =	1.1	Modefied

Modulus of subgrade Reaction, K_s

$$k_s = \frac{E_s}{B(1-\nu_s{}^2)}$$

Ks= 3,687.72 KN/m^3

Pseudo Coupled

Ks,ave=	3,687.72	KN/m^3
A_1=	36	m^2
A_2=	45	m^2
A_3=	63	m^2

$$k_{s1} = k_{s,ave} \times \frac{A_1 + A_2 + A_3}{A_1 + 1.5A_2 + 2A_3}$$

Ks_1=	2,313.87	KN/m^3
Ks_2=	3,470.80	KN/m^3
Ks_3=	4,627.73	KN/m^3

4) Model Case_4: Symetrically loaded rectangular (aspect ratio of 3) plate

This first non-square symmetrically loaded plate model example is chosen to test the effectiveness of the newly calibrated Kerr equivalent Pasternak model for the analysis of plates underlain by a very soft clay/loose sand.

Table 7: Dimension and Parameters used for plate of size 24mx8mx0.75m loaded symmetrically

L(m)	B(m)	h(m)	E_P(GPa)	ν_p	Es(MPa)	ν_s	R_s	Load Case	e_x(m)	e_y(m)	χ_{chart}	$\chi_{modified}$
24	8	0.75	32	0.2	20	0.42	0.0267	M4	0	0	1.25	2.35

Figure 46. shows a symetrically loaded raft having a similar grid pattern (center to center of the load location) in both directions.

The Worku's_AdJ model is most appropriate for this model case because the plate is not square (having an aspect ratio of 3), necessitating an adjustment to the calibration factor.

Because of this, the calibration factor, which was calculated from the chart using the relative rigidity of the plate and the soil stiffness, is 1.25 whereas the updated value is 2.35. The MATLAB program developed for the Worku's_AdJ model also incorporates this change to the edge stiffness. As a result, the deflection output from the Worku's model and the Worku's_AdJ model will obviously differ, as demonstrated in figure 51 and Figure 52.

Figure 47 shows the three dimenssional continuum finite element model (cFEM) of the current model as modeled and analysed on PLAXIS 3D. The model extent of the soil is 168 meter in the lateral and 96 meters in the vertical direction. A mesh size starting from 0.5 meter around the plate and going to 5 meters at the edge boundary of the soil model is employed. A total of 80,016 elements are generated. 3D solid section with 10-noded tetrahedral elements is used for the soil while the mat is modelled as a two-dimensional plate element with 6-noded triangles.

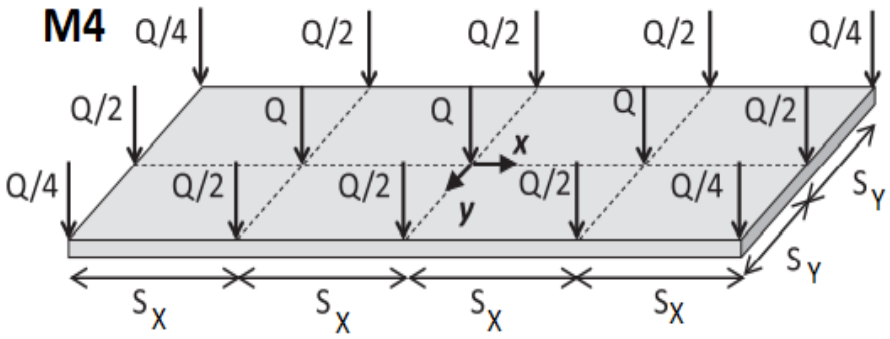

Figure 46: Load configuration used for a plate of size 24mx8mx0.75m

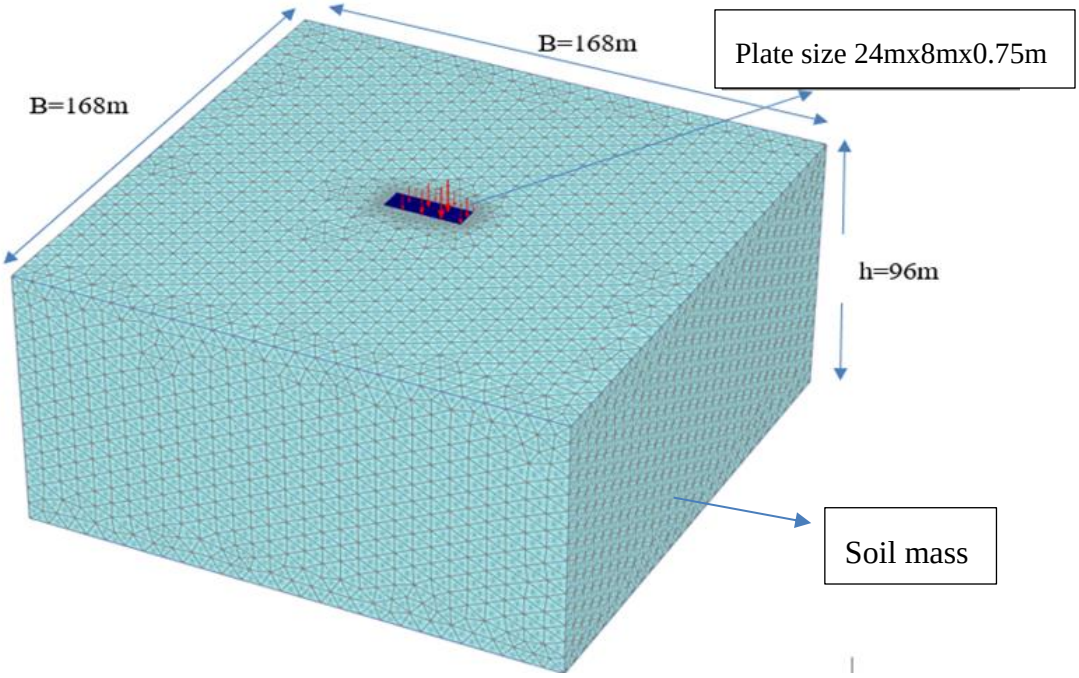

Figure 47: cFEM size of 168mx168mx96m

Figure 48 and Figure 49, respectively, display the vertical deformation produced by the Single Parameter Subgrade Model (Winkler) and the Pseudo Coupled Analysis Model. The commercial CSi SAFE software is used to simulate and analyze both. The Winkler model produced a vertical deformation output that ranged from 69.56 mm to 85.64 mm, whereas the

Pseudo coupled technique produced a vertical deformation output that ranged from 70.00 mm to 79.35 mm.

The maximum error at the side of the eccentrically loaded area for the two single parameter subgrade models (Winkler and the Pseudo Coupled) was 31% and 22%, respectively, with the Winkler model giving the largest error.

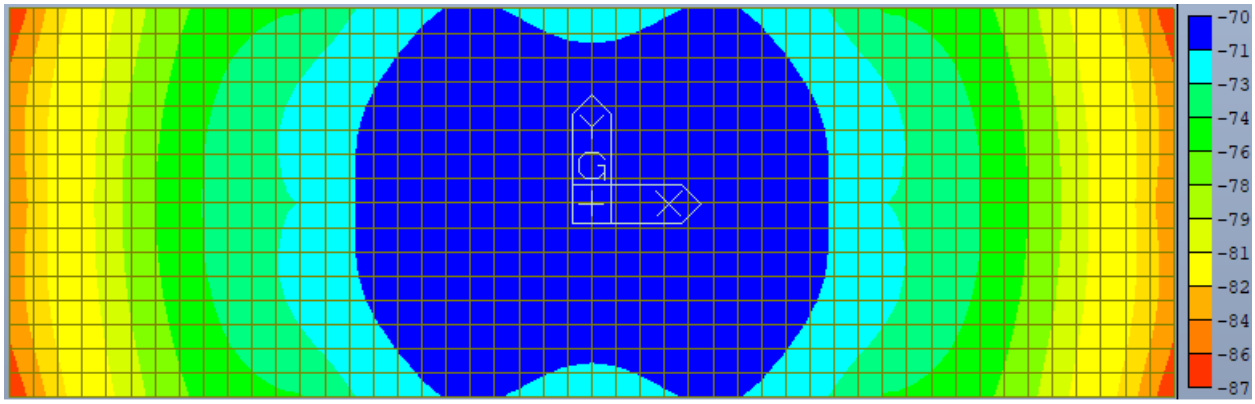

Figure 48: Winkler Model Output for symmetrically loaded plate of size 24mx8mx0.75m

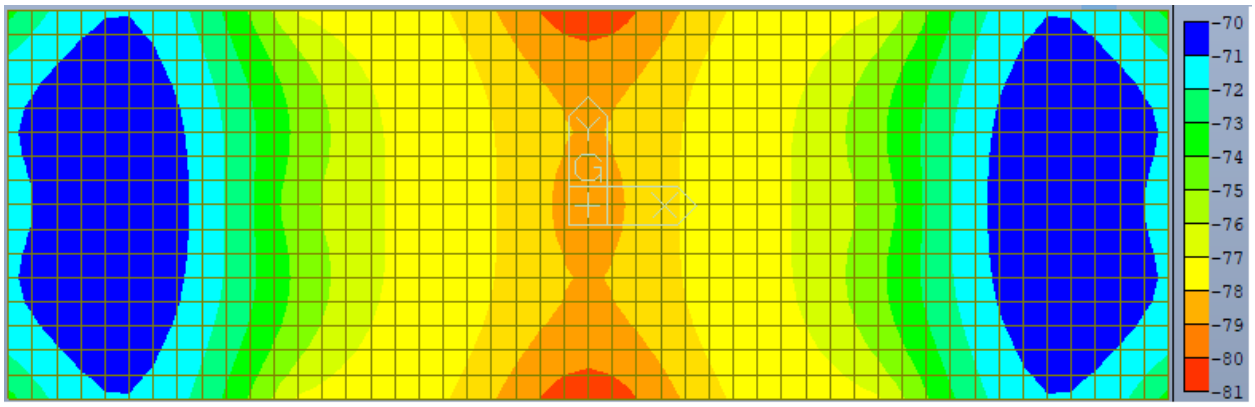

Figure 49: Pseudo Coupled Model Output for symmetrically loaded plate of size 24mx8mx0.75m

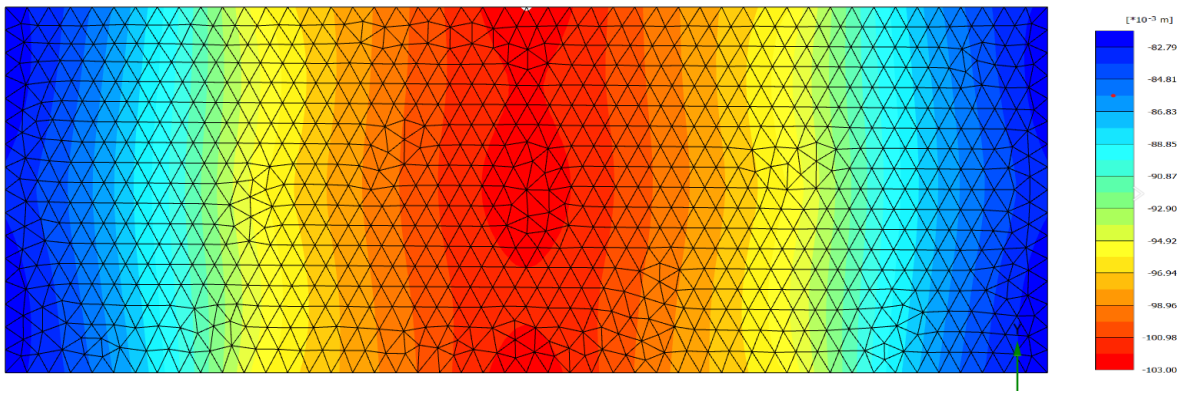

Figure 50: cFEM Model Output for symmetrically loaded plate of size 24mx8mx0.75m

The maximum error in the deformation value produced by the original Worku model and the adjusted Worku's model is 25% and 9%, respectively. As was stated before, one should employ Worku's_AdJ model rather than the original Worku model for problems that are asymmetrically loaded. Matter of fact, when compared to the other models (Winkler-resulted in maximum error of 31%, Pseudo coupled- resulted in maximum error of 22%, and Vlasov-resulted in maximum error of 27%), the Worku model (without adjustment) produced an acceptable result (maximum error of 25%).

The two-parameter subgrade model, which was studied using the GEO5's Slab module, produced a comparably satisfactory deformation result (maximum error of 25%) as seen in figure 53.

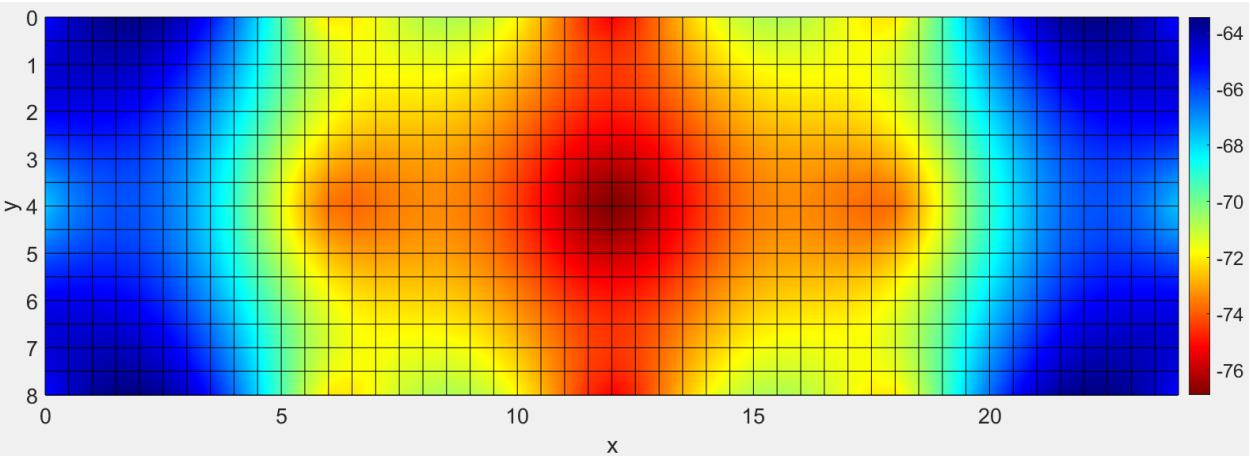

Figure 51: Worku Model Output for symmetrically loaded plate of size 24mx8mx0.75m

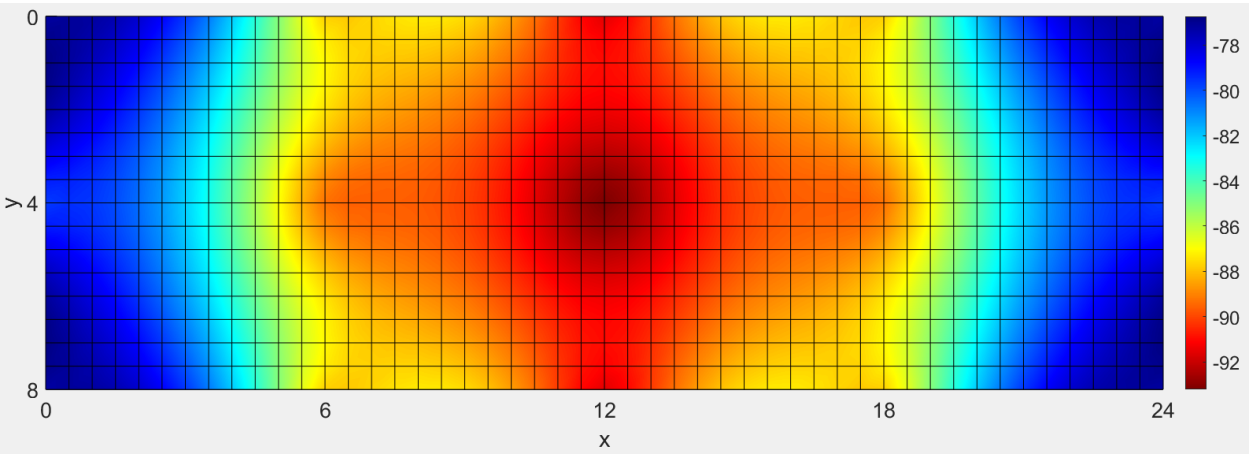

Figure 52: Worku's_AdJ Model Output for symmetrically loaded plate of size 24mx8mx0.75m

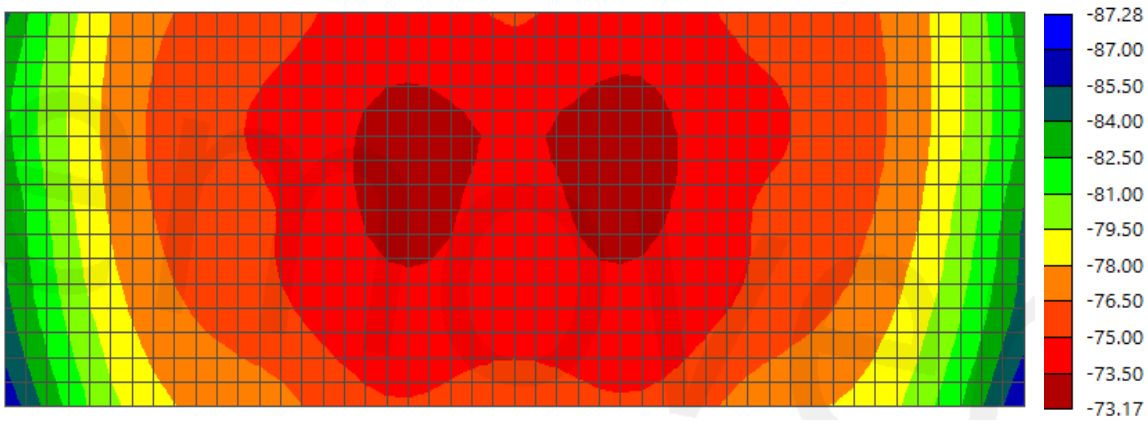

Figure 53: GEO5 Output for symmetrically loaded plate of size 24mx8mx0.75m

Regardless of the values stipulated, it is believed that the deformation pattern displayed by all except the Winkler and Vlasov models is satisfactory given the absence of eccentricity in both directions ($e_x = e_y = 0$). In contrast to the other mechanical models, the Winkler and Vlasov models both exhibited an inverted bowl form, which is ascribed to the lack of an additional edge stiffener at the plate's edge.

The aspect ratio effect had to be addressed by tweaking the calibration values owing to the non-square plate shape. After modification, it was assigned a value of 2.35 instead of the initial calibration factor, which was almost 1.25 as read from the chart.

As seen in Figure 50 and Figure 52, despite the fact that the plate used for the analysis had an aspect ratio of 3, using the adjusted calibration value stated above along with the Kerr equivalent Pasternak model of Worku written in MATLAB algorithm produced an acceptable vertical deformation result (an error of less than 10%) when compared to the cFEM.

Therefore, this model can be used to analyze and design a rectangular raft foundation.

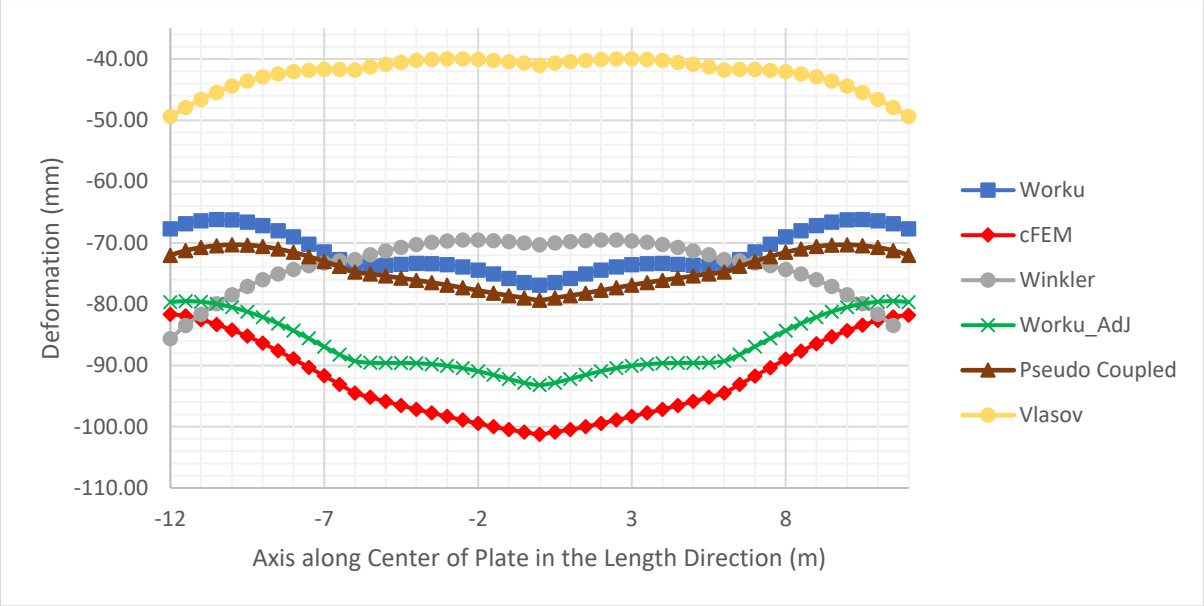

Figure 54: Vertical deformation along the center of the plate in the Length direction

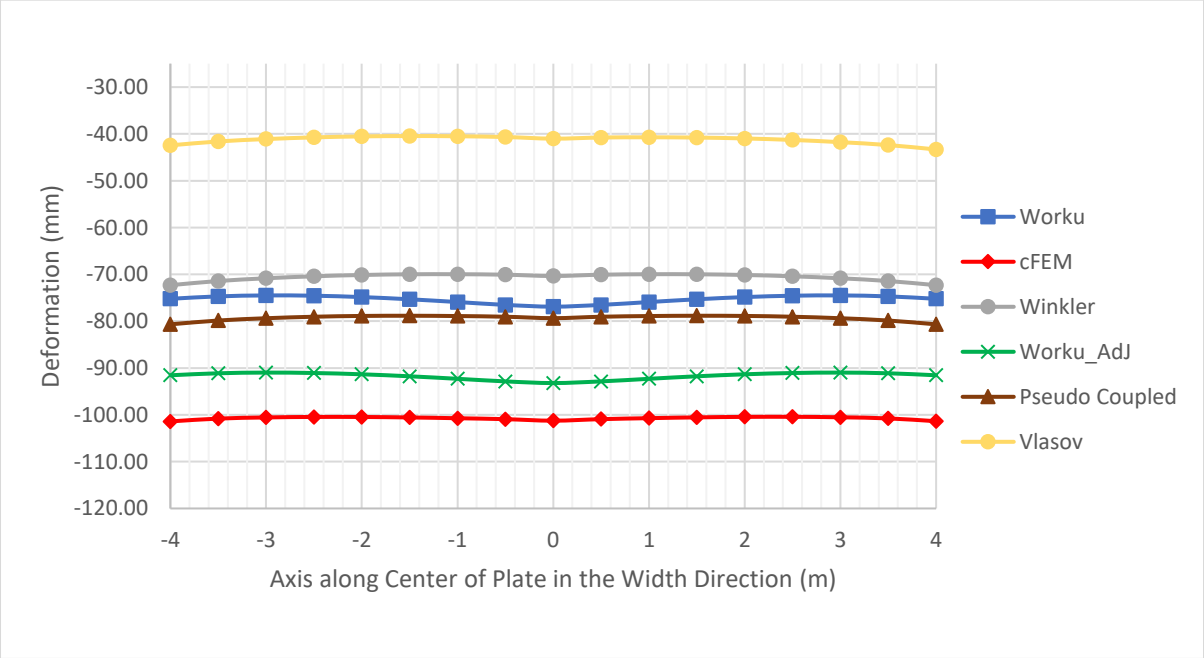

Figure 55: Vertical deformation along the center of the plate in the Width direction

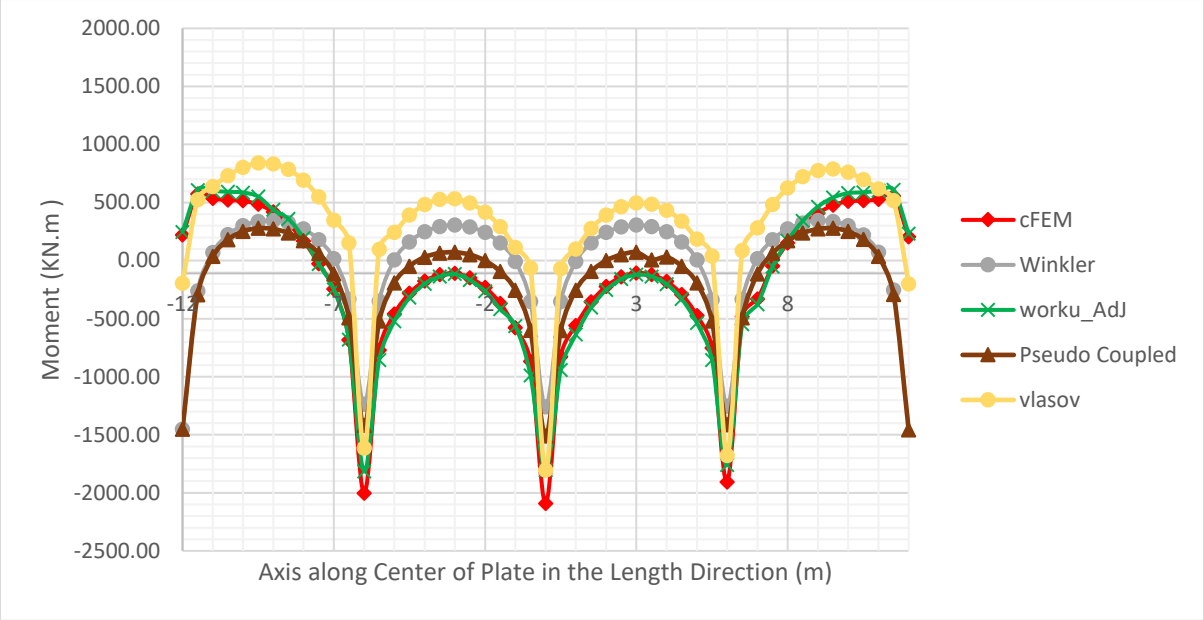

Figure 56: moment values along the center of the plate in the length direction

The bending moment results obtained using Worku's_AdJ model demonstrate enhanced agreement with the continuum finite element analysis performed in PLAXIS 3D. The maximum discrepancy in moment values within most of the span is less than 5 % and at the point of loading is 13.8 %, indicating that Worku's two-parameter foundation model reliably captures both the magnitude and distribution of bending moments in rectangular raft foundations.

Table 8: Deformation output for plate of size 24mx8mx0.75m loaded symmetrically

Coordinate	Worku	Worku Modefied	cFEM	Winkler	Pseudo Coupled	GEO-5	Worku Error (%)	Worku Modified Error (%)
-12	-67.70	-79.65	-81.64	-85.64	-72.03	-49.39	17.08	2.43
-11.5	-66.88	-79.50	-81.92	-83.49	-71.25	-47.92	18.36	2.96
-11	-66.39	-79.62	-82.55	-81.65	-70.77	-46.61	19.58	3.55
-10.5	-66.18	-79.96	-83.32	-79.96	-70.46	-45.45	20.56	4.02
-10	-66.25	-80.51	-84.22	-78.46	-70.32	-44.44	21.33	4.40
-9.5	-66.59	-81.23	-85.24	-77.14	-70.37	-43.60	21.88	4.71
-9	-67.19	-82.12	-86.38	-76.02	-70.60	-42.93	22.22	4.93
-8.5	-68.02	-83.16	-87.63	-75.08	-71.00	-42.42	22.38	5.10
-8	-69.04	-84.33	-88.95	-74.33	-71.55	-42.06	22.38	5.19
-7.5	-70.23	-85.61	-90.32	-73.74	-72.24	-41.84	22.25	5.22
-7	-71.50	-86.94	-91.71	-73.29	-73.02	-41.72	22.04	5.21
-6.5	-72.74	-88.24	-93.08	-72.93	-73.85	-41.69	21.86	5.20
-6	-73.69	-89.29	-94.49	-72.75	-74.79	-41.80	22.02	5.51
-5.5	-73.83	-89.58	-95.18	-71.95	-75.06	-41.27	22.43	5.89
-5	-73.68	-89.60	-95.89	-71.31	-75.41	-40.87	23.16	6.56
-4.5	-73.50	-89.60	-96.55	-70.75	-75.75	-40.53	23.87	7.19
-4	-73.38	-89.65	-97.17	-70.28	-76.11	-40.26	24.48	7.73
-3.5	-73.39	-89.80	-97.76	-69.93	-76.48	-40.07	24.93	8.15
-3	-73.57	-90.06	-98.35	-69.69	-76.89	-39.98	25.19	8.43
-2.5	-73.92	-90.45	-98.92	-69.57	-77.32	-39.97	25.28	8.57
-2	-74.43	-90.95	-99.48	-69.56	-77.76	-40.06	25.18	8.58
-1.5	-75.08	-91.55	-100.01	-69.65	-78.20	-40.22	24.92	8.46
-1	-75.80	-92.20	-100.48	-69.82	-78.61	-40.43	24.56	8.24
-0.5	-76.49	-92.84	-100.87	-70.03	-78.98	-40.67	24.16	7.96
0	-76.90	-93.21	-101.25	-70.35	-79.35	-41.01	24.05	7.94
0.5	-76.49	-92.84	-100.86	-70.03	-78.98	-40.67	24.16	7.96
1	-75.80	-92.20	-100.48	-69.82	-78.61	-40.43	24.56	8.23
1.5	-75.08	-91.55	-100.00	-69.65	-78.20	-40.22	24.92	8.45
2	-74.43	-90.95	-99.48	-69.56	-77.76	-40.06	25.17	8.57
2.5	-73.92	-90.45	-98.92	-69.57	-77.32	-39.97	25.27	8.56
3	-73.57	-90.06	-98.34	-69.69	-76.89	-39.98	25.19	8.42
3.5	-73.39	-89.80	-97.76	-69.93	-76.48	-40.07	24.92	8.14
4	-73.38	-89.65	-97.16	-70.28	-76.11	-40.26	24.48	7.73
4.5	-73.50	-89.60	-96.55	-70.75	-75.75	-40.53	23.87	7.19
5	-73.68	-89.60	-95.90	-71.31	-75.41	-40.87	23.17	6.56
5.5	-73.83	-89.58	-95.19	-71.95	-75.06	-41.27	22.44	5.90
6	-73.69	-89.29	-94.51	-72.75	-74.79	-41.80	22.03	5.52
6.5	-72.74	-88.24	-93.11	-72.93	-73.85	-41.69	21.88	5.22
7	-71.50	-86.94	-91.75	-73.29	-73.02	-41.72	22.07	5.24
7.5	-70.23	-85.61	-90.37	-73.74	-72.24	-41.84	22.28	5.27
8	-69.04	-84.33	-89.00	-74.33	-71.55	-42.06	22.42	5.25
8.5	-68.02	-83.16	-87.69	-75.08	-71.00	-42.42	22.44	5.17
9	-67.19	-82.12	-86.46	-76.02	-70.60	-42.93	22.29	5.02
9.5	-66.59	-81.23	-85.33	-77.14	-70.37	-43.60	21.96	4.81
10	-66.25	-80.51	-84.32	-78.46	-70.32	-44.44	21.43	4.52
10.5	-66.18	-79.96	-83.43	-79.96	-70.46	-45.45	20.68	4.16
11	-66.39	-79.62	-82.68	-81.65	-70.77	-46.61	19.71	3.71
11.5	-66.88	-79.50	-82.07	-83.49	-71.25	-47.92	18.50	3.13
12	-67.70	-79.65	-81.80	-85.64	-72.03	-49.39	17.24	2.62

Model Parameters

L=	24	m
B=	8	m
h=	0.75	m
A_R=	3	Aspect Ratio
e_x=	0	m
e_y=	0	m
E_p=	32	GPa
v_p=	0.2	
E_S=	20	MPa
v_s=	0.42	

Flexural Rigidity

$$D = \frac{E_p h^3{}_s}{12(1 - v_p{}^2)}$$

D= 1,171.88 MNm

Relative Rigidity

$$R_s = \frac{8D(1 - v_s{}^2)}{\pi L^2 B E_s}$$

Rs 0.027 Relative rigidity

Load Type= C8

Q= 5400 KN

Calibration Factor

chi, χ = 1.25 From Chart

chi_M, χ_M = 2.35 Modefied

Modulus of subgrade Reaction, K_s

$$k_s = \frac{E_s}{B(1 - v_s{}^2)}$$

Ks= 3,035.45 KN/m^3

Pseudo Coupled

Ks,ave= 3,035.45 KN/m^3

A_1= 48 m^2

A_2= 60 m^2

A_3= 84 m^2

$$k_{s1} = k_{s,ave} \times \frac{A_1 + A_2 + A_3}{A_1 + 1.5A_2 + 2A_3}$$

Ks_1= 1,904.60 KN/m^3

Ks_2= 2,856.90 KN/m^3

Ks_3= 3,809.20 KN/m^3

Coordinate	Worku	Worku Modefied	cFEM	Winkler	Pseudo Coupled	GEO-5	Worku Error (%)	Worku Modified Error (%)
-4	-75.22	-91.56	-101.41	-72.31	-80.67	-42.44	25.83	9.72
-3.5	-74.70	-91.13	-100.80	-71.42	-79.86	-41.61	25.90	9.60
-3	-74.50	-90.98	-100.56	-70.84	-79.37	-41.10	25.92	9.53
-2.5	-74.56	-91.07	-100.45	-70.41	-79.05	-40.74	25.78	9.34
-2	-74.85	-91.35	-100.46	-70.13	-78.88	-40.53	25.49	9.07
-1.5	-75.32	-91.77	-100.56	-69.98	-78.84	-40.45	25.10	8.74
-1	-75.91	-92.30	-100.73	-69.97	-78.90	-40.50	24.64	8.36
-0.5	-76.52	-92.86	-100.93	-70.07	-79.05	-40.66	24.18	7.99
0	-76.90	-93.21	-101.25	-70.35	-79.35	-41.01	24.05	7.94
0.5	-76.52	-92.86	-100.92	-70.07	-79.05	-40.77	24.18	7.99
1	-75.91	-92.30	-100.72	-69.97	-78.90	-40.72	24.63	8.35
1.5	-75.32	-91.77	-100.55	-69.98	-78.84	-40.78	25.09	8.73
2	-74.85	-91.35	-100.44	-70.13	-78.88	-40.97	25.48	9.06
2.5	-74.56	-91.07	-100.43	-70.41	-79.05	-41.29	25.76	9.32
3	-74.50	-90.98	-100.53	-70.84	-79.37	-41.76	25.89	9.50
3.5	-74.70	-91.13	-100.76	-71.42	-79.86	-42.38	25.87	9.57
4	-75.22	-91.56	-101.36	-72.31	-80.67	-43.32	25.79	9.68

5) Model Case_5: Asymetrically loaded (one direction) rectangular raft

This load configuration, designated M5, represents a rectangular raft foundation having an aspect ratio of 3 and loaded asymmetrically in one direction ($e_x = 3 \& e_y = 0$). The relevant data are given in table 9. The relative rigidity (R_s) determined according to equation (12) is also included in the eighth column.

The value of the calibration is obtained from Figure 13 by entering with the relative rigidity and soil stiffness. However, for the Worku'AdJ model this value should be modified as the raft is not a square.

Thus, the original calibration value, which was determined from the calibration chart using the relative rigidity of the plate and the soil's stiffness, is 1.9, whereas the modified value is 3.0. Therefore, Worku's model uses the original calibration value of 1.9 while Worku's AdJ model uses the value of 3.0.

Table 9: Dimension and Parameters used for plate of size 24mx8mx0.8m loaded asymmetrically

L(m)	B(m)	h(m)	E_P(GPa)	ν_p	Es(MPa)	ν_s	R_s	Load Case	e_x(m)	e_y(m)	χ_{chart}	$\chi_{modified}$
24	8	0.8	32	0.2	60	0.26	0.0122	M5	3	0	1.9	3.0

The raft geometry with the load configuration used for this scenario is shown in figure 57.

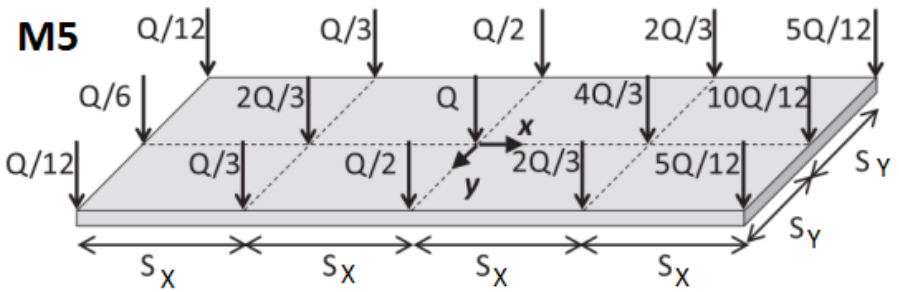

Figure 57: Load configuration used for a plate of size 24mx8mx0.8m

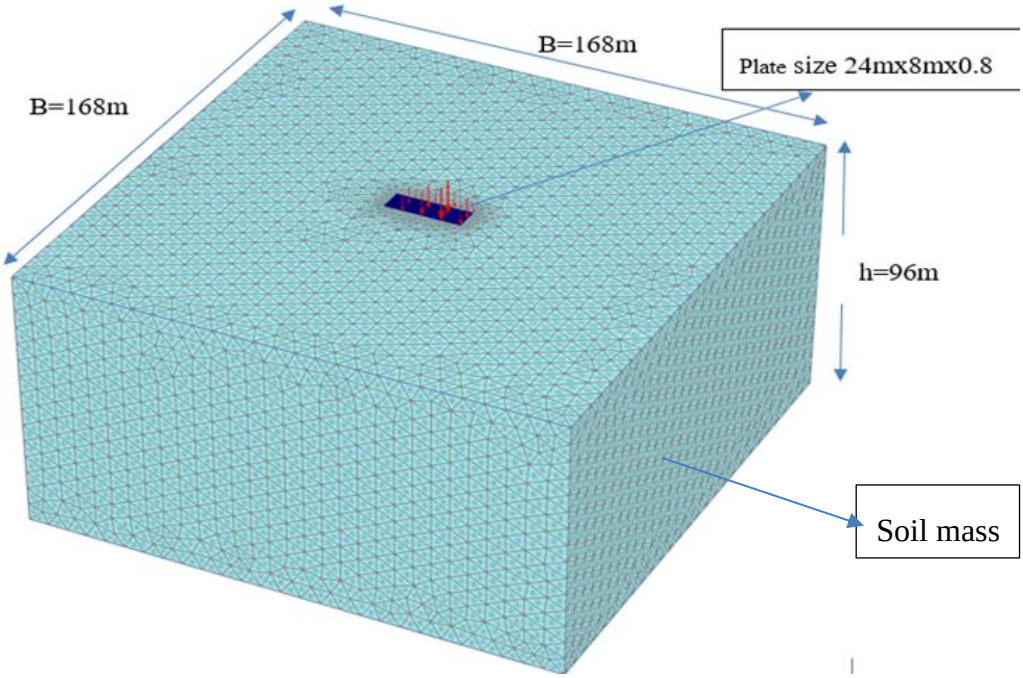

Figure 58: cFEM size of 168mx168mx96m

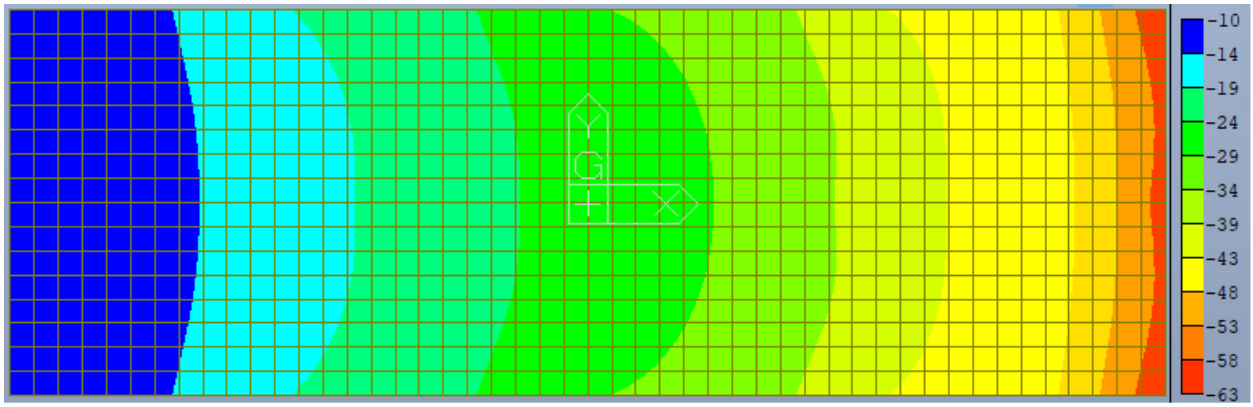

Figure 59: Winkler Model Output for unsymmetrically loaded plate of size 24mx8mx0.8m

Figure 59 and 60, respectively, display the vertical deformation produced by the Single Parameter Subgrade Model (Winkler) and the Pseudo Coupled Analysis Model. The commercial CSi SAFE software is used to simulate and analyze both. The Winkler model produced a vertical deformation output that ranged from 9.82 mm to 60.24 mm, whereas

Pseudo coupled technique produced a vertical deformation output that ranged from 6.98 mm to 49.78 mm.

The maximum error at the side of the eccentrically loaded area for the two single parameter subgrade models (Winkler and the Pseudo Coupled) was 45% and 61%, respectively, with the Pseudo coupled model giving the largest error.

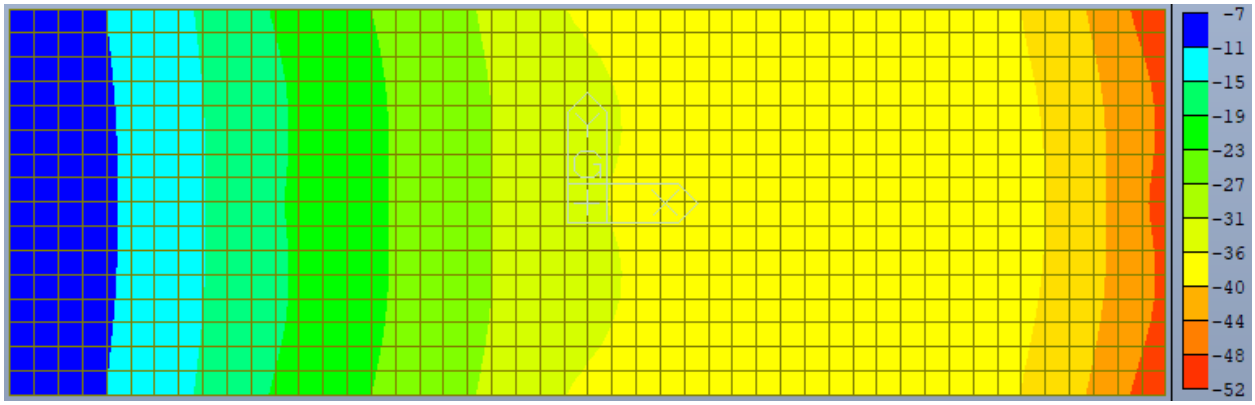

Figure 60: Pseudo Coupled Model Output for unsymmetrically loaded plate of size 24mx8mx0.8m

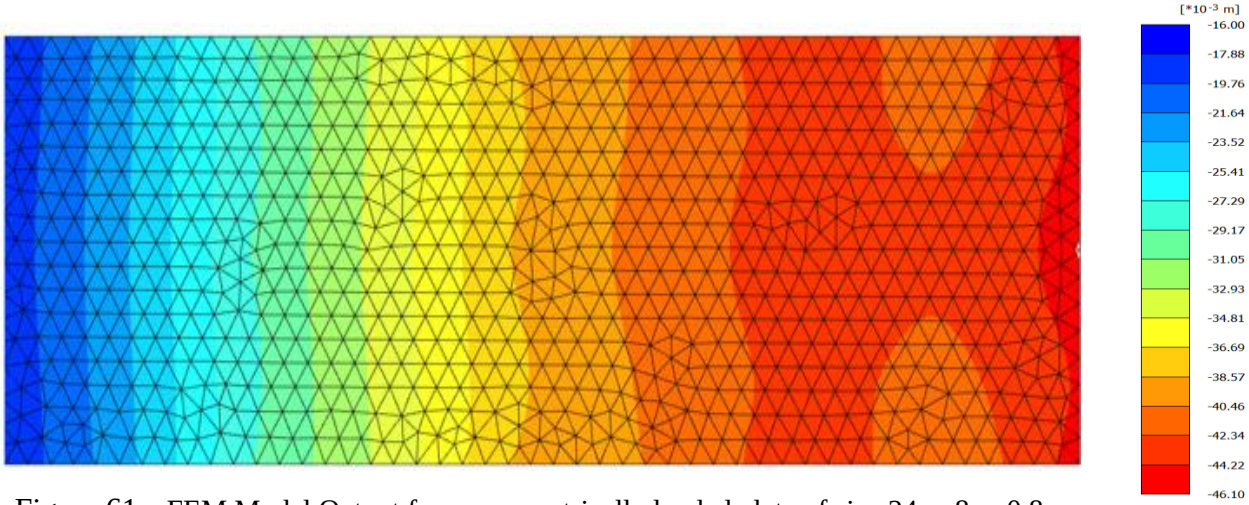

Figure 61: cFEM Model Output for unsymmetrically loaded plate of size 24mx8mx0.8m

The maximum error in the deformation value produced by Worku's model and Worku's_AdJ model is 18% and 8%, respectively. As was stated before, one should employ the adjusted Worku's_AdJ model rather than the original Worku's model for problems that are asymmetrically loaded. Matter of fact, when compared to the other models (Winkler-resulted in maximum error of 45%, Pseudo coupled- resulted in maximum error of 61%, and Vlasov-resulted in maximum error of 58%), Worku's model (without adjustment) produced an acceptable result (maximum error of 18%).

The two-parameter subgrade model, which was studied using the GEO5's Slab module, produced unrealistic deformation result (maximum error of 58%) as seen in figure 64.

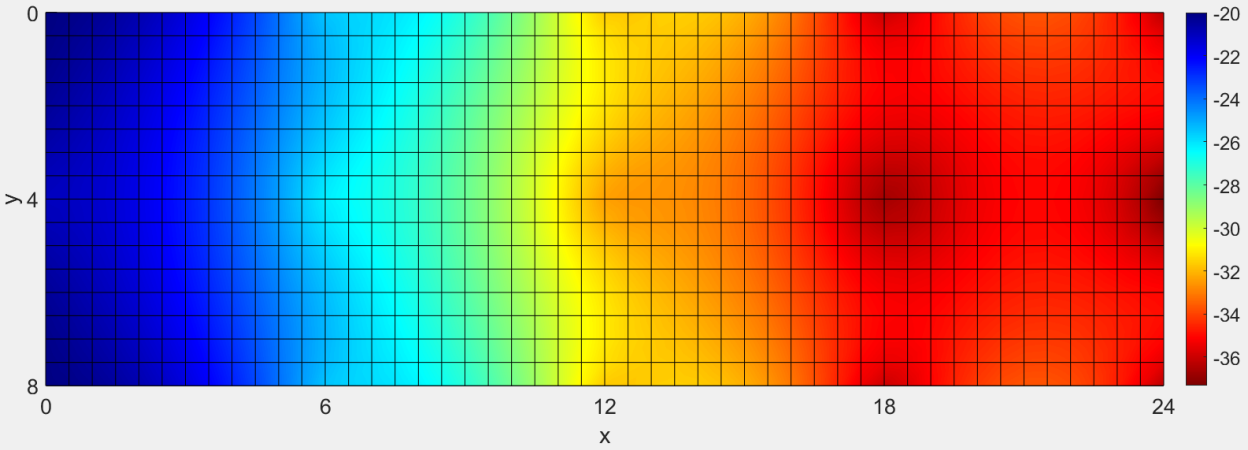

Figure 62: Worku's Model Output for asymmetrically loaded plate of size 24mx8mx0.8m

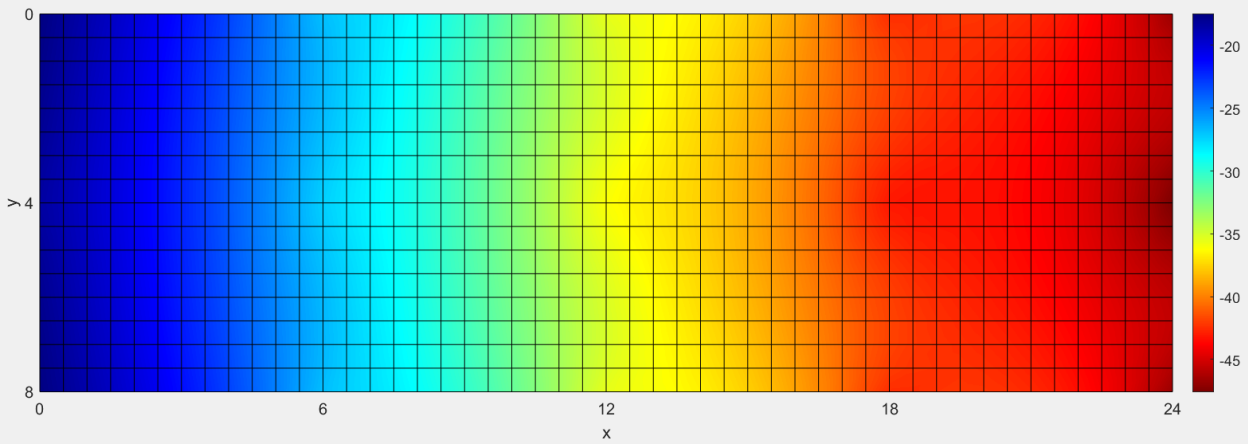

Figure 63: Worku's AdJ Model Output for asymmetrically loaded plate of size 24mx8mx0.8m

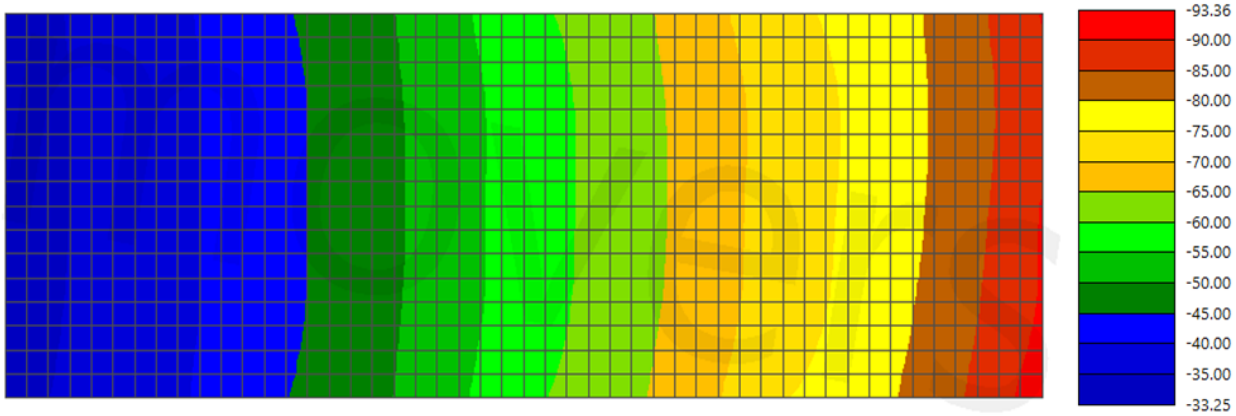

Figure 64: GEO5 Output for unsymmetrically loaded plate of size 24mx8mx0.8m

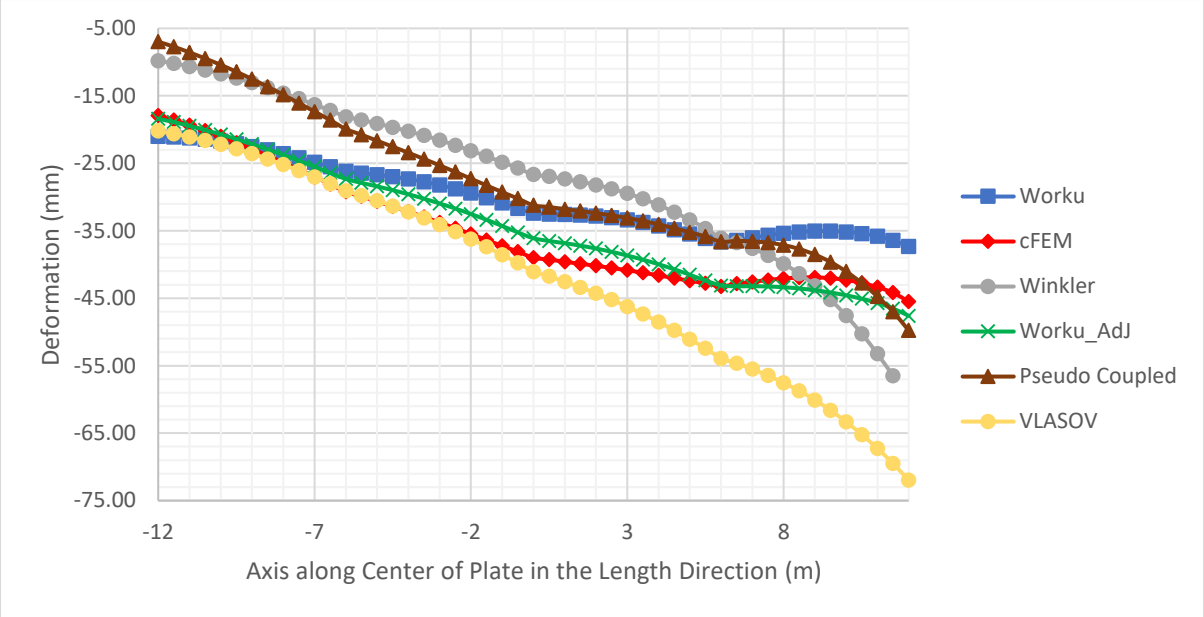

Figure 65: Vertical deformation along the center of the plate in the Length (X- direction)

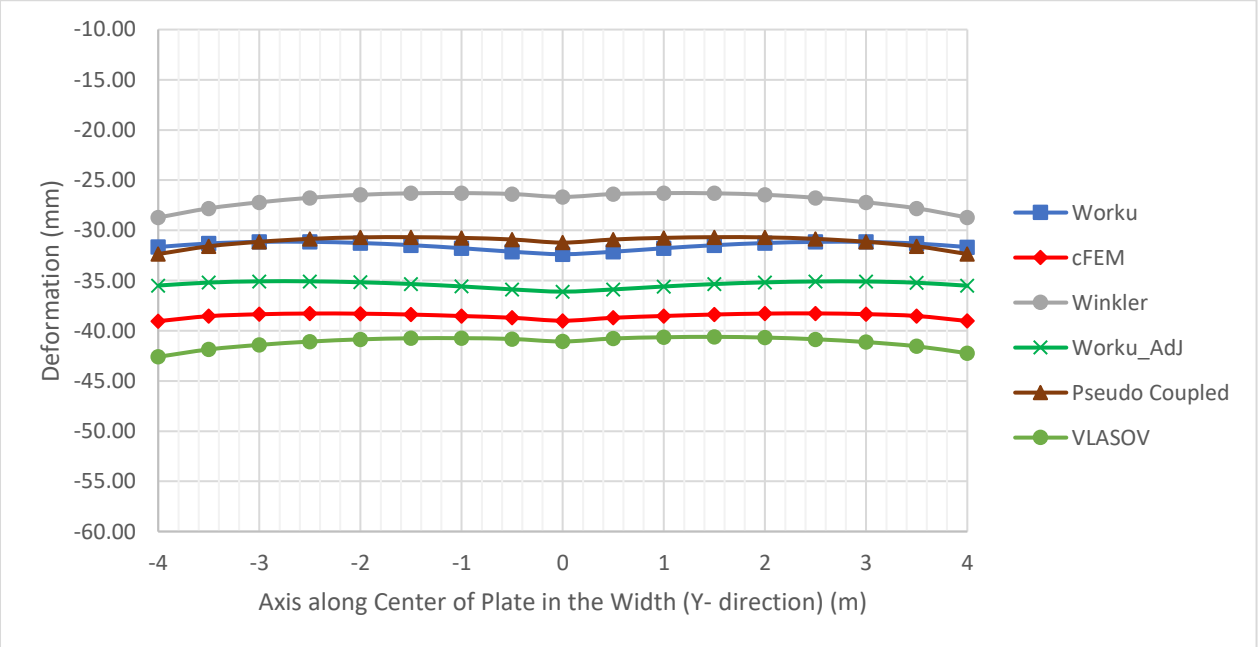

Figure 66: Vertical deformation along the center of the plate in the Width Y- direction (symmetrically loaded side)

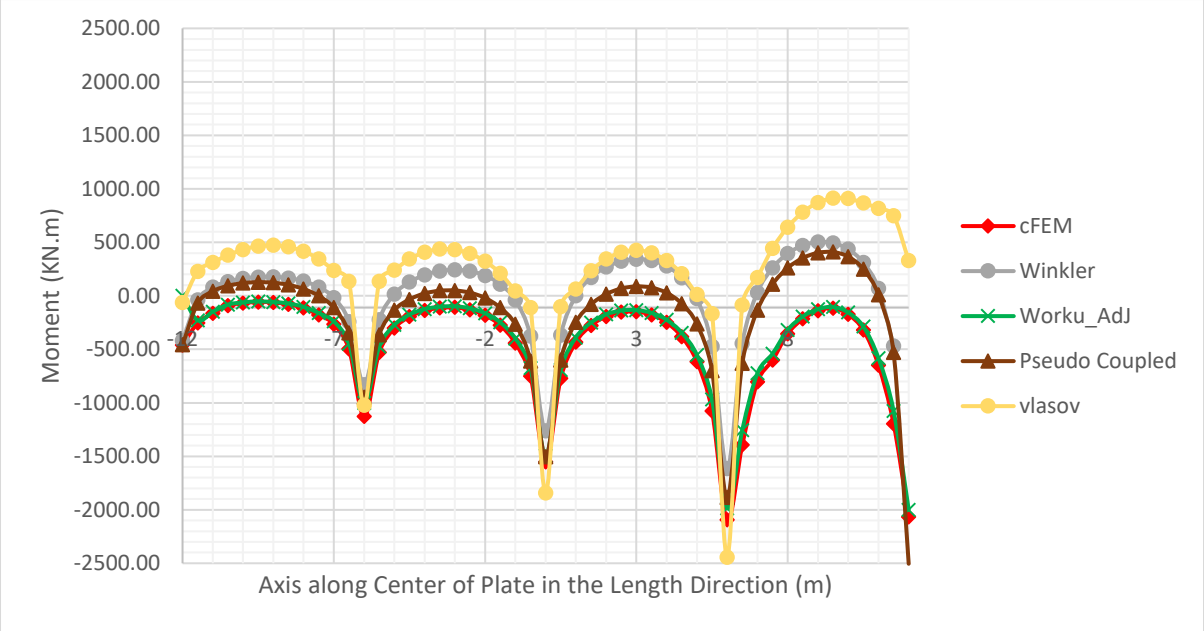

Figure 67: moment values along the center of the plate in the length (X- direction)

Due to the combined effect of both high aspect ratio and load eccentricity, this model posed a more complex bending behavior. Worku's AdJ model, which incorporates adjustments for both geometry and eccentricity, accurately captured the shifted moment profile. It showed the maximum negative moment skewed toward the loaded side, indicating strong top reinforcement demand in that area, and corresponding positive moment on the opposite side requiring bottom reinforcement. The cFEM result showed Worku's_AdJ model, with a deviation in moment values of less than 8 %, confirming its reliability. While winkler and vlasov model exhibit exaggerated values yielding unrealistically higher errors. While pseudo-coupled approach shows a better performance than both vlasov and winkler it still exhibits a higher error values at the mid-span.

Table 10: Deformation output for plate of size 24mx8mx0.8m loaded asymmetrically

Coordinate	Worku	Worku Modefied	cFEM	Winkler	Pseudo Coupled	GEO-5	Worku Error (%)	Worku Modified Error (%)
-12	-21.03	-18.40	-17.90	-9.82	-6.98	-20.19	-17.45	-2.75
-11.5	-21.09	-18.89	-18.57	-10.18	-7.72	-20.61	-13.56	-1.72
-11	-21.23	-19.45	-19.34	-10.64	-8.56	-21.09	-9.76	-0.56
-10.5	-21.45	-20.07	-20.16	-11.16	-9.46	-21.62	-6.39	0.48
-10	-21.74	-20.72	-21.03	-11.73	-10.41	-22.20	-3.38	1.43
-9.5	-22.09	-21.42	-21.93	-12.36	-11.43	-22.85	-0.72	2.32
-9	-22.51	-22.16	-22.89	-13.05	-12.51	-23.57	1.63	3.16
-8.5	-23.00	-22.94	-23.88	-13.79	-13.65	-24.35	3.69	3.93
-8	-23.55	-23.76	-24.91	-14.59	-14.85	-25.19	5.45	4.61
-7.5	-24.16	-24.62	-25.96	-15.43	-16.08	-26.09	6.92	5.17
-7	-24.83	-25.51	-27.02	-16.29	-17.34	-27.03	8.12	5.58
-6.5	-25.53	-26.44	-28.08	-17.16	-18.60	-28.01	9.10	5.84
-6	-26.16	-27.32	-29.20	-18.09	-19.92	-29.08	10.40	6.44
-5.5	-26.47	-27.90	-29.90	-18.57	-20.76	-29.76	11.47	6.70
-5	-26.71	-28.42	-30.65	-19.11	-21.66	-30.53	12.86	7.27
-4.5	-26.99	-28.98	-31.40	-19.66	-22.54	-31.34	14.06	7.70
-4	-27.33	-29.59	-32.17	-20.25	-23.44	-32.20	15.05	8.01
-3.5	-27.74	-30.25	-32.96	-20.88	-24.36	-33.11	15.83	8.22
-3	-28.22	-30.95	-33.77	-21.57	-25.31	-34.09	16.44	8.36
-2.5	-28.78	-31.71	-34.62	-22.32	-26.28	-35.13	16.86	8.41
-2	-29.42	-32.51	-35.49	-23.12	-27.28	-36.23	17.10	8.38
-1.5	-30.13	-33.37	-36.37	-23.96	-28.28	-37.38	17.16	8.23
-1	-30.90	-34.29	-37.24	-24.83	-29.27	-38.56	17.04	7.93
-0.5	-31.70	-35.24	-38.09	-25.71	-30.22	-39.76	16.79	7.49
0	-32.38	-36.11	-39.00	-26.67	-31.22	-41.07	16.99	7.42
0.5	-32.54	-36.52	-39.27	-26.95	-31.48	-41.76	17.12	7.00
1	-32.59	-36.84	-39.59	-27.33	-31.80	-42.56	17.68	6.95
1.5	-32.68	-37.21	-39.89	-27.73	-32.08	-43.39	18.09	6.73
2	-32.83	-37.63	-40.20	-28.20	-32.38	-44.27	18.33	6.37
2.5	-33.06	-38.12	-40.51	-28.77	-32.72	-45.22	18.40	5.90
3	-33.38	-38.67	-40.86	-29.45	-33.10	-46.24	18.30	5.34
3.5	-33.78	-39.29	-41.22	-30.25	-33.55	-47.34	18.05	4.70
4	-34.28	-39.96	-41.62	-31.18	-34.06	-48.52	17.63	3.97
4.5	-34.85	-40.71	-42.02	-32.24	-34.62	-49.77	17.05	3.12
5	-35.50	-41.52	-42.42	-33.40	-35.23	-51.07	16.32	2.12
5.5	-36.16	-42.38	-42.78	-34.65	-35.85	-52.42	15.47	0.95
6	-36.65	-43.11	-43.24	-36.10	-36.61	-53.92	15.24	0.30
6.5	-36.44	-43.22	-42.85	-36.74	-36.51	-54.63	14.97	-0.87
7	-36.04	-43.22	-42.57	-37.61	-36.58	-55.51	15.34	-1.52
7.5	-35.68	-43.26	-42.30	-38.64	-36.77	-56.47	15.66	-2.28
8	-35.38	-43.37	-42.07	-39.88	-37.13	-57.53	15.91	-3.09
8.5	-35.17	-43.56	-41.94	-41.36	-37.70	-58.73	16.13	-3.87
9	-35.06	-43.82	-41.91	-43.14	-38.53	-60.09	16.34	-4.54
9.5	-35.06	-44.15	-42.03	-45.21	-39.63	-61.62	16.59	-5.05
10	-35.17	-44.57	-42.30	-47.59	-41.04	-63.32	16.87	-5.36
10.5	-35.41	-45.08	-42.74	-50.27	-42.75	-65.21	17.16	-5.47
11	-35.80	-45.72	-43.37	-53.24	-44.74	-67.27	17.44	-5.42
11.5	-36.41	-46.53	-44.18	-56.49	-47.01	-69.50	17.58	-5.32
12	-37.32	-47.61	-45.50	-60.24	-49.78	-71.97	17.98	-4.62

Model Parameters		
L=	24	m
B=	8	m
h=	0.8	m
A_R=	3	Aspect Ratio
e_x=	3	m
e_y=	0	m
E_p=	32	GPa
v_p=	0.2	
E_S=	60	MPa
v_s=	0.26	

Flexural Rigidity

$$D = \frac{E_p h^3{}_s}{12(1 - v_p{}^2)}$$

D= 1,422.22 MNm

Relative Rigidity

$$R_s = \frac{8D(1 - v_s{}^2)}{\pi L^2 B E_s}$$

Rs 0.012 Relative rigidity

Load Type= C10

Q= 5400 KN

Calibration Factor

chi, χ = 1.9 From Chart

chi_M, χ_M = 3.00 Modefied

Modulus of subgrade Reaction, K_s

$$k_s = \frac{E_s}{B(1 - v_s{}^2)}$$

Ks= 8,043.76 KN/m^3

Pseudo Coupled

Ks,ave= 8,043.76 KN/m^3

A_1= 48 m^2

A_2= 60 m^2

A_3= 84 m^2

$$k_{s1} = k_{s,ave} \times \frac{A_1 + A_2 + A_3}{A_1 + 1.5A_2 + 2A_3}$$

Ks_1= 5,047.06 KN/m^3

Ks_2= 7,570.60 KN/m^3

Ks_3= 10,094.13 KN/m^3

Coordinate	Worku	Worku Modefied	cFEM	Winkler	Pseudo Coupled	GEO-5	Worku Error (%)	Worku Modified Error (%)
-4	-31.66	-35.50	-39.05	-28.72	-32.36	-42.60	18.92	9.09
-3.5	-31.31	-35.20	-38.55	-27.81	-31.59	-41.86	18.79	8.68
-3	-31.15	-35.08	-38.36	-27.21	-31.14	-41.41	18.80	8.56
-2.5	-31.14	-35.08	-38.28	-26.76	-30.85	-41.08	18.65	8.37
-2	-31.26	-35.17	-38.30	-26.46	-30.70	-40.86	18.38	8.17
-1.5	-31.48	-35.34	-38.39	-26.31	-30.68	-40.75	18.01	7.93
-1	-31.78	-35.59	-38.53	-26.29	-30.75	-40.74	17.53	7.65
-0.5	-32.13	-35.88	-38.71	-26.38	-30.91	-40.82	17.00	7.30
0	-32.38	-36.11	-39.00	-26.67	-31.22	-41.07	16.99	7.42
0.5	-32.13	-35.89	-38.71	-26.38	-30.91	-40.77	16.99	7.29
1	-31.78	-35.59	-38.53	-26.29	-30.75	-40.65	17.52	7.63
1.5	-31.48	-35.35	-38.38	-26.31	-30.68	-40.61	17.99	7.90
2	-31.26	-35.18	-38.29	-26.46	-30.70	-40.68	18.36	8.13
2.5	-31.15	-35.09	-38.28	-26.76	-30.85	-40.85	18.62	8.32
3	-31.16	-35.09	-38.35	-27.21	-31.14	-41.13	18.76	8.49
3.5	-31.31	-35.22	-38.53	-27.81	-31.59	-41.55	18.74	8.60
4	-31.67	-35.52	-39.03	-28.72	-32.36	-42.24	18.86	9.00

6) Model_Case_6: Asymetrically loaded (both directions) rectangular raft

The option to use this model was made to account for the fact that most foundations are not square and are typically loaded asymmetrically. The plate size for this model was 24mx8mx0.8m, with an aspect ratio of 3. In the analysis of thin plates, this model illustrates the combined effects of aspect ratio and both side eccentricity.

Table 11: Dimension and Parameters used for plate of size 24mx8mx0.8m loaded asymmetrically

L(m)	B(m)	h(m)	E_P(GPa)	ν_p	Es(MPa)	ν_s	R_s	Load	e_x(m)	e_y(m)	χ_{chart}	$\chi_{modified}$
24	8	0.8	32	0.2	70	0.22	0.0107	M6	3	2	2.1	3.2

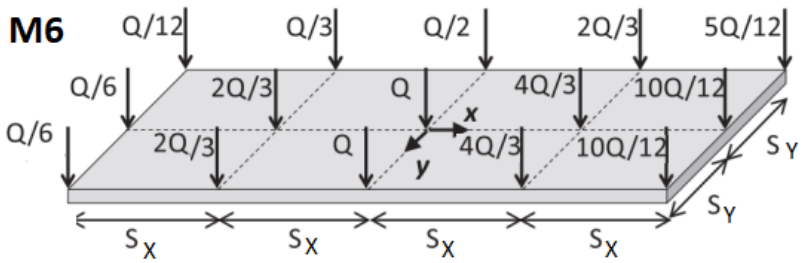

Figure 68: Load configuration used for a plate of size 24mx8mx0.8m

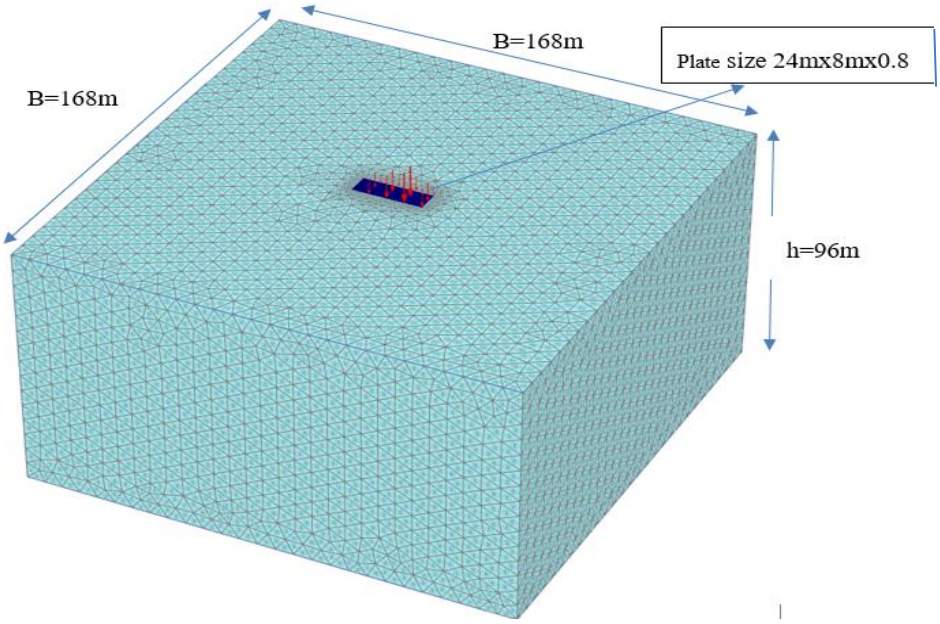

Figure 69: cFEM size of 168mx168mx96m

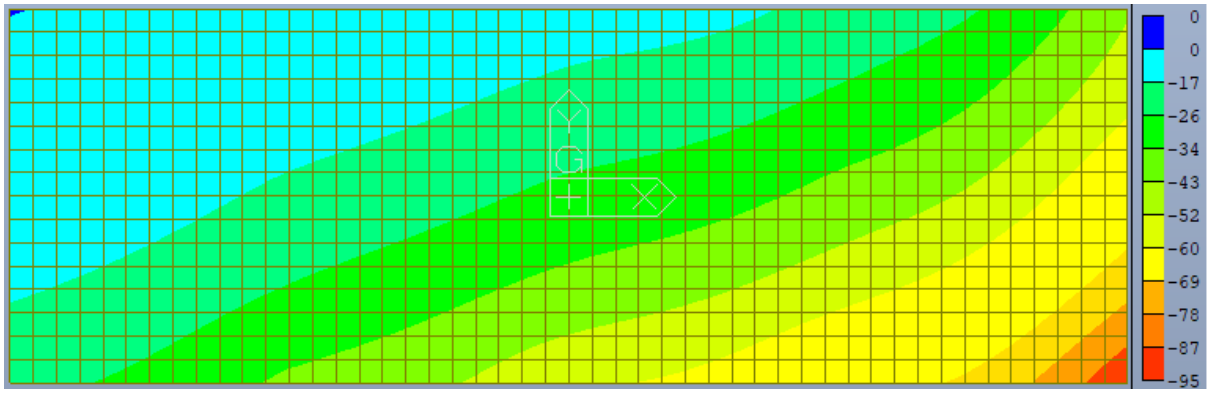

Figure 70: Winkler Model Output for asymmetrically loaded plate of size 24mx8mx0.8m

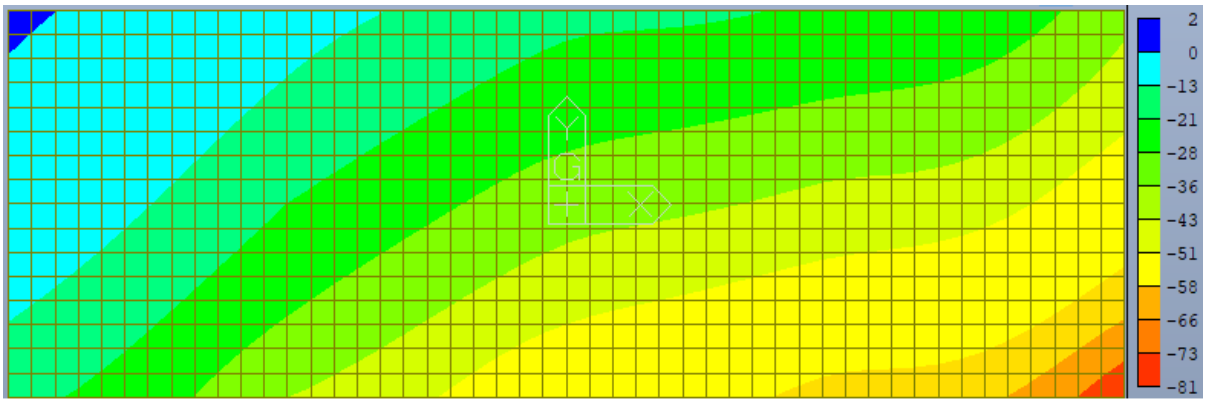

Figure 71: Pseudo Coupled Model Output for asymmetrically loaded plate of size 24mx8mx0.8m

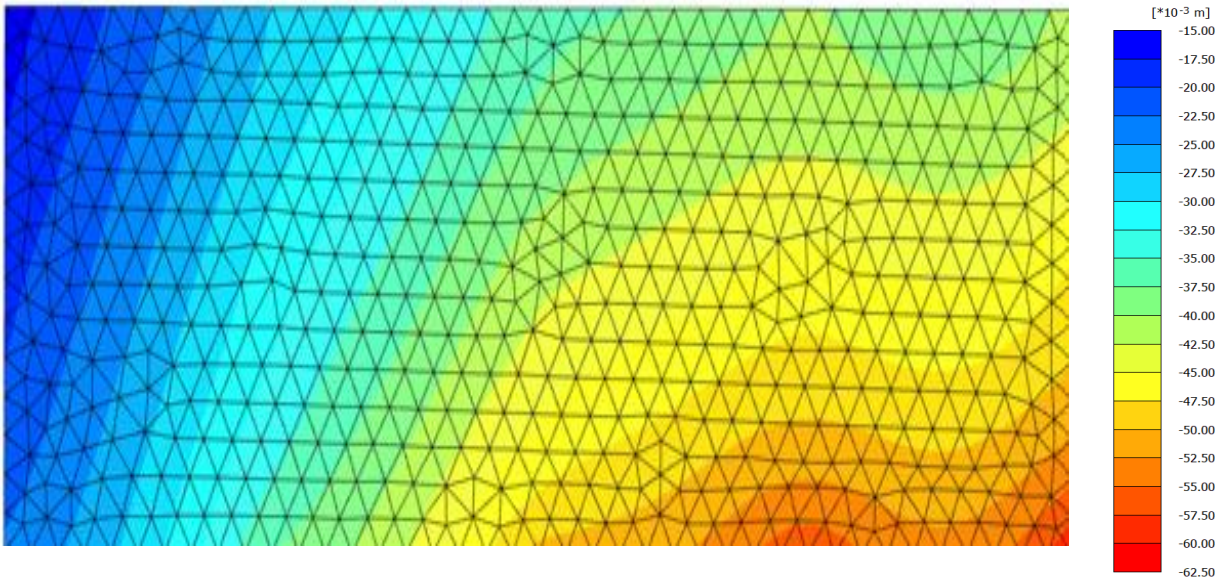

Figure 72: cFEM Model Output for asymmetrically loaded plate of size 24mx8mx0.8m

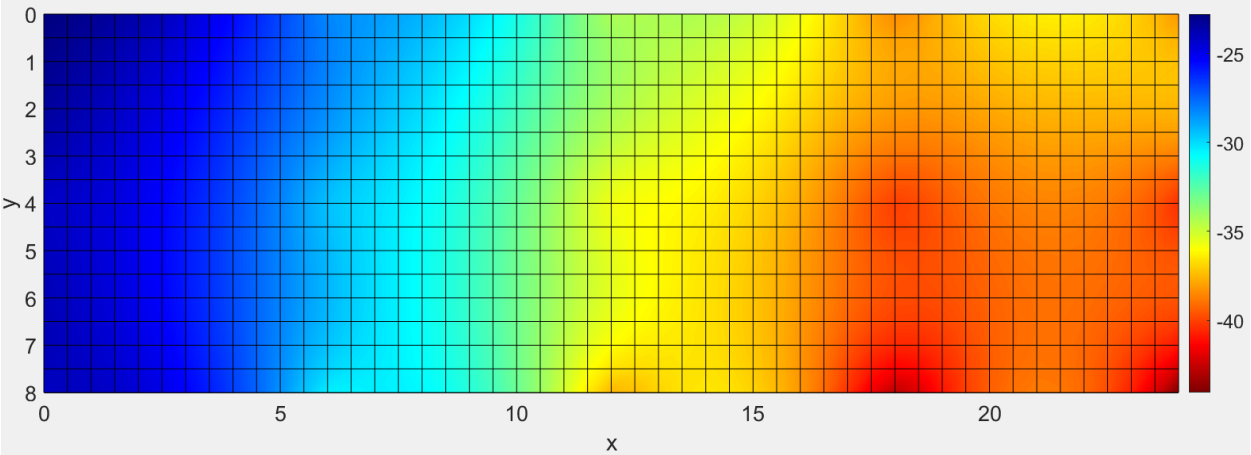

Figure 73: Worku's Model Output for asymmetrically loaded plate of size 24mx8mx0.8m

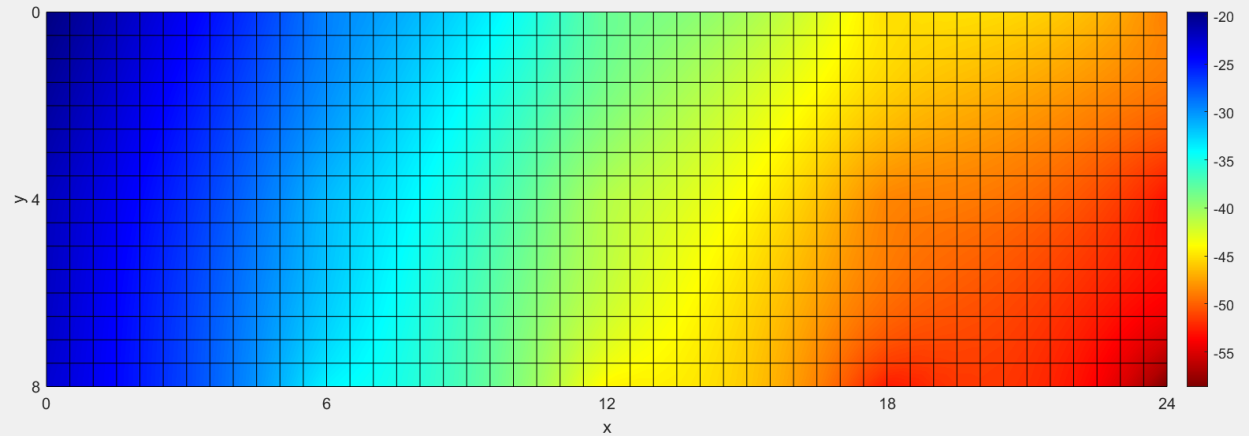

Figure 74: Worku's_AdJ Model Output for asymmetrically loaded plate of size 24mx8mx0.8m

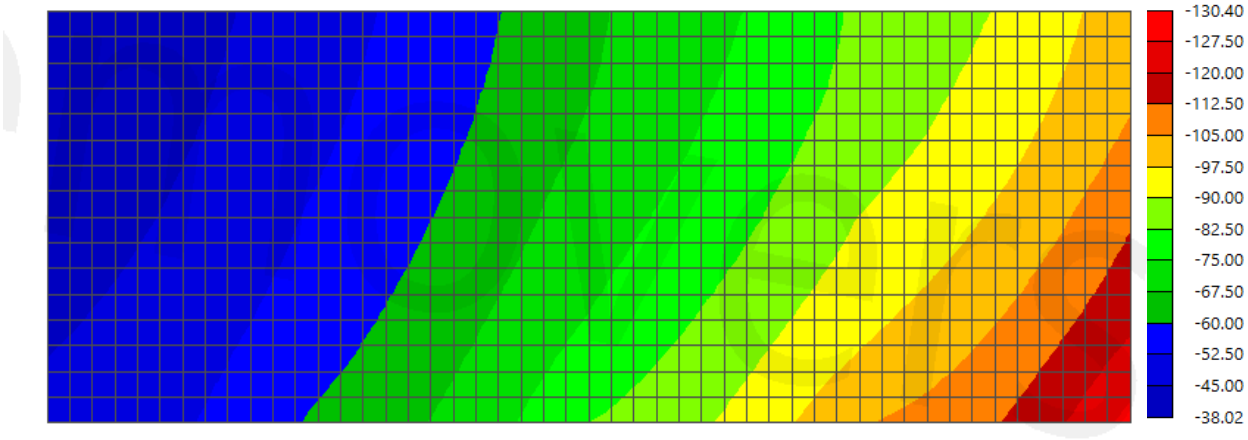

Figure 75: GEO5 output for unsymmetrically loaded plate of size 24mx8mx0.8m

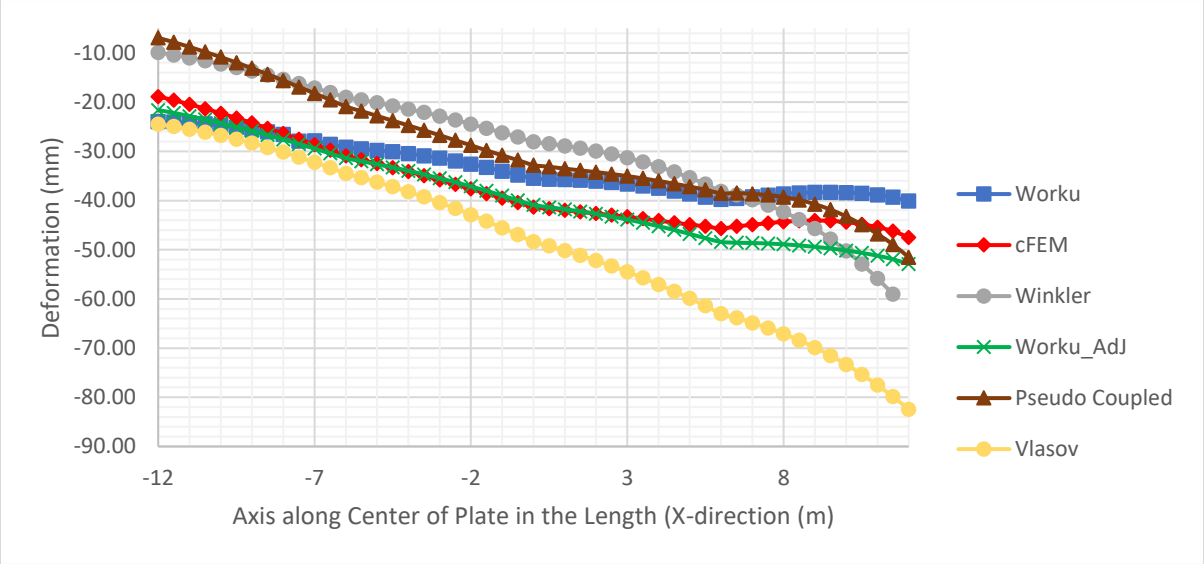

Figure 76: Vertical deformation along the center of the plate in the Length direction

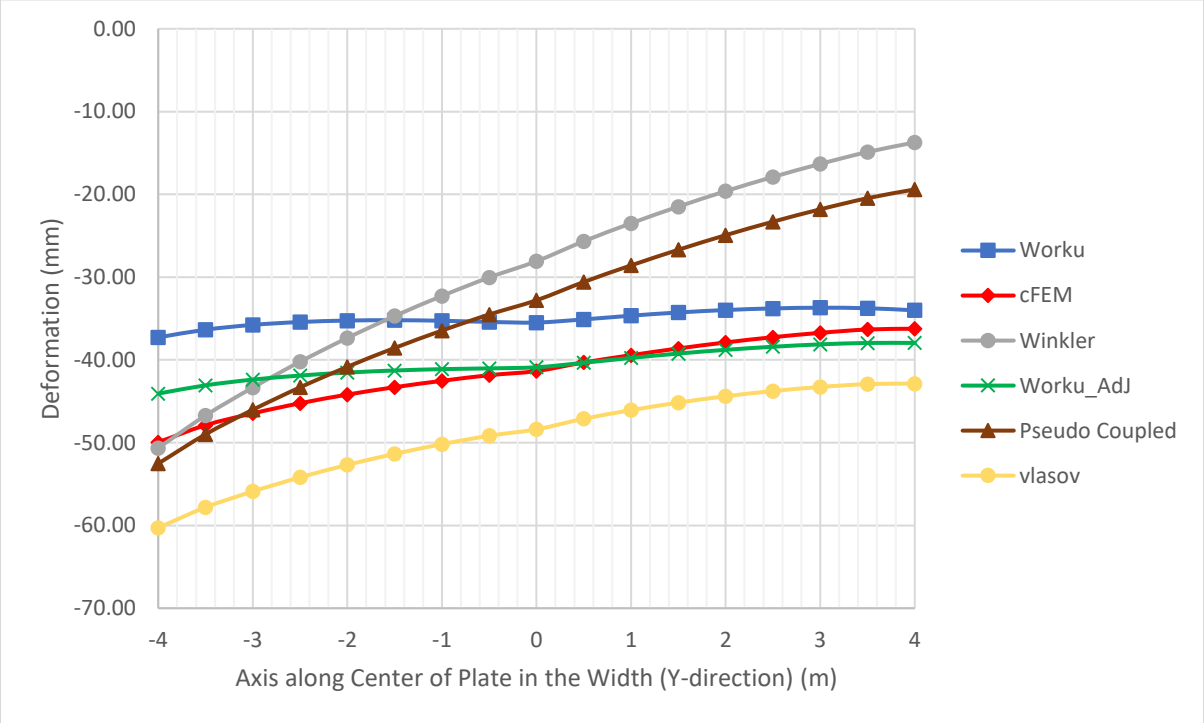

Figure 77: Vertical deformation along the center of the plate in the Width (Y- direction)

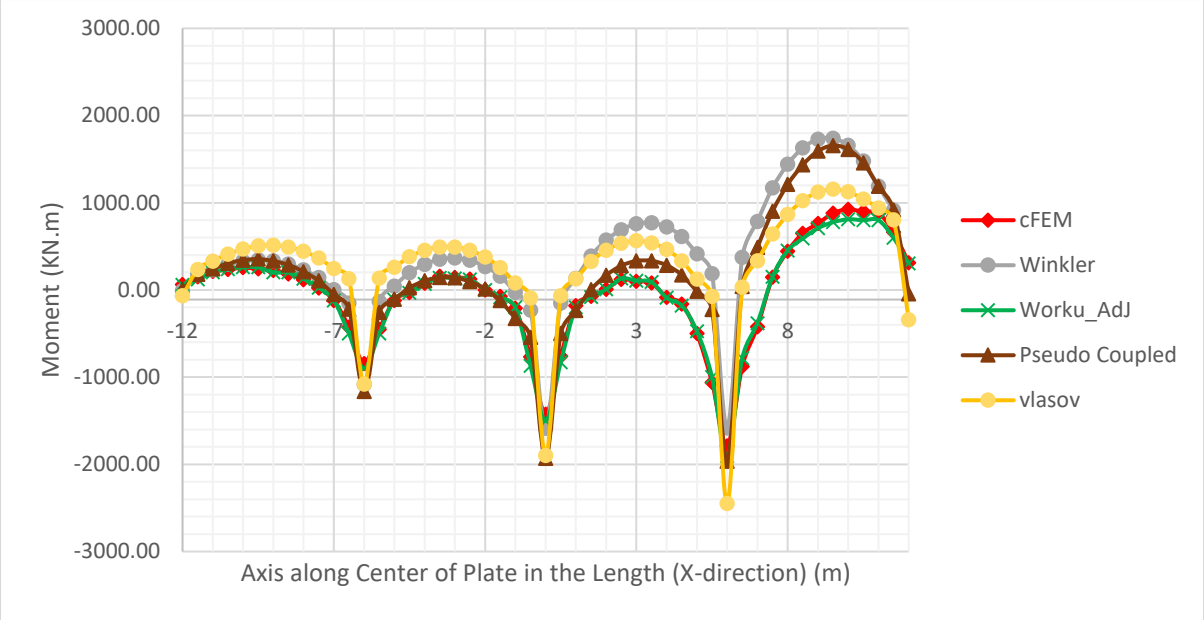

Figure 78: moment values along the center of the plate in the length (X-direction)

This configuration closely reflects many real-life scenarios where building loads are not perfectly centered, and foundation shapes are non-square. The Worku's_AdJ model once again performed exceptionally well, adapting to both the elongated geometry and the bidirectional load imbalance. It correctly identified the location of maximum negative bending moment, which was no longer centrally located but shifted diagonally toward the more heavily loaded quadrant. This resulted in an irregular but realistic distribution of top and bottom reinforcement zones. The modified Worku model stayed within a 12% error range, clearly demonstrating its robustness. Vlasov attempted to capture the shift in moments but fell short in magnitude and shape by yielding an error of 60% or more. This case conclusively shows that the Worku's model, when properly calibrated, is a practical and safe tool for real-world raft foundation design, even under complex loading and geometry conditions.

Table 12: Deformation output for plate of size 24mx8mx0.8m loaded asymmetrically

Coordinate	Worku	Worku Modefied	cFEM	Winkler	GEO-5	Pseudo Coupled	Worku Error (%)	Worku Modified Error (%)
-12	-23.93	-21.61	-18.87	-9.93	-24.47	-6.94	-26.83	-12.66
-11.5	-24.03	-22.19	-19.61	-10.41	-24.96	-7.82	-22.56	-11.64
-11	-24.20	-22.84	-20.44	-10.98	-25.51	-8.78	-18.39	-10.48
-10.5	-24.45	-23.53	-21.32	-11.59	-26.11	-9.79	-14.64	-9.39
-10	-24.75	-24.27	-22.25	-12.24	-26.78	-10.84	-11.25	-8.32
-9.5	-25.12	-25.04	-23.22	-12.94	-27.51	-11.95	-8.18	-7.27
-9	-25.55	-25.85	-24.24	-13.70	-28.32	-13.12	-5.41	-6.23
-8.5	-26.04	-26.70	-25.30	-14.50	-29.20	-14.34	-2.93	-5.22
-8	-26.59	-27.57	-26.40	-15.35	-30.15	-15.60	-0.74	-4.27
-7.5	-27.96	-28.49	-27.52	-16.23	-31.16	-16.90	-1.60	-3.42
-7	-27.85	-29.44	-28.65	-17.13	-32.23	-18.21	2.77	-2.70
-6.5	-28.55	-30.42	-29.77	-18.03	-33.33	-19.53	4.11	-2.15
-6	-29.18	-31.36	-30.94	-19.00	-34.53	-20.89	5.69	-1.34
-5.5	-29.51	-32.02	-31.70	-19.54	-35.34	-21.83	6.90	-1.00
-5	-29.78	-32.63	-32.50	-20.15	-36.25	-22.80	8.37	-0.39
-4.5	-30.09	-33.28	-33.31	-20.77	-37.20	-23.77	9.64	0.09
-4	-30.46	-33.96	-34.12	-21.41	-38.21	-24.74	10.72	0.46
-3.5	-30.89	-34.69	-34.96	-22.10	-39.27	-25.72	11.63	0.76
-3	-31.39	-35.46	-35.83	-22.83	-40.41	-26.73	12.38	1.01
-2.5	-31.95	-36.28	-36.72	-23.62	-41.61	-27.75	13.00	1.22
-2	-32.58	-37.13	-37.65	-24.45	-42.88	-28.78	13.46	1.36
-1.5	-33.27	-38.04	-38.58	-25.32	-44.19	-29.81	13.75	1.40
-1	-34.02	-38.99	-39.50	-26.21	-45.54	-30.82	13.87	1.31
-0.5	-34.81	-39.97	-40.40	-27.10	-46.91	-31.79	13.84	1.05
0	-35.48	-40.89	-41.34	-28.08	-48.38	-32.79	14.18	1.10
0.5	-35.67	-41.37	-41.64	-28.43	-49.23	-33.13	14.33	0.66
1	-35.76	-41.77	-41.99	-28.89	-50.19	-33.51	14.84	0.52
1.5	-35.88	-42.22	-42.31	-29.37	-51.18	-33.87	15.19	0.22
2	-36.07	-42.71	-42.63	-29.92	-52.21	-34.23	15.39	-0.20
2.5	-36.32	-43.26	-42.96	-30.55	-53.31	-34.61	15.45	-0.71
3	-36.65	-43.87	-43.31	-31.28	-54.48	-35.03	15.39	-1.26
3.5	-37.05	-44.52	-43.69	-32.13	-55.73	-35.50	15.21	-1.85
4	-37.52	-45.22	-44.09	-33.10	-57.06	-36.02	14.90	-2.49
4.5	-38.07	-45.98	-44.50	-34.19	-58.46	-36.59	14.46	-3.22
5	-38.67	-46.80	-44.90	-35.37	-59.91	-37.18	13.86	-4.06
5.5	-39.31	-47.66	-45.25	-36.64	-61.40	-37.79	13.13	-5.06
6	-39.78	-48.41	-45.68	-38.11	-63.03	-38.54	12.92	-5.65
6.5	-39.58	-48.58	-45.26	-38.86	-63.86	-38.50	12.53	-6.84
7	-39.23	-48.64	-44.93	-39.84	-64.86	-38.64	12.68	-7.62
7.5	-38.91	-48.74	-44.60	-40.97	-65.92	-38.89	12.77	-8.49
8	-38.65	-48.91	-44.33	-42.30	-67.10	-39.29	12.81	-9.37
8.5	-38.46	-49.13	-44.14	-43.87	-68.40	-39.90	12.86	-10.17
9	-38.35	-49.41	-44.07	-45.70	-69.88	-40.74	12.98	-10.82
9.5	-38.33	-49.76	-44.15	-47.82	-71.52	-41.85	13.19	-11.27
10	-38.39	-50.16	-44.39	-50.23	-73.35	-43.23	13.52	-11.50
10.5	-38.56	-50.64	-44.81	-52.91	-75.36	-44.89	13.95	-11.51
11	-38.86	-51.22	-45.42	-55.85	-77.54	-46.81	14.45	-11.33
11.5	-39.33	-51.95	-46.21	-59.02	-79.88	-48.95	14.88	-11.04
12	-40.08	-52.91	-47.50	-62.63	-82.43	-51.54	15.62	-10.23

	Model Parameters	
L=	24	m
B=	8	m
h=	0.8	m
A_R=	3	Aspect Ratio
e_x=	3	m
e_y=	0.8	m
E_p=	32	GPa
ν_p=	0.2	
E_s=	70	MPa
ν_s=	0.25	
	Flexural Rigidity	
	$D = \frac{E_p h^3{}_s}{12(1-{\nu_p}^2)}$	
D=	1,422.22	MNm
	Relative Rigidity	
	$R_s = \frac{8D(1-{\nu_s}^2)}{\pi L^2 B E_s}$	
Rs	0.011	Relative rigidity
Load Type=	C10M	
Q=	5400	KN
	Calibration Factor	
chi, χ =	2.1	From Chart
chi$_M$, χ_M =	3.20	Modefied
	Modulus of subgrade Reaction, K_s	
	$k_s = \frac{E_s}{B(1-{\nu_s}^2)}$	
Ks=	9,333.33	KN/m^3
	Pseudo Coupled	
Ks,ave=	9,333.33	KN/m^3
A_1=	48	m^2
A_2=	60	m^2
A_3=	84	m^2
	$k_{s1} = k_{s,ave} \times \frac{A_1 + A_2 + A_3}{A_1 + 1.5A_2 + 2A_3}$	
Ks$_1$=	5,856.21	KN/m^3
Ks$_2$=	8,784.31	KN/m^3
Ks$_3$=	11,712.42	KN/m^3

Coordinate	Worku	Worku Modefied	cFEM	Winkler	GE0-5	Pseudo Coupled	Worku Error (%)	Worku Modified Error (%)
-4	-37.28	-44.07	-49.94	-50.64	-60.28	-52.52	25.36	11.76
-3.5	-36.35	-43.07	-47.89	-46.72	-57.81	-48.99	24.10	10.06
-3	-35.77	-42.38	-46.46	-43.34	-55.89	-46.02	23.01	8.77
-2.5	-35.42	-41.89	-45.23	-40.22	-54.19	-43.31	21.69	7.40
-2	-35.25	-41.53	-44.19	-37.35	-52.68	-40.83	20.24	6.02
-1.5	-35.20	-41.28	-43.30	-34.70	-51.35	-38.55	18.69	4.66
-1	-35.27	-41.11	-42.53	-32.27	-50.18	-36.46	17.06	3.32
-0.5	-35.41	-41.02	-41.85	-30.04	-49.16	-34.51	15.38	1.97
0	-35.48	-40.89	-41.34	-28.08	-48.38	-32.79	14.18	1.10
0.5	-35.11	-40.35	-40.31	-25.66	-47.11	-30.58	12.90	-0.10
1	-34.66	-39.76	-39.43	-23.50	-46.07	-28.58	12.10	-0.83
1.5	-34.27	-39.23	-38.62	-21.48	-45.16	-26.69	11.25	-1.57
2	-33.97	-38.78	-37.89	-19.62	-44.39	-24.93	10.33	-2.30
2.5	-33.78	-38.41	-37.26	-17.90	-43.76	-23.30	9.34	-3.00
3	-33.70	-38.12	-36.73	-16.32	-43.27	-21.81	8.26	-3.65
3.5	-33.76	-37.95	-36.32	-14.89	-42.92	-20.46	7.07	-4.29
4	-34.01	-37.95	-36.23	-13.73	-42.87	-19.40	6.14	-4.52

CHAPTER FIVE

5. CONCLUSION AND RECOMMENDATION

5. 1 Conclusion

The following major conclusions may be drawn:

1. For the analysis of thin plates of any dimension and load configuration resting on an elastic foundation problem, Worku's Kerr equivalent Pasternak model can be utilized, producing results that are in strong agreement with those of cFEM.
2. Comparisons with rigorous continuum finite element analysis (cFEM) demonstrated that Worku's two-parameter model better predicts deformations and bending moment.
3. The Winkler's model, while widely used due to its simplicity for implementation, consistently demonstrated limitations in precisely predicting the structural response of raft foundations compared to the continuum finite element model (cFEM).
4. The pseudo-coupled model provided enhanced accuracy over the Winkler method, yet still showed notable deviances from the continuum finite element benchmark, indicating limitations in fully capturing shear interactions within the soil-foundation system.
5. Though the Vlasov model exhibited considerable errors near corners and eccentrically loaded zones, its close agreement with the general trend of cFEM results indicates that its accuracy can likely be improved through additional calibration efforts.
6. One just needs to figure out the soil property and the relative stiffness of a plate in order to use the calibration chart created by Worku and Minwuyelet (2022).
7. In almost all cases, the calibration chart developed by Worku and Minwuyelet (2022) in conjunction with the calibrated Kerr equivalent Pasternak model gives consistently better results with the cFEM outputs.
8. Practicing Engineers can analyze mat foundation and even conduct parametric studies with ease by using the model and the corresponding calibration chart once the validation is done.

5. 2 Recommendation

1. To validate the computational findings, large-scale experiments need be carried out.
2. The performance of the model and the calibration chart for thick plates should be verified since the scope of this work is confined to thin rectangular plates subjected to vertical loading only.
3. Developers of structural foundation design software are encouraged to integrate this model into their platforms once validation is done. Doing so would make this method more accessible to practicing engineers and increase its use in day-to-day design work.

REFERENCES

ACI 336.2R-88. (2002). Suggested Analysis and Design Procedures for Combined Footings and Mats. (Reapproved 2002), American Concrete Institute.

Baban, T. M. (2016). *Shallow Foundations Discussions and Problem Solving.* United Kingdom: John Wiley & Sons, Ltd.

Bowles, J. E. (1995). *Foundation Analysis and Design.* New York: McGraw-Hill Companies,Inc.

Brown, P. T. (1975). The behaviour of uniformly loaded piled strip footings. *Soils and Foundation*, 15, 13–21.

Burland, J. B. (1977). Behaviour of foundations and structures. *Proc. 9th Int. Conf. on Soil Mech. and Found. Engrg., Vol. 2*, (pp. 495-546). Tokyo.

Butterfield, R. a. (1971). The elastic analysis of compressible piles and pile groups. *Géotechnique*, 21, 1, 43–60.

Cheung YK, Z. O. (1965). Plates and tanks on elastic foundations: an application of finite element method. . *Int. J. Solids Struct*, 451–461.

Couduto D. P. (2001). *Foundation Design Principles and Practices.* Prentice Hall.

D. Loukidis, G.-P. T. (2017). Spatial distribution of Winkler spring stiffness for rectangular mat foundation analysis. *Engineering Structures Elsevier Ltd.*, 443–459.

Dunham, C. W. (1962). *Foundations of structures.* New York: McGraw-Hill,.

E.J., U. (1995). Design and performance of mat foundations;state-of-the-art review. *ACI*, 95-116.

Hemsley, J. A. (2000). Developments in raft analysis and design. In J. A. Hemsley, *Design applications of raft foundations* (p. 495). London: Thomas Telford Ltd.

Horvath, R. J. (2010). Practical Subgrade Model for Improved Soil-Structure Interaction Analysis: Software Implementation. *Practice Periodical on Structural Design and Construction, ASCE*, 278-286.

Minwuyelet and Worku (2024). A Method of Implementation of a Rigorous Analytical Subgrade Model to the (FE) Analysis of Plates on an Elastic Foundation. Manuscript submitted for publication.

Poulos, H. G. (1991). Analysis of piled strip foundation. *Comp. Methods & Advances in Geomech.(eds G. Beer et al.)* (pp. 1, 183–191). Balkema, Rotterdam: Proceedings of the Seventh International Confrence on Computer methods and advances in Geomechanics.

Reissner E. (1958). Deflection of plates on viscoelastic foundation. *Journal of Applied Mechanics (ASME)*, 144–145.

Shukla, S. N. (1984). A simplified method for design of mats on elastic foundations-Shukla. *ACI Journal*, 469-475.

Szilard, R. (2004). *Theories and Applications of Plate Analysis Classical, Numerical and Engineering Methods.* Hoboken, New Jersey: John Wiley & Sons, Inc.

Vlazov VZ & Leontiev UN. (1966). Beams, Plates and Shells on Elastic Foundations. *Israel Program for Scientific Translations, Jerusalem (translated from Russian),*.

worku, A. (2009). Proposed Higher Order Continuum Based Models for an Elastic subgrade. *EEA,volume 26*, 1-10.

Worku, A. (2009). Winkler's Single-Parameter Subgrade Model from the perspective of an improoved approach of continuum-based subgrade modeling. *Journal of EEA, Vol. 26*, 11-22.

worku, A. (2010). A generalized Formulation of Continuum Models for Elastic Foundations. *GeoFlorida 2010:Advances in Analysis,Modeling & Design* (pp. 1641-1650). ASCE.

worku, A. (2013). Cakibrated Analytical Formulas for Foundation Model Parameters. *International Journal of Geomechanics*, 340-347.

worku, A. (2014). Development of a Calibrated Pasternak Foundation Model for Practical Use. *International Journal of Geotechnical Engineering*, 26-33.

ANNEX

ANNEX A: TABULAR DATA FOR DEFORMATION VALUES AND ERROR PERCENTAGE

Deformation and percentage error of M1 24mx24mx2.2m

Coordin	Worku	CFEM	Winkl	Pseudo Couple	Vlaso	ERROR (%)			
						rku Erro	inkler	Pseud	vlasov
-12	-46.83	-47.94	-66.81	-66.46	-56.13	-2.37	39.36	38.64	17.09
-11.5	-46.85	-47.96	-66.64	-66.38	-56.14	-2.37	38.96	38.41	14.58
-11	-46.88	-48.05	-66.54	-66.36	-56.02	-2.50	38.49	38.12	14.23
-10.5	-46.92	-48.15	-66.46	-66.36	-55.93	-2.64	38.00	37.81	13.90
-10	-46.97	-48.27	-66.38	-66.38	-55.86	-2.77	37.51	37.50	13.58
-9.5	-47.03	-48.40	-66.31	-66.40	-55.79	-2.91	37.02	37.19	13.25
-9	-47.10	-48.53	-66.26	-66.43	-55.73	-3.04	36.52	36.88	12.92
-8.5	-47.17	-48.67	-66.20	-66.47	-55.68	-3.17	36.04	36.58	12.60
-8	-47.25	-48.81	-66.20	-66.52	-55.64	-3.29	35.64	36.28	12.28
-7.5	-47.33	-48.95	-66.16	-66.57	-55.61	-3.41	35.16	35.99	11.98
-7	-47.42	-49.10	-66.13	-66.63	-55.58	-3.53	34.69	35.71	11.67
-6.5	-47.50	-49.25	-66.10	-66.70	-55.56	-3.67	34.23	35.44	11.37
-6	-47.57	-49.45	-66.09	-66.83	-55.55	-3.94	33.66	35.15	10.99
-5.5	-47.61	-49.47	-66.14	-66.78	-55.49	-3.92	33.68	34.99	10.84
-5	-47.63	-49.55	-66.02	-66.80	-55.44	-4.03	33.23	34.80	10.62
-4.5	-47.65	-49.63	-65.96	-66.81	-55.40	-4.15	32.91	34.63	10.42
-4	-47.67	-49.70	-65.91	-66.84	-55.37	-4.27	32.61	34.47	10.23
-3.5	-47.69	-49.78	-65.85	-66.86	-55.34	-4.37	32.28	34.33	10.06
-3	-47.72	-49.84	-65.82	-66.89	-55.32	-4.45	32.06	34.20	9.90
-2.5	-47.75	-49.90	-65.81	-66.91	-55.31	-4.52	31.87	34.08	9.77
-2	-47.78	-49.96	-65.80	-66.94	-55.31	-4.57	31.71	33.99	9.67
-1.5	-47.81	-50.01	-65.81	-66.97	-55.31	-4.60	31.58	33.91	9.58
-1	-47.85	-50.06	-65.82	-67.00	-55.32	-4.62	31.48	33.85	9.51
-0.5	-47.88	-50.10	-65.84	-67.00	-55.34	-4.64	31.41	33.73	9.47
0	-47.89	-50.19	-65.92	-67.12	-55.39	-4.79	31.34	33.73	9.39
0.5	-47.88	-50.10	-65.84	-67.00	-55.34	-4.64	31.41	33.73	9.47
1	-47.85	-50.06	-65.82	-67.00	-55.32	-4.62	31.48	33.85	9.51
1.5	-47.81	-50.01	-65.81	-66.97	-55.31	-4.60	31.58	33.91	9.58
2	-47.78	-49.96	-65.80	-66.94	-55.31	-4.56	31.72	33.99	9.67
2.5	-47.75	-49.90	-65.81	-66.91	-55.31	-4.51	31.88	34.09	9.78
3	-47.72	-49.84	-65.82	-66.89	-55.32	-4.45	32.07	34.20	9.91
3.5	-47.69	-49.77	-65.85	-66.86	-55.34	-4.36	32.29	34.33	10.06
4	-47.67	-49.70	-65.91	-66.84	-55.37	-4.26	32.62	34.48	10.24
4.5	-47.65	-49.63	-65.96	-66.81	-55.40	-4.14	32.92	34.64	10.42
5	-47.63	-49.55	-66.02	-66.80	-55.44	-4.02	33.24	34.81	10.63
5.5	-47.61	-49.47	-66.14	-66.78	-55.49	-3.91	33.69	35.00	10.85
6	-47.57	-49.44	-66.09	-66.83	-55.57	-3.93	33.67	35.16	11.03
6.5	-47.50	-49.24	-66.10	-66.70	-55.55	-3.66	34.25	35.45	11.36
7	-47.42	-49.09	-66.13	-66.63	-55.56	-3.52	34.70	35.72	11.64
7.5	-47.33	-48.95	-66.16	-66.57	-55.58	-3.40	35.18	36.00	11.94
8	-47.25	-48.80	-66.20	-66.52	-55.61	-3.28	35.66	36.30	12.24
8.5	-47.17	-48.66	-66.20	-66.47	-55.64	-3.16	36.05	36.59	12.54
9	-47.10	-48.52	-66.26	-66.43	-55.68	-3.03	36.54	36.90	12.85
9.5	-47.03	-48.39	-66.31	-66.40	-55.73	-2.90	37.03	37.21	13.17
10	-46.97	-48.27	-66.38	-66.38	-55.86	-2.76	37.53	37.52	13.59
10.5	-46.92	-48.15	-66.46	-66.36	-55.93	-2.62	38.02	37.83	13.91
11	-46.88	-48.04	-66.54	-66.36	-56.02	-2.49	38.51	38.14	14.24
11.5	-46.85	-47.95	-66.64	-66.38	-56.14	-2.36	38.98	38.43	14.59
12	-46.83	-47.93	-66.81	-66.46	-56.13	-2.36	39.38	38.66	14.61

Deformation and percentage error for M2 12mx12mx1.1m along the length

Coordin	Work	Worku Modefied	cFEM	Wink	Pseudo Couple	VLAS	WORK	ERROR(%) MODIFIE	WINKLI	PSEUD	VLASC
-6	-33.41	-31.22	-30.13	-27.29	-30.14	-24.51	10.88	3.62	10.41	0.03	22.94
-5.5	-33.39	-31.53	-30.57	-29.08	-31.74	-25.47	9.21	3.11	5.15	3.67	20.04
-5	-33.44	-31.90	-31.14	-30.97	-33.45	-26.44	7.41	2.45	0.56	6.91	17.77
-4.5	-33.57	-32.34	-31.74	-32.89	-35.20	-27.43	5.76	1.91	3.51	9.83	15.71
-4	-33.75	-32.85	-32.37	-34.85	-36.99	-28.42	4.27	1.49	7.13	12.49	13.90
-3.5	-34.00	-33.42	-33.03	-36.85	-38.80	-29.42	2.94	1.19	10.38	14.88	12.25
-3	-34.30	-34.04	-33.70	-38.88	-40.65	-30.42	1.76	0.99	13.31	17.09	10.79
-2.5	-34.65	-34.71	-34.40	-40.95	-42.53	-31.43	0.71	0.90	15.99	19.11	9.45
-2	-35.04	-35.43	-35.11	-43.05	-44.44	-32.45	0.21	0.89	18.44	20.99	8.21
-1.5	-35.46	-36.18	-35.84	-45.19	-46.37	-33.47	1.05	0.95	20.70	22.71	7.07
-1	-35.90	-36.94	-36.57	-47.37	-48.33	-34.50	1.83	1.02	22.80	24.33	6.00
-0.5	-36.32	-37.69	-37.30	-49.58	-50.31	-35.55	2.64	1.04	24.77	25.85	4.94
0	-36.64	-38.35	-38.12	-51.91	-52.39	-36.60	3.89	0.59	26.56	27.23	4.16
0.5	-36.70	-38.74	-38.55	-53.89	-54.10	-37.63	4.81	0.50	28.45	28.74	2.45
1	-36.66	-39.05	-39.07	-55.98	-55.92	-38.62	6.17	0.06	30.21	30.13	1.17
1.5	-36.61	-39.34	-39.60	-58.12	-57.76	-39.63	7.55	0.64	31.87	31.45	0.09
2	-36.57	-39.66	-40.14	-60.31	-59.64	-40.65	8.89	1.19	33.45	32.70	1.26
2.5	-36.57	-40.02	-40.70	-62.56	-61.56	-41.68	10.16	1.68	34.94	33.88	2.35
3	-36.62	-40.43	-41.30	-64.86	-63.54	-42.72	11.33	2.09	36.33	35.01	3.34
3.5	-36.73	-40.91	-41.92	-67.23	-65.56	-43.76	12.40	2.41	37.64	36.05	4.20
4	-36.91	-41.47	-42.59	-69.67	-67.64	-44.82	13.35	2.64	38.86	37.03	4.97
4.5	-37.16	-42.11	-43.31	-72.17	-69.79	-45.89	14.19	2.77	39.99	37.94	5.62
5	-37.51	-42.85	-44.08	-74.74	-72.00	-46.97	14.91	2.80	41.02	38.77	6.14
5.5	-37.96	-43.70	-44.93	-77.38	-74.28	-48.06	15.50	2.73	41.94	39.52	6.52
6	-38.54	-44.68	-46.01	-80.24	-76.79	-49.20	16.22	2.90	42.66	40.09	6.49

Deformation and percentage error for M2 12mx12mx1.1m along the width

Coordin	Work	Worku Modefie	cFEM	Wink	Pseudo Couple	VLAS	rku Err	ERROR(%) modifiec	WINKLI	PSEUD	VLASC
-6	-35.98	-37.58	-38.09	-53.76	-53.46	-36.06	5.56	1.34	41.12	40.34	5.34
-5.5	-35.68	-37.30	-37.77	-53.23	-53.01	-35.68	5.55	1.25	40.93	40.35	5.54
-5	-35.48	-37.11	-37.63	-52.85	-52.73	-35.47	5.72	1.37	40.44	40.13	5.74
-4.5	-35.36	-37.01	-37.54	-52.53	-52.49	-35.31	5.80	1.41	39.92	39.82	5.95
-4	-35.33	-36.99	-37.50	-52.26	-52.31	-35.21	5.78	1.35	39.37	39.50	6.10
-3.5	-35.36	-37.03	-37.49	-52.04	-52.18	-35.15	5.67	1.21	38.82	39.19	6.24
-3	-35.46	-37.14	-37.51	-51.87	-52.09	-35.13	5.48	1.00	38.28	38.87	6.35
-2.5	-35.61	-37.30	-37.56	-51.75	-52.05	-35.17	5.20	0.71	37.78	38.57	6.37
-2	-35.80	-37.50	-37.63	-51.68	-52.04	-35.25	4.86	0.36	37.32	38.28	6.33
-1.5	-36.03	-37.73	-37.72	-51.66	-52.07	-35.37	4.48	0.03	36.94	38.03	6.24
-1	-36.28	-37.98	-37.82	-51.68	-52.13	-35.53	4.08	0.42	36.63	37.82	6.07
-0.5	-36.51	-38.22	-37.93	-51.74	-52.21	-35.73	3.75	0.75	36.41	37.64	5.80
0	-36.64	-38.35	-38.12	-51.91	-52.39	-35.97	3.89	0.59	36.16	37.42	5.65
0.5	-36.51	-38.22	-37.93	-51.74	-52.21	-36.12	3.74	0.76	36.42	37.66	4.76
1	-36.28	-37.99	-37.82	-51.68	-52.13	-36.2	4.06	0.45	36.66	37.85	4.27
1.5	-36.03	-37.74	-37.71	-51.66	-52.07	-36.31	4.44	0.07	37.00	38.08	3.71
2	-35.80	-37.50	-37.62	-51.68	-52.04	-36.45	4.82	0.31	37.39	38.35	3.10
2.5	-35.61	-37.30	-37.54	-51.75	-52.05	-36.64	5.14	0.64	37.86	38.66	2.39
3	-35.46	-37.14	-37.48	-51.87	-52.09	-36.87	5.41	0.92	38.38	38.97	1.64
3.5	-35.36	-37.04	-37.46	-52.04	-52.18	-37.14	5.59	1.12	38.94	39.31	0.84
4	-35.33	-36.99	-37.46	-52.26	-52.31	-37.45	5.69	1.25	39.51	39.65	0.02
4.5	-35.37	-37.02	-37.50	-52.53	-52.49	-37.81	5.69	1.29	40.08	39.98	0.83
5	-35.48	-37.12	-37.58	-52.85	-52.73	-38.22	5.60	1.24	40.63	40.31	1.70
5.5	-35.68	-37.30	-37.72	-53.23	-53.01	-38.68	5.41	1.10	41.13	40.55	2.55
6	-35.98	-37.59	-38.03	-53.76	-53.46	-39.31	5.41	1.18	41.34	40.56	3.35

Deformation and percentage error for M3 12mx12mx1.2m along the length

Coordin	Work	Worku Modefie	cFEM	Winkl	Pseudo Couple	Vlaso	rku Err	WORKU MODIFIED Error (%	winkler	pseud	vlaso
-6	-25.76	-25.20	-22.80	-19.44	-21.80	-24.87	12.99	10.53	14.74	4.39	9.07
-5.5	-25.74	-25.43	-23.15	-20.91	-23.12	-25.51	11.18	9.86	9.68	0.14	10.19
-5	-25.77	-25.72	-23.61	-22.48	-24.54	-26.19	9.16	8.94	4.78	3.94	10.93
-4.5	-25.85	-26.05	-24.10	-24.08	-25.98	-26.91	7.29	8.13	0.07	7.82	11.68
-4	-25.98	-26.44	-24.61	-25.70	-27.46	-27.66	5.58	7.43	4.44	11.59	12.41
-3.5	-26.15	-26.86	-25.14	-27.53	-28.96	-28.44	4.04	6.85	9.51	15.20	13.13
-3	-26.37	-27.33	-25.69	-29.03	-30.48	-29.24	2.64	6.37	13.01	18.65	13.83
-2.5	-26.62	-27.83	-26.25	-30.74	-32.03	-30.08	1.39	6.00	17.09	22.01	14.58
-2	-26.90	-28.36	-26.83	-32.47	-33.60	-30.94	0.26	5.71	21.02	25.24	15.32
-1.5	-27.21	-28.92	-27.42	-34.23	-35.19	-31.84	0.76	5.49	24.86	28.36	16.14
-1	-27.52	-29.49	-28.01	-36.03	-36.80	-32.76	1.73	5.29	28.64	31.39	16.97
-0.5	-27.83	-30.05	-28.60	-37.84	-38.42	-33.71	2.71	5.05	32.29	34.32	17.85
0	-28.06	-30.54	-29.28	-39.77	-40.14	-34.69	4.17	4.28	35.81	37.07	18.46
0.5	-28.10	-30.83	-29.62	-41.37	-41.53	-35.60	5.12	4.10	39.69	40.23	20.21
1	-28.06	-31.05	-30.03	-43.08	-43.01	-36.44	6.56	3.39	43.45	43.21	21.34
1.5	-28.01	-31.26	-30.46	-44.83	-44.52	-37.31	8.02	2.65	47.19	46.17	22.50
2	-27.98	-31.49	-30.90	-46.62	-46.06	-38.22	9.43	1.94	50.90	49.08	23.71
2.5	-27.97	-31.75	-31.35	-48.45	-47.63	-39.16	10.77	1.28	54.54	51.92	24.90
3	-28.00	-32.05	-31.83	-50.33	-49.24	-40.14	12.03	0.68	58.11	54.69	26.10
3.5	-28.08	-32.39	-32.34	-52.26	-50.89	-41.16	13.18	0.16	61.59	57.36	27.27
4	-28.20	-32.79	-32.88	-54.24	-52.58	-42.22	14.24	0.28	64.96	59.91	28.40
4.5	-28.38	-33.25	-33.46	-56.27	-54.32	-43.33	15.18	0.64	68.17	62.35	29.50
5	-28.62	-33.77	-34.08	-58.36	-56.12	-44.50	16.01	0.92	71.23	64.66	30.56
5.5	-28.95	-34.37	-34.76	-60.50	-57.98	-45.68	16.73	1.12	74.04	66.79	31.41
6	-29.37	-35.07	-35.65	-62.84	-60.03	-46.98	17.63	1.63	76.25	68.37	31.77

Deformation and percentage error for M3 12mx12mx1.1m along the width

Coordin	Worku	Worku Modefie	cFEM	Winkl	Pseudo Couple	vlasov	Worku	Error (%	winkler	pseud	vlaso
-6	-29.37	-35.07	-35.65	-62.84	-60.03	-47.75	17.63	1.62	76.26	68.38	33.94
-5.5	-28.95	-34.37	-34.76	-60.50	-57.98	-46.29	16.72	1.11	74.06	66.81	33.17
-5	-28.62	-33.77	-34.08	-58.36	-56.12	-45.03	16.01	0.91	71.25	64.67	32.13
-4.5	-28.38	-33.25	-33.46	-56.27	-54.32	-43.82	15.17	0.63	68.19	62.36	30.98
-4	-28.20	-32.79	-32.88	-54.24	-52.58	-42.67	14.23	0.27	64.97	59.92	29.78
-3.5	-28.08	-32.39	-32.34	-52.26	-50.89	-41.55	13.18	0.17	61.60	57.37	28.49
-3	-28.00	-32.05	-31.83	-50.33	-49.24	-40.48	12.02	0.69	58.12	54.69	27.17
-2.5	-27.97	-31.75	-31.35	-48.45	-47.63	-39.44	10.77	1.28	54.54	51.93	25.80
-2	-27.98	-31.49	-30.89	-46.62	-46.06	-38.45	9.43	1.94	50.90	49.09	24.46
-1.5	-28.01	-31.26	-30.46	-44.83	-44.52	-37.48	8.02	2.65	47.20	46.18	23.06
-1	-28.06	-31.05	-30.03	-43.08	-43.01	-36.55	6.56	3.39	43.45	43.22	21.70
-0.5	-28.10	-30.83	-29.62	-41.37	-41.53	-35.66	5.12	4.10	39.69	40.23	20.41
0	-28.06	-30.54	-29.28	-39.77	-40.14	-34.69	4.17	4.28	35.81	37.07	18.46
0.5	-27.83	-30.05	-28.60	-37.84	-38.42	-33.65	2.71	5.05	32.29	34.31	17.64
1	-27.52	-29.49	-28.01	-36.03	-36.80	-32.64	1.73	5.29	28.64	31.39	16.54
1.5	-27.21	-28.92	-27.42	-34.23	-35.19	-31.66	0.76	5.49	24.86	28.36	15.48
2	-26.90	-28.36	-26.83	-32.47	-33.60	-30.71	0.26	5.71	21.02	25.24	14.46
2.5	-26.62	-27.83	-26.25	-30.74	-32.03	-29.79	1.39	6.00	17.09	22.01	13.47
3	-26.37	-27.33	-25.69	-29.03	-30.48	-28.90	2.64	6.37	13.01	18.65	12.50
3.5	-26.15	-26.86	-25.14	-27.35	-28.96	-28.04	4.04	6.85	8.80	15.20	11.54
4	-25.98	-26.44	-24.61	-25.70	-27.46	-27.21	5.58	7.43	4.44	11.59	10.58
4.5	-25.85	-26.05	-24.10	-24.08	-25.98	-26.41	7.29	8.13	0.07	7.82	9.60
5	-25.77	-25.72	-23.61	-22.48	-24.54	-25.64	9.16	8.94	4.78	3.95	8.60
5.5	-25.74	-25.43	-23.15	-20.91	-23.12	-24.90	11.18	9.86	9.68	0.13	7.56
6	-25.76	-25.20	-22.80	-19.44	-21.80	-24.26	12.99	10.54	14.74	4.39	6.40

Deformation and percentage error for M4 8mx24mx0.75m along the length

Coordin	Work	Worku Modefi	cFEM	Winkl	Pseudo Coupl	GEO-	ku Er	odifi	winkl	pseu	vlas
-12	-67.70	-79.65	-81.64	-85.64	-72.03	-49.39	17.08	2.43	4.90	11.77	39.50
-11.5	-66.88	-79.50	-81.92	-83.49	-71.25	-47.92	18.36	2.96	1.91	13.03	41.51
-11	-66.39	-79.62	-82.55	-81.65	-70.77	-46.61	19.58	3.55	1.09	14.27	43.54
-10.5	-66.18	-79.96	-83.32	-79.96	-70.46	-45.45	20.56	4.02	4.03	15.43	45.45
-10	-66.25	-80.51	-84.22	-78.46	-70.32	-44.44	21.33	4.40	6.83	16.50	47.23
-9.5	-66.59	-81.23	-85.24	-77.14	-70.37	-43.60	21.88	4.71	9.50	17.45	48.85
-9	-67.19	-82.12	-86.38	-76.02	-70.60	-42.93	22.22	4.93	12.00	18.27	50.30
-8.5	-68.02	-83.16	-87.63	-75.08	-71.00	-42.42	22.38	5.10	14.32	18.97	51.59
-8	-69.04	-84.33	-88.95	-74.33	-71.55	-42.06	22.38	5.19	16.43	19.56	52.71
-7.5	-70.23	-85.61	-90.32	-73.74	-72.24	-41.84	22.25	5.22	18.36	20.02	53.68
-7	-71.50	-86.94	-91.71	-73.29	-73.02	-41.72	22.04	5.21	20.09	20.38	54.51
-6.5	-72.74	-88.24	-93.08	-72.93	-73.85	-41.69	21.86	5.20	21.65	20.66	55.21
-6	-73.69	-89.29	-94.49	-72.75	-74.79	-41.80	22.02	5.51	23.01	20.85	55.76
-5.5	-73.83	-89.58	-95.18	-71.95	-75.06	-41.27	22.43	5.89	24.41	21.14	56.64
-5	-73.68	-89.60	-95.89	-71.31	-75.41	-40.87	23.16	6.56	25.64	21.36	57.38
-4.5	-73.50	-89.60	-96.55	-70.75	-75.75	-40.53	23.87	7.19	26.72	21.54	58.02
-4	-73.38	-89.65	-97.17	-70.28	-76.11	-40.26	24.48	7.73	27.67	21.67	58.57
-3.5	-73.39	-89.80	-97.76	-69.93	-76.48	-40.07	24.93	8.15	28.47	21.77	59.01
-3	-73.57	-90.06	-98.35	-69.69	-76.89	-39.98	25.19	8.43	29.14	21.82	59.35
-2.5	-73.92	-90.45	-98.92	-69.57	-77.32	-39.97	25.28	8.57	29.67	21.84	59.60
-2	-74.43	-90.95	-99.48	-69.56	-77.76	-40.06	25.18	8.58	30.08	21.84	59.73
-1.5	-75.08	-91.55	-100.01	-69.65	-78.20	-40.22	24.92	8.46	30.35	21.81	59.78
-1	-75.80	-92.20	-100.48	-69.82	-78.61	-40.43	24.56	8.24	30.51	21.77	59.76
-0.5	-76.49	-92.84	-100.87	-70.03	-78.98	-40.67	24.16	7.96	30.57	21.70	59.68
0	-76.90	-93.21	-101.25	-70.35	-79.35	-41.01	24.05	7.94	30.52	21.63	59.50
0.5	-76.49	-92.84	-100.86	-70.03	-78.98	-40.67	24.16	7.96	30.57	21.70	59.68
1	-75.80	-92.20	-100.48	-69.82	-78.61	-40.43	24.56	8.23	30.51	21.76	59.76
1.5	-75.08	-91.55	-100.00	-69.65	-78.20	-40.22	24.92	8.45	30.35	21.80	59.78
2	-74.43	-90.95	-99.48	-69.56	-77.76	-40.06	25.17	8.57	30.07	21.83	59.73
2.5	-73.92	-90.45	-98.92	-69.57	-77.32	-39.97	25.27	8.56	29.67	21.83	59.59
3	-73.57	-90.06	-98.34	-69.69	-76.89	-39.98	25.19	8.42	29.14	21.81	59.35
3.5	-73.39	-89.80	-97.76	-69.93	-76.48	-40.07	24.92	8.14	28.47	21.77	59.01
4	-73.38	-89.65	-97.16	-70.28	-76.11	-40.26	24.48	7.73	27.67	21.67	58.56
4.5	-73.50	-89.60	-96.55	-70.75	-75.75	-40.53	23.87	7.19	26.72	21.54	58.02
5	-73.68	-89.60	-95.90	-71.31	-75.41	-40.87	23.17	6.56	25.64	21.36	57.38
5.5	-73.83	-89.58	-95.19	-71.95	-75.06	-41.27	22.44	5.90	24.41	21.15	56.64
6	-73.69	-89.29	-94.51	-72.75	-74.79	-41.80	22.03	5.52	23.02	20.87	55.77
6.5	-72.74	-88.24	-93.11	-72.93	-73.85	-41.69	21.88	5.22	21.67	20.68	55.22
7	-71.50	-86.94	-91.75	-73.29	-73.02	-41.72	22.07	5.24	20.12	20.41	54.53
7.5	-70.23	-85.61	-90.37	-73.74	-72.24	-41.84	22.28	5.27	18.40	20.06	53.70
8	-69.04	-84.33	-89.00	-74.33	-71.55	-42.06	22.42	5.25	16.49	19.61	52.74
8.5	-68.02	-83.16	-87.69	-75.08	-71.00	-42.42	22.44	5.17	14.38	19.04	51.63
9	-67.19	-82.12	-86.46	-76.02	-70.60	-42.93	22.29	5.02	12.08	18.35	50.35
9.5	-66.59	-81.23	-85.33	-77.14	-70.37	-43.60	21.96	4.81	9.60	17.53	48.91
10	-66.25	-80.51	-84.32	-78.46	-70.32	-44.44	21.43	4.52	6.95	16.60	47.30
10.5	-66.18	-79.96	-83.43	-79.96	-70.46	-45.45	20.68	4.16	4.16	15.55	45.52
11	-66.39	-79.62	-82.68	-81.65	-70.77	-46.61	19.71	3.71	1.25	14.40	43.63
11.5	-66.88	-79.50	-82.07	-83.49	-71.25	-47.92	18.50	3.13	1.73	13.18	41.61
12	-67.70	-79.65	-81.80	-85.64	-72.03	-49.39	17.24	2.62	4.69	11.95	39.62

Deformation and percentage error for M4 8mx24mx0.75m along the width

Coordin	Work	Worku Modefi	cFEM	Winkl	Pseudo Coupl	vlasc	ku Er	ERROR (%) odifi	winkl	pseu	vlaso
-4	-75.22	-91.56	-101.41	-72.31	-80.67	-42.44	25.83	9.72	28.70	20.45	58.15
-3.5	-74.70	-91.13	-100.80	-71.42	-79.86	-41.61	25.90	9.60	29.15	20.78	58.72
-3	-74.50	-90.98	-100.56	-70.84	-79.37	-41.10	25.92	9.53	29.55	21.07	59.13
-2.5	-74.56	-91.07	-100.45	-70.41	-79.05	-40.74	25.78	9.34	29.91	21.31	59.44
-2	-74.85	-91.35	-100.46	-70.13	-78.88	-40.53	25.49	9.07	30.19	21.48	59.66
-1.5	-75.32	-91.77	-100.56	-69.98	-78.84	-40.45	25.10	8.74	30.41	21.60	59.78
-1	-75.91	-92.30	-100.73	-69.97	-78.90	-40.50	24.64	8.36	30.54	21.67	59.79
-0.5	-76.52	-92.86	-100.93	-70.07	-79.05	-40.66	24.18	7.99	30.58	21.68	59.71
0	-76.90	-93.21	-101.25	-70.35	-79.35	-41.01	24.05	7.94	30.52	21.63	59.50
0.5	-76.52	-92.86	-100.92	-70.07	-79.05	-40.77	24.18	7.99	30.57	21.67	59.60
1	-75.91	-92.30	-100.72	-69.97	-78.90	-40.72	24.63	8.35	30.53	21.66	59.57
1.5	-75.32	-91.77	-100.55	-69.98	-78.84	-40.78	25.09	8.73	30.40	21.59	59.44
2	-74.85	-91.35	-100.44	-70.13	-78.88	-40.97	25.48	9.06	30.18	21.47	59.21
2.5	-74.56	-91.07	-100.43	-70.41	-79.05	-41.29	25.76	9.32	29.89	21.29	58.89
3	-74.50	-90.98	-100.53	-70.84	-79.37	-41.76	25.89	9.50	29.53	21.05	58.46
3.5	-74.70	-91.13	-100.76	-71.42	-79.86	-42.38	25.87	9.57	29.12	20.75	57.94
4	-75.22	-91.56	-101.36	-72.31	-80.67	-43.32	25.79	9.68	28.66	20.42	57.26

Deformation and percentage error for M5 8mx24mx0.8m along the length

Coordin	Worku	Worku Modefie	cFEM	Winkle	Pseudo Couple	VLASO	RKU Err	ERROR (%) ODIFIEDE	WINKLE	PSEUD	VLASOV
-12	-21.03	-18.40	-17.90	-9.82	-6.98	-20.19	-17.45	-2.75	45.15	61.01	12.78
-11.5	-21.09	-18.89	-18.57	-10.18	-7.72	-20.61	-13.56	-1.72	45.18	58.43	10.99
-11	-21.23	-19.45	-19.34	-10.64	-8.56	-21.09	-9.76	-0.56	44.99	55.75	9.03
-10.5	-21.45	-20.07	-20.16	-11.16	-9.46	-21.62	-6.39	0.48	44.65	53.08	7.23
-10	-21.74	-20.72	-21.03	-11.73	-10.41	-22.20	-3.38	1.43	44.21	50.49	5.59
-9.5	-22.09	-21.42	-21.93	-12.36	-11.43	-22.85	-0.72	2.32	43.65	47.89	4.17
-9	-22.51	-22.16	-22.89	-13.05	-12.51	-23.57	1.63	3.16	42.98	45.34	2.98
-8.5	-23.00	-22.94	-23.88	-13.79	-13.65	-24.35	3.69	3.93	42.25	42.84	1.97
-8	-23.55	-23.76	-24.91	-14.59	-14.85	-25.19	5.45	4.61	41.42	40.38	1.14
-7.5	-24.16	-24.62	-25.96	-15.43	-16.08	-26.09	6.92	5.17	40.56	38.05	0.51
-7	-24.83	-25.51	-27.02	-16.29	-17.34	-27.03	8.12	5.58	39.72	35.83	0.02
-6.5	-25.53	-26.44	-28.08	-17.16	-18.60	-28.01	9.10	5.84	38.90	33.77	0.26
-6	-26.16	-27.32	-29.20	-18.09	-19.92	-29.08	10.40	6.44	38.04	31.78	0.41
-5.5	-26.47	-27.90	-29.90	-18.57	-20.76	-29.76	11.47	6.70	37.89	30.56	0.46
-5	-26.71	-28.42	-30.65	-19.11	-21.66	-30.53	12.86	7.27	37.66	29.34	0.40
-4.5	-26.99	-28.98	-31.40	-19.66	-22.54	-31.34	14.06	7.70	37.39	28.22	0.20
-4	-27.33	-29.59	-32.17	-20.25	-23.44	-32.20	15.05	8.01	37.05	27.13	0.10
-3.5	-27.74	-30.25	-32.96	-20.88	-24.36	-33.11	15.83	8.22	36.64	26.08	0.47
-3	-28.22	-30.95	-33.77	-21.57	-25.31	-34.09	16.44	8.36	36.13	25.06	0.94
-2.5	-28.78	-31.71	-34.62	-22.32	-26.28	-35.13	16.86	8.41	35.52	24.08	1.48
-2	-29.42	-32.51	-35.49	-23.12	-27.28	-36.23	17.10	8.38	34.85	23.12	2.10
-1.5	-30.13	-33.37	-36.37	-23.96	-28.28	-37.38	17.16	8.23	34.11	22.23	2.79
-1	-30.90	-34.29	-37.24	-24.83	-29.27	-38.56	17.04	7.93	33.33	21.41	3.54
-0.5	-31.70	-35.24	-38.09	-25.71	-30.22	-39.76	16.79	7.49	32.51	20.67	4.38
0	-32.38	-36.11	-39.00	-26.67	-31.22	-41.07	16.99	7.42	31.62	19.95	5.31
0.5	-32.54	-36.52	-39.27	-26.95	-31.48	-41.76	17.12	7.00	31.37	19.83	6.35
1	-32.59	-36.84	-39.59	-27.33	-31.80	-42.56	17.68	6.95	30.97	19.68	7.50
1.5	-32.68	-37.21	-39.89	-27.73	-32.08	-43.39	18.09	6.73	30.49	19.59	8.76
2	-32.83	-37.63	-40.20	-28.20	-32.38	-44.27	18.33	6.37	29.84	19.44	10.14
2.5	-33.06	-38.12	-40.51	-28.77	-32.72	-45.22	18.40	5.90	28.99	19.24	11.62
3	-33.38	-38.67	-40.86	-29.45	-33.10	-46.24	18.30	5.34	27.92	18.98	13.18
3.5	-33.78	-39.29	-41.22	-30.25	-33.55	-47.34	18.05	4.70	26.62	18.62	14.83
4	-34.28	-39.96	-41.62	-31.18	-34.06	-48.52	17.63	3.97	25.08	18.16	16.59
4.5	-34.85	-40.71	-42.02	-32.24	-34.62	-49.77	17.05	3.12	23.27	17.61	18.45
5	-35.50	-41.52	-42.42	-33.40	-35.23	-51.07	16.32	2.12	21.26	16.95	20.40
5.5	-36.16	-42.38	-42.78	-34.65	-35.85	-52.42	15.47	0.95	19.01	16.21	22.52
6	-36.65	-43.11	-43.24	-36.10	-36.61	-53.92	15.24	0.30	16.51	15.33	24.71
6.5	-36.44	-43.22	-42.85	-36.74	-36.51	-54.63	14.97	-0.87	14.26	14.80	27.49
7	-36.04	-43.22	-42.57	-37.61	-36.58	-55.51	15.34	-1.52	11.66	14.08	30.39
7.5	-35.68	-43.26	-42.30	-38.64	-36.77	-56.47	15.66	-2.28	8.65	13.07	33.51
8	-35.38	-43.37	-42.07	-39.88	-37.13	-57.53	15.91	-3.09	5.21	11.75	36.74
8.5	-35.17	-43.56	-41.94	-41.36	-37.70	-58.73	16.13	-3.87	1.37	10.10	40.05
9	-35.06	-43.82	-41.91	-43.14	-38.53	-60.09	16.34	-4.54	2.93	8.07	43.37
9.5	-35.06	-44.15	-42.03	-45.21	-39.63	-61.62	16.59	-5.05	7.57	5.71	46.61
10	-35.17	-44.57	-42.30	-47.59	-41.04	-63.32	16.87	-5.36	12.50	2.99	49.68
10.5	-35.41	-45.08	-42.74	-50.27	-42.75	-65.21	17.16	-5.47	17.61	0.01	52.56
11	-35.80	-45.72	-43.37	-53.24	-44.74	-67.27	17.44	-5.42	22.77	3.17	55.12
11.5	-36.41	-46.53	-44.18	-56.49	-47.01	-69.50	17.58	-5.32	27.86	6.41	57.31
12	-37.32	-47.61	-45.50	-60.24	-49.78	-71.97	17.98	-4.62	32.39	9.40	58.17

Deformation and percentage error for M5 8mx24mx0.8m along the width

Coordin	Worku	Worku Modefie	cFEM	Winkle	Pseudo Couple	VLASO	RKU Err	ERROR (%) ODIFIEDE	WINKLE	PSEUD	VLASOV
-4	-31.66	-35.50	-39.05	-28.72	-32.36	-42.60	18.92	9.09	26.45	17.13	9.10
-3.5	-31.31	-35.20	-38.55	-27.81	-31.59	-41.86	18.79	8.68	27.85	18.05	8.59
-3	-31.15	-35.08	-38.36	-27.21	-31.14	-41.41	18.80	8.56	29.07	18.82	7.95
-2.5	-31.14	-35.08	-38.28	-26.76	-30.85	-41.08	18.65	8.37	30.10	19.42	7.30
-2	-31.26	-35.17	-38.30	-26.46	-30.70	-40.86	18.38	8.17	30.92	19.84	6.68
-1.5	-31.48	-35.34	-38.39	-26.31	-30.68	-40.75	18.01	7.93	31.47	20.08	6.15
-1	-31.78	-35.59	-38.53	-26.29	-30.75	-40.74	17.53	7.65	31.77	20.20	5.73
-0.5	-32.13	-35.88	-38.71	-26.38	-30.91	-40.82	17.00	7.30	31.85	20.15	5.45
0	-32.38	-36.11	-39.00	-26.67	-31.22	-41.07	16.99	7.42	31.62	19.95	5.31
0.5	-32.13	-35.89	-38.71	-26.38	-30.91	-40.77	16.99	7.29	31.85	20.14	5.33
1	-31.78	-35.59	-38.53	-26.29	-30.75	-40.65	17.52	7.63	31.77	20.19	5.50
1.5	-31.48	-35.35	-38.38	-26.31	-30.68	-40.61	17.99	7.90	31.46	20.07	5.80
2	-31.26	-35.18	-38.29	-26.46	-30.70	-40.68	18.36	8.13	30.90	19.83	6.23
2.5	-31.15	-35.09	-38.28	-26.76	-30.85	-40.85	18.62	8.32	30.08	19.40	6.73
3	-31.16	-35.09	-38.35	-27.21	-31.14	-41.13	18.76	8.49	29.05	18.80	7.25
3.5	-31.31	-35.22	-38.53	-27.81	-31.59	-41.55	18.74	8.60	27.83	18.02	7.83
4	-31.67	-35.52	-39.03	-28.72	-32.36	-42.24	18.86	9.00	26.41	17.09	8.23

Deformation and percentage error for M6 8mx24mx0.8m along the width

Coordin	Worku	Worku Modefie	cFEM	Winkle	Pseudo Couple	VLASO	RKU Err	ERROR (%) ODIFIEDE	WINKLE	PSEUD	VLASOV
-4	-37.28	-44.07	-49.94	-50.64	-60.28	-52.52	-25.36	11.76	1.41	20.70	5.17
-3.5	-36.35	-43.07	-47.89	-46.72	-57.81	-48.99	-24.10	10.06	2.45	20.72	2.30
-3	-35.77	-42.38	-46.46	-43.34	-55.89	-46.02	-23.01	8.77	6.71	20.31	0.93
-2.5	-35.42	-41.89	-45.23	-40.22	-54.19	-43.31	-21.69	7.40	11.08	19.80	4.25
-2	-35.25	-41.53	-44.19	-37.35	-52.68	-40.83	-20.24	6.02	15.49	19.21	7.60
-1.5	-35.20	-41.28	-43.30	-34.70	-51.35	-38.55	-18.69	4.66	19.85	18.60	10.95
-1	-35.27	-41.11	-42.53	-32.27	-50.18	-36.46	-17.06	3.32	24.11	18.00	14.27
-0.5	-35.41	-41.02	-41.85	-30.04	-49.16	-34.51	-15.38	1.97	28.22	17.47	17.53
0	-35.48	-40.89	-41.34	-28.08	-48.38	-32.79	-14.18	1.10	32.09	17.02	20.68
0.5	-35.11	-40.35	-40.31	-25.66	-47.11	-30.58	-12.90	0.10	36.33	16.88	24.12
1	-34.66	-39.76	-39.43	-23.50	-46.07	-28.58	-12.10	0.84	40.40	16.85	27.51
1.5	-34.27	-39.23	-38.62	-21.48	-45.16	-26.69	-11.25	1.60	44.37	16.95	30.88
2	-33.97	-38.78	-37.89	-19.62	-44.39	-24.93	-10.33	2.36	48.22	17.16	34.20
2.5	-33.78	-38.41	-37.26	-17.90	-43.76	-23.30	-9.34	3.09	51.96	17.46	37.45
3	-33.70	-38.12	-36.73	-16.32	-43.27	-21.81	-8.26	3.79	55.56	17.81	40.62
3.5	-33.76	-37.95	-36.32	-14.89	-42.92	-20.46	-7.07	4.48	59.02	18.16	43.67
4	-34.01	-37.95	-36.23	-13.73	-42.87	-19.40	-6.14	4.73	62.11	18.32	46.45

Deformation and percentage error for M6 8mx24mx0.8m along the length

Coordin	Worku	Worku Modefie	cFEM	Winkle	Pseudo Couple	VLASO	RKU Er	ERROR (%) ODIFIEDE	WINKLE	PSEUD	VLASOV
-12	-23.93	-21.61	-18.87	-9.93	-24.47	-6.94	26.83	14.49	47.38	29.67	63.25
-11.5	-24.03	-22.19	-19.61	-10.41	-24.96	-7.82	22.56	13.18	46.88	27.31	60.14
-11	-24.20	-22.84	-20.44	-10.98	-25.51	-8.78	18.39	11.71	46.28	24.79	57.06
-10.5	-24.45	-23.53	-21.32	-11.59	-26.11	-9.79	14.64	10.36	45.65	22.45	54.11
-10	-24.75	-24.27	-22.25	-12.24	-26.78	-10.84	11.25	9.08	44.98	20.36	51.27
-9.5	-25.12	-25.04	-23.22	-12.94	-27.51	-11.95	8.18	7.84	44.26	18.47	48.52
-9	-25.55	-25.85	-24.24	-13.70	-28.32	-13.12	5.41	6.65	43.49	16.83	45.87
-8.5	-26.04	-26.70	-25.30	-14.50	-29.20	-14.34	2.93	5.51	42.68	15.41	43.32
-8	-26.59	-27.57	-26.40	-15.35	-30.15	-15.60	0.74	4.46	41.85	14.22	40.88
-7.5	-27.96	-28.49	-27.52	-16.23	-31.16	-16.90	1.60	3.54	41.02	13.25	38.58
-7	-27.85	-29.44	-28.65	-17.13	-32.23	-18.21	2.77	2.78	40.21	12.51	36.42
-6.5	-28.55	-30.42	-29.77	-18.03	-33.33	-19.53	4.11	2.20	39.42	11.96	34.41
-6	-29.18	-31.36	-30.94	-19.00	-34.53	-20.89	5.69	1.36	38.61	11.59	32.49
-5.5	-29.51	-32.02	-31.70	-19.54	-35.34	-21.83	6.90	1.01	38.35	11.49	31.15
-5	-29.78	-32.63	-32.50	-20.15	-36.25	-22.80	8.37	0.39	38.01	11.52	29.85
-4.5	-30.09	-33.28	-33.31	-20.77	-37.20	-23.77	9.64	0.09	37.65	11.69	28.63
-4	-30.46	-33.96	-34.12	-21.41	-38.21	-24.74	10.72	0.46	37.24	11.99	27.49
-3.5	-30.89	-34.69	-34.96	-22.10	-39.27	-25.72	11.63	0.76	36.78	12.33	26.41
-3	-31.39	-35.46	-35.83	-22.83	-40.41	-26.73	12.38	1.01	36.26	12.79	25.40
-2.5	-31.95	-36.28	-36.72	-23.62	-41.61	-27.75	13.00	1.22	35.69	13.30	24.44
-2	-32.58	-37.13	-37.65	-24.45	-42.88	-28.78	13.46	1.36	35.05	13.90	23.55
-1.5	-33.27	-38.04	-38.58	-25.32	-44.19	-29.81	13.75	1.40	34.37	14.55	22.73
-1	-34.02	-38.99	-39.50	-26.21	-45.54	-30.82	13.87	1.31	33.66	15.28	21.99
-0.5	-34.81	-39.97	-40.40	-27.10	-46.91	-31.79	13.84	1.05	32.92	16.12	21.31
0	-35.48	-40.89	-41.34	-28.08	-48.38	-32.79	14.18	1.10	32.09	17.02	20.68
0.5	-35.67	-41.37	-41.64	-28.43	-49.23	-33.13	14.33	0.66	31.72	18.23	20.43
1	-35.76	-41.77	-41.99	-28.89	-50.19	-33.51	14.84	0.52	31.20	19.53	20.19
1.5	-35.88	-42.22	-42.31	-29.37	-51.18	-33.87	15.19	0.22	30.58	20.96	19.95
2	-36.07	-42.71	-42.63	-29.92	-52.21	-34.23	15.39	0.20	29.82	22.48	19.71
2.5	-36.32	-43.26	-42.96	-30.55	-53.31	-34.61	15.45	0.71	28.89	24.10	19.44
3	-36.65	-43.87	-43.31	-31.28	-54.48	-35.03	15.39	1.27	27.78	25.78	19.12
3.5	-37.05	-44.52	-43.69	-32.13	-55.73	-35.50	15.21	1.88	26.46	27.55	18.75
4	-37.52	-45.22	-44.09	-33.10	-57.06	-36.02	14.90	2.56	24.93	29.40	18.31
4.5	-38.07	-45.98	-44.50	-34.19	-58.46	-36.59	14.46	3.33	23.18	31.36	17.79
5	-38.67	-46.80	-44.90	-35.37	-59.91	-37.18	13.86	4.24	21.21	33.44	17.18
5.5	-39.31	-47.66	-45.25	-36.64	-61.40	-37.79	13.13	5.33	19.02	35.69	16.48
6	-39.78	-48.41	-45.68	-38.11	-63.03	-38.54	12.92	5.99	16.56	37.99	15.63
6.5	-39.58	-48.58	-45.26	-38.86	-63.86	-38.50	12.53	7.34	14.13	41.11	14.93
7	-39.23	-48.64	-44.93	-39.84	-64.86	-38.64	12.68	8.25	11.33	44.36	14.00
7.5	-38.91	-48.74	-44.60	-40.97	-65.92	-38.89	12.77	9.28	8.15	47.79	12.81
8	-38.65	-48.91	-44.33	-42.30	-67.10	-39.29	12.81	10.33	4.57	51.38	11.36
8.5	-38.46	-49.13	-44.14	-43.87	-68.40	-39.90	12.86	11.32	0.61	54.98	9.60
9	-38.35	-49.41	-44.07	-45.70	-69.88	-40.74	12.98	12.13	3.71	58.57	7.55
9.5	-38.33	-49.76	-44.15	-47.82	-71.52	-41.85	13.19	12.70	8.33	62.00	5.21
10	-38.39	-50.16	-44.39	-50.23	-73.35	-43.23	13.52	13.00	13.15	65.23	2.61
10.5	-38.56	-50.64	-44.81	-52.91	-75.36	-44.89	13.95	13.01	18.07	68.16	0.17
11	-38.86	-51.22	-45.42	-55.85	-77.54	-46.81	14.45	12.77	22.97	70.72	3.05
11.5	-39.33	-51.95	-46.21	-59.02	-79.88	-48.95	14.88	12.41	27.73	72.86	5.93
12	-40.08	-52.91	-47.50	-62.63	-82.43	-51.54	15.62	11.40	31.85	73.54	8.50

ANNEX B: MOMENT VALUES AND PERCENTAGE ERROR

Moment and percentage error of M1 24mx24mx2.2m

						ERROR %			
oordi	Worku	CFEM	Winkle	Pseudo Coupled	VLASO	rku Err	winkle	pseudo	vlasov
-12	228.67	254.24	-1546.70	-2204.92	-211.60	10.06	708.36	967.26	183.23
-11.5	601.54	670.81	-344.17	-1009.70	585.00	10.33	151.31	250.52	12.79
-11	592.23	657.95	7.96	-655.40	697.00	9.99	98.79	199.61	5.94
-10.5	408.92	450.00	183.30	-486.70	716.40	9.13	59.27	208.16	59.20
-10	299.50	330.00	281.62	-404.70	729.30	9.24	14.66	222.64	121.00
-9.5	185.75	195.00	330.38	-372.50	732.40	4.74	69.43	291.03	275.59
-9	-48.09	-50.69	342.51	-381.50	717.90	5.14	775.70	652.61	1516.26
-8.5	-110.78	-118.56	321.10	-424.60	677.80	6.57	370.83	258.13	671.69
-8	-297.33	-314.51	265.12	-506.80	604.20	5.46	184.30	61.14	292.11
-7.5	-488.66	-539.60	159.40	-634.27	485.60	9.44	129.54	17.54	189.99
-7	-777.85	-797.47	-8.30	-834.70	299.90	2.46	98.96	4.67	137.61
-6.5	-1061.46	-1198.66	-360.50	-1215.36	-28.10	11.45	69.92	1.39	97.66
-6	-2656.11	-2610.96	-1243.03	-2150.59	-1039.70	1.73	52.39	17.63	60.18
-5.5	-1588.24	-1430.25	-363.38	-1268.50	-35.90	11.05	74.59	11.31	97.49
-5	-1067.95	-1186.61	-11.50	-941.80	283.90	10.00	99.03	20.63	123.93
-4.5	-973.66	-1092.96	150.20	-792.60	460.40	10.91	113.74	27.48	142.12
-4	-958.45	-1053.84	258.50	-711.60	567.70	9.05	124.53	32.48	153.87
-3.5	-940.08	-1051.20	309.70	-675.80	626.00	10.57	129.46	35.71	159.55
-3	-974.94	-1083.26	327.20	-675.20	643.60	10.00	130.20	37.67	159.41
-2.5	-1021.98	-1146.65	308.90	-705.73	622.60	10.87	126.94	38.45	154.30
-2	-1111.27	-1243.64	256.40	-770.10	560.90	10.64	120.62	38.08	145.10
-1.5	-1225.03	-1383.37	155.50	-879.50	450.00	11.45	111.24	36.42	132.53
-1	-1429.39	-1588.21	-16.23	-1060.24	269.90	10.00	98.98	33.24	116.99
-0.5	-1945.03	-1938.16	-367.95	-1420.10	-53.90	0.35	81.02	26.73	97.22
0	-2827.09	-3134.13	-1253.70	-2303.27	-1062.10	9.80	60.00	26.51	66.11
0.5	-1945.03	-1817.96	-377.20	-1422.60	-55.40	6.99	79.25	21.75	96.95
1	-1466.52	-1518.36	-11.70	-1057.93	266.90	3.41	99.23	30.32	117.58
1.5	-1258.77	-1398.64	155.30	-880.30	445.40	10.00	111.10	37.06	131.85
2	-1134.63	-1249.59	255.30	-769.70	554.60	9.20	120.43	38.40	144.38
2.5	-1045.20	-1150.22	309.10	-706.70	614.60	9.13	126.87	38.56	153.43
3	-997.00	-1085.87	326.70	-674.60	633.80	8.18	130.09	37.87	158.37
3.5	-958.39	-1053.77	310.10	-676.20	614.40	9.05	129.43	35.83	158.30
4	-955.05	-1056.72	256.80	-712.17	554.40	9.62	124.30	32.61	152.46
4.5	-999.44	-1104.93	155.90	-794.13	445.60	9.55	114.11	28.13	140.33
5	-1099.46	-1199.40	-20.20	-937.40	268.10	8.33	98.32	21.84	122.35
5.5	-1488.25	-1452.39	-368.84	-1264.80	-52.40	2.47	74.60	12.92	96.39
6	-2756.11	-2610.46	-1279.40	-2154.60	-1056.30	5.58	50.99	17.46	59.54
6.5	-1194.14	-1215.71	-361.10	-1214.20	-44.20	1.77	70.30	0.12	96.36
7	-773.67	-848.53	-10.70	-831.90	284.80	8.82	98.74	1.96	133.56
7.5	-454.60	-505.11	161.30	-636.20	471.90	10.00	131.93	25.95	193.43
8	-269.31	-288.12	265.16	-507.47	592.30	6.53	192.03	76.13	305.57
8.5	-115.40	-124.63	321.30	-425.90	667.80	7.41	357.79	241.72	635.81
9	48.24	43.60	342.60	-380.90	709.90	10.64	685.74	973.58	1528.13
9.5	164.60	182.89	329.80	-372.30	726.40	10.00	80.32	303.56	297.17
10	289.30	314.78	280.80	-403.90	724.90	8.09	10.79	228.31	130.29
10.5	397.58	438.42	183.30	-486.30	713.60	9.32	58.19	210.92	62.77
11	508.63	564.03	10.20	-651.30	695.60	9.82	98.19	215.47	23.33
11.5	600.98	676.64	-354.20	-998.90	584.50	11.18	152.35	247.63	13.62
12	220.18	239.09	-1532.60	-2160.86	-211.70	7.91	741.01	1003.77	188.54

Moment and error percentage for M2 12mx12mx1.2m along the length

Coordin	Worku Ad	cFEM	Winkle	Pseudo Coupled	vlasov	WORKU AdJ Error (%	winkler2	pseudo	vlasov2
-6	-1085.09	-959.06	-1110.62	-1207.10	-156.80	13.14	15.80	25.86	83.65
-5.5	-677.97	-676.70	-296.50	-375.20	382.00	0.19	56.18	44.55	156.45
-5	-481.14	-480.26	-55.30	-181.20	454.80	0.18	88.49	62.27	194.70
-4.5	-362.88	-342.26	64.60	-75.70	489.50	6.03	118.87	77.88	243.02
-4	-229.42	-260.47	131.20	-22.50	524.20	11.92	150.37	91.36	301.25
-3.5	-249.98	-228.89	163.80	-5.20	547.60	9.22	171.56	97.73	339.25
-3	-261.60	-235.45	168.30	-17.20	552.20	11.11	171.48	92.69	334.53
-2.5	-227.52	-253.92	145.50	-53.10	532.10	10.40	157.30	79.09	309.55
-2	-368.55	-323.25	90.60	-123.30	480.80	14.01	128.03	61.86	248.74
-1.5	-458.46	-436.55	-7.90	-233.60	388.10	5.02	98.19	46.49	188.90
-1	-628.56	-634.90	-170.70	-405.60	231.70	1.00	73.11	36.12	136.49
-0.5	-891.00	-878.53	-518.30	-760.90	85.30	1.42	41.00	13.39	109.71
0	-1496.73	-1754.91	-1423.30	-1664.10	-1802.40	14.71	18.90	5.17	2.71
0.5	-899.10	-864.44	-491.90	-740.20	130.40	4.01	43.10	14.37	115.08
1	-643.95	-583.40	-123.70	-371.90	320.40	10.38	78.80	36.25	154.92
1.5	-432.76	-396.20	60.10	-182.90	517.80	9.23	115.17	53.84	230.69
2	-335.00	-320.79	175.10	-60.90	647.40	4.43	154.58	81.02	301.82
2.5	-266.12	-256.00	238.30	16.10	730.50	3.95	193.09	106.29	385.35
3	-259.64	-242.96	262.60	52.00	776.80	6.86	208.08	121.40	419.72
3.5	-283.13	-271.17	246.10	55.10	792.60	4.41	190.75	120.32	392.29
4	-343.88	-331.43	183.10	11.80	785.40	3.76	155.25	103.56	336.97
4.5	-563.76	-515.19	57.03	-97.40	767.40	9.43	111.07	81.09	248.95
5	-810.00	-750.60	-173.90	-305.50	758.70	7.91	76.83	59.30	201.08
5.5	-1210.95	-1162.86	-640.10	-686.30	683.60	4.14	44.95	40.98	158.79
6	-1906.00	-1787.25	-2247.10	-2320.20	-310.90	6.64	25.73	29.82	82.60

Moment and error percentage for M3 12mx12mx1.1m along the length

Coordin	Worku Modefied	cFEM	Winkle	Pseudo Coupled	vlasov	worku Ad	winkler2	pseudo	vlasov2
-6	-1000.00	-1026.65	-963.75	-1087.40	-1103.30	2.60	6.13	5.92	7.47
-5.5	-700.00	-691.58	-162.80	-257.10	-240.80	1.22	76.46	62.82	65.18
-5	-537.49	-517.46	80.40	-57.50	-30.00	3.87	115.54	88.89	94.20
-4.5	-314.56	-341.19	201.90	50.50	107.90	7.80	159.18	114.80	131.62
-4	-261.85	-277.15	270.10	105.60	189.40	5.52	197.46	138.10	168.34
-3.5	-233.00	-243.60	306.10	125.70	232.30	4.35	225.66	151.60	195.36
-3	-242.00	-249.25	313.10	115.30	244.50	2.91	225.62	146.26	198.09
-2.5	-278.00	-273.20	293.30	83.10	227.30	1.76	207.36	130.42	183.20
-2	-346.40	-349.03	242.10	16.60	176.70	0.75	169.36	104.76	150.63
-1.5	-501.96	-459.05	148.10	-89.70	82.20	9.35	132.26	80.46	117.91
-1	-684.00	-645.91	-11.70	-260.50	-81.60	5.90	98.19	59.67	87.37
-0.5	-900.00	-896.01	-350.70	-606.30	-332.90	0.44	60.86	32.33	62.85
0	-1602.00	-1782.71	-1239.30	-1514.20	-1802.40	10.14	30.48	15.06	1.10
0.5	-900.00	-939.72	-321.50	-583.60	-303.90	4.23	65.79	37.90	67.66
1	-675.00	-688.51	51.00	-205.50	-22.10	1.96	107.41	70.15	96.79
1.5	-484.52	-446.78	243.20	-10.40	168.20	8.45	154.43	97.67	137.65
2	-303.60	-330.28	364.90	121.20	284.20	8.08	210.48	136.70	186.05
2.5	-294.20	-275.86	443.10	210.40	350.80	6.65	260.63	176.27	227.17
3	-272.60	-258.61	483.80	262.70	374.70	5.41	287.08	201.58	244.89
3.5	-285.20	-279.78	490.40	286.90	356.30	1.94	275.28	202.54	227.35
4	-322.87	-352.89	459.10	273.10	288.20	8.51	230.10	177.39	181.67
4.5	-448.23	-487.98	379.10	209.10	151.20	8.15	177.69	142.85	130.99
5	-827.95	-794.38	218.20	67.70	-93.10	4.23	127.47	108.52	88.28
5.5	-1200.00	-1256.60	-118.10	-208.20	-481.40	4.50	90.60	83.43	61.69
6	-1600.00	-1755.14	-1304.40	-1438.10	-2182.4	8.84	25.68	18.06	24.34

Moment and error percentage for M4 24mx8mx0.75m along the length

Coordin	Worku A	cFEM	Winkl	Pseudo Couple	vlasov	ERROR (%)			
						WORK	winkle	pseud	vlasov
-12	247.00	220.80	-1452.50	-1451.20	-195.50	-11.86	757.83	757.24	188.54
-11.5	608.27	573.74	-261.40	-293.90	523.10	-6.02	145.56	151.22	8.83
-11	589.70	534.18	69.70	36.40	636.80	-10.39	86.95	93.19	19.21
-10.5	582.40	520.87	222.70	180.70	731.10	-11.81	57.24	65.31	40.36
-10	576.17	515.08	300.90	252.10	804.10	-11.86	41.58	51.06	56.11
-9.5	541.63	484.53	338.10	278.90	840.10	-11.78	30.22	42.44	73.38
-9	475.13	419.32	344.90	272.70	834.30	-13.31	17.75	34.97	98.96
-8.5	349.01	315.54	324.90	237.70	785.00	-10.61	2.97	24.67	148.78
-8	183.12	169.78	274.10	171.90	691.12	-7.86	61.44	1.25	307.06
-7.5	-28.84	-26.47	178.80	62.20	549.80	-8.96	775.54	335.00	2177.25
-7	-248.70	-243.58	17.70	-115.30	348.90	-2.10	107.27	52.66	243.24
-6.5	-681.62	-682.44	-333.70	-493.50	152.00	0.12	51.10	27.69	122.27
-6	-1762.53	-2003.97	-1235.90	-1419.50	-1615.70	12.05	38.33	29.17	19.37
-5.5	-855.84	-771.25	-350.60	-520.80	98.40	-10.97	54.54	32.47	112.76
-5	-501.23	-459.68	5.50	-192.00	242.10	-9.04	101.20	58.23	152.67
-4.5	-295.86	-281.51	160.70	-48.50	391.00	-5.10	157.09	82.77	238.90
-4	-184.62	-176.02	248.70	29.40	482.10	-4.88	241.29	116.70	373.89
-3.5	-132.79	-121.24	292.60	65.20	528.00	-9.52	341.33	153.78	535.49
-3	-115.61	-109.94	305.30	71.80	532.20	-5.16	377.71	165.31	584.10
-2.5	-161.52	-147.50	289.50	51.30	495.50	-9.51	296.28	134.78	435.94
-2	-253.41	-231.04	241.80	-0.50	417.20	-9.68	204.66	99.78	280.58
-1.5	-401.36	-367.66	152.10	-94.40	293.90	-9.17	141.37	74.32	179.94
-1	-564.32	-579.36	-6.60	-254.60	113.20	2.60	98.86	56.06	119.54
-0.5	-952.46	-868.82	-352.70	-601.60	-61.80	-9.63	59.40	30.76	92.89
0	-1801.21	-2090.41	-1260.30	-1511.20	-1806.30	13.83	39.71	27.71	13.59
0.5	-892.25	-828.02	-353.10	-602.90	-68.20	-7.76	57.36	27.19	91.76
1	-626.39	-559.39	-8.10	-254.60	100.50	-11.98	98.55	54.49	117.97
1.5	-396.52	-356.41	152.10	-94.30	275.00	-11.25	142.68	73.54	177.16
2	-242.88	-222.22	242.30	0.57	392.20	-9.30	209.04	100.26	276.49
2.5	-158.62	-140.93	290.10	51.20	464.50	-12.55	305.85	136.33	429.60
3	-119.95	-107.16	305.30	71.60	495.40	-11.93	384.89	166.81	562.28
3.5	-130.85	-119.44	292.80	6.70	485.70	-9.55	345.14	105.61	506.64
4	-192.31	-178.84	248.30	29.60	434.60	-7.53	238.84	116.55	343.01
4.5	-311.19	-291.19	160.30	-48.80	338.70	-6.87	155.05	83.24	216.32
5	-495.41	-472.74	5.70	-193.40	185.50	-4.80	101.21	59.09	139.24
5.5	-792.46	-752.47	-339.10	-520.90	38.00	-5.32	54.93	30.77	105.05
6	-1642.83	-1907.11	-1252.40	-1413.10	-1679.10	13.86	34.33	25.90	11.96
6.5	-532.96	-482.54	-333.40	-493.40	86.40	-10.45	30.91	2.25	117.91
7	-301.16	-331.40	16.50	-115.70	282.00	9.12	104.98	65.09	185.09
7.5	-51.20	-46.57	180.20	62.80	482.80	-9.94	486.95	234.85	1136.73
8	157.23	151.22	272.50	170.20	625.50	-3.97	80.20	12.55	313.63
8.5	315.62	300.48	323.90	237.30	722.10	-5.04	7.80	21.03	140.32
9	429.86	408.03	344.50	272.70	776.10	-5.35	15.57	33.17	90.21
9.5	508.25	477.13	337.60	278.80	788.50	-6.52	29.24	41.57	65.26
10	551.94	510.68	301.20	251.90	761.20	-8.08	41.02	50.67	49.06
10.5	562.41	516.62	221.90	181.70	698.90	-8.86	57.05	64.83	35.28
11	590.95	527.61	71.70	36.20	616.90	-12.01	86.41	93.14	16.92
11.5	601.51	558.47	-252.70	-290.50	515.50	-7.71	145.25	152.02	7.69
12	221.50	204.31	-1432.50	-1457.30	-199.30	-8.41	801.13	813.27	197.55

Moment and error percentage for M5 24mx8mx0.8m along the length

Coordi	Worku AdJ	cFEM	Winkle	Pseudo Couple	vlasov	ERROR (%) WORKU2	winkler2	pseudo	vlasov2
-12	-500.00	-459.71	-419.36	-458.30	-63.20	-8.76	8.78	0.31	86.25
-11.5	-237.24	-254.40	-38.89	-69.20	227.60	6.75	84.71	72.80	189.47
-11	-152.86	-164.71	80.27	42.80	311.40	7.20	148.73	125.98	289.05
-10.5	-83.45	-90.85	133.19	93.80	380.00	8.15	246.61	203.25	518.27
-10	-62.28	-68.02	162.00	119.20	433.00	8.44	338.15	275.23	736.55
-9.5	-53.42	-57.71	175.83	127.80	464.80	7.43	404.68	321.45	905.41
-9	-58.16	-61.29	177.65	122.70	473.40	5.11	389.86	300.20	872.41
-8.5	-73.59	-78.74	166.17	102.80	457.60	6.54	311.05	230.56	681.18
-8	-109.84	-114.28	137.89	64.70	416.20	3.89	220.66	156.61	464.19
-7.5	-172.24	-178.32	81.89	-0.30	346.10	3.41	145.92	99.83	294.09
-7	-259.23	-265.02	-16.94	-111.30	237.80	2.19	93.61	58.00	189.73
-6.5	-459.39	-497.08	-240.40	-347.50	134.10	7.58	51.64	30.09	126.98
-6	-1029.50	-1128.33	-831.65	-948.20	-1021.10	8.76	26.29	15.96	9.50
-5.5	-516.96	-529.13	-223.58	-364.20	135.60	2.30	57.75	31.17	125.63
-5	-291.27	-302.37	15.77	-133.70	239.40	3.67	105.22	55.78	179.17
-4.5	-190.84	-195.00	128.08	-33.60	344.90	2.13	165.68	82.77	276.87
-4	-129.64	-137.71	195.81	22.50	407.80	5.86	242.19	116.34	396.12
-3.5	-109.24	-113.29	231.82	47.90	436.30	3.57	304.63	142.28	485.13
-3	-101.47	-108.21	243.38	50.10	432.20	6.23	324.90	146.30	499.39
-2.5	-124.83	-130.23	231.69	29.60	395.10	4.14	277.91	122.73	403.39
-2	-172.79	-181.08	190.16	-19.90	323.10	4.58	205.02	89.01	278.43
-1.5	-257.41	-275.07	108.31	-110.80	211.40	6.42	139.37	59.72	176.85
-1	-418.20	-443.13	-39.54	-266.20	45.50	5.63	91.08	39.93	110.27
-0.5	-701.61	-749.20	-377.18	-608.50	-110.60	6.35	49.66	18.78	85.24
0	-1496.16	-1551.29	-1261.46	-1504.90	-1840.90	3.55	18.68	2.99	18.67
0.5	-725.67	-770.05	-367.96	-599.80	-100.50	5.76	52.22	22.11	86.95
1	-415.51	-432.98	1.37	-246.50	63.70	4.04	100.32	43.07	114.71
1.5	-254.61	-277.95	170.87	-80.40	233.90	8.40	161.48	71.07	184.15
2	-181.39	-192.39	269.14	15.60	344.20	5.72	239.89	108.11	278.91
2.5	-143.65	-152.73	322.87	68.50	407.20	5.95	311.39	144.85	366.61
3	-139.87	-148.10	342.90	88.10	426.00	5.56	331.53	159.49	387.64
3.5	-164.21	-177.37	329.65	77.00	400.70	7.42	285.85	143.41	325.91
4	-232.57	-248.78	278.62	27.80	329.30	6.51	212.00	111.17	232.37
4.5	-365.47	-383.37	169.36	-72.90	205.90	4.67	144.18	80.98	153.71
5	-601.58	-614.92	-27.59	-263.40	11.60	2.17	95.51	57.17	101.89
5.5	-987.42	-1076.31	-471.60	-697.80	-167.30	8.26	56.18	35.17	84.46
6	-1948.63	-2094.30	-1615.28	-1882.70	-2442.40	6.96	22.87	10.10	16.62
6.5	-1321.50	-1393.72	-445.79	-631.00	-86.30	5.18	68.01	54.73	93.81
7	-764.52	-804.71	31.49	-134.80	172.40	4.99	103.91	83.25	121.42
7.5	-560.38	-601.25	260.44	109.10	444.10	6.80	143.32	118.15	173.86
8	-338.23	-354.30	395.20	260.60	641.60	4.53	211.55	173.55	281.09
8.5	-201.89	-215.44	471.58	353.30	782.20	6.29	318.89	263.99	463.07
9	-128.55	-138.98	502.59	402.10	872.20	7.51	461.62	389.31	727.56
9.5	-109.63	-115.60	493.95	409.40	913.10	5.17	527.28	454.14	889.86
10	-163.58	-173.45	436.48	365.90	909.00	5.69	351.65	310.95	624.07
10.5	-291.71	-318.57	310.60	250.20	868.30	8.43	197.50	178.54	372.56
11	-613.36	-647.06	70.30	10.20	817.10	5.21	110.86	101.58	226.28
11.5	-1105.17	-1194.63	-469.56	-528.10	748.20	7.49	60.69	55.79	162.63
12	-1897.63	-2066.07	-2430.79	-2504.40	330.70	8.15	17.65	21.22	116.01

Moment and error percentage for M6 24mx8mx0.8m along the length

Coordi	Worku AdJ	cFEM	Winkle	Pseudo Couple	vlasov	ERROR (%) WORKU2	winkler2	pseudo	vlasov2
-12	60.86	62.05	-7.79	-66.30	6.75	1.92	112.55	206.85	89.12
-11.5	138.60	149.86	176.12	236.20	179.05	7.51	17.52	57.62	19.48
-11	202.87	212.22	232.19	331.50	241.02	4.41	9.41	56.21	13.57
-10.5	239.67	233.39	297.60	409.40	305.91	-2.69	27.51	75.41	31.07
-10	249.63	256.14	330.98	469.40	342.31	2.54	29.22	83.26	33.64
-9.5	258.91	241.76	344.51	504.70	354.03	-7.09	42.50	108.76	46.44
-9	208.29	222.94	333.45	512.80	332.12	6.57	49.57	130.02	48.97
-8.5	201.84	184.86	297.79	493.00	287.10	-9.19	61.09	166.69	55.30
-8	129.78	118.75	232.16	444.60	210.56	-9.29	95.51	274.40	77.31
-7.5	25.17	23.01	141.62	365.10	106.21	-9.38	515.42	1486.56	361.52
-7	-113.60	-120.00	1.71	245.70	-50.89	5.33	101.42	304.75	57.59
-6.5	-456.34	-427.74	-151.29	129.20	-218.70	-6.69	64.63	130.21	48.87
-6	-902.74	-844.16	-1083.55	-1078.70	-1163.29	-6.94	28.36	27.78	37.80
-5.5	-493.85	-450.00	-131.02	136.90	-256.96	-9.74	70.88	130.42	42.90
-5	-110.63	-120.00	45.43	259.10	-106.95	7.81	137.86	315.92	10.88
-4.5	-32.84	-30.00	198.39	380.30	24.53	-9.47	761.31	1367.67	181.77
-4	70.73	76.00	294.33	455.70	104.59	6.93	287.28	499.61	37.62
-3.5	143.91	156.91	350.90	492.80	142.39	8.29	123.63	214.06	9.26
-3	132.54	142.44	365.45	492.70	140.70	6.95	156.56	245.90	1.22
-2.5	121.90	123.58	340.39	454.80	95.84	1.36	175.44	268.02	22.45
-2	48.75	50.23	268.97	377.70	11.07	2.95	435.48	651.94	77.96
-1.5	-81.56	-75.37	158.07	257.00	-122.46	-8.21	309.73	440.98	62.48
-1	-200.00	-210.00	-27.32	78.90	-327.88	4.76	86.99	137.57	56.13
-0.5	-812.59	-767.95	-231.19	-92.40	-544.30	-5.81	69.90	87.97	29.12
0	-1500.00	-1424.21	-1586.11	-1898.30	-1930.69	-5.32	11.37	33.29	35.56
0.5	-828.02	-760.24	-150.89	-66.50	-500.08	-8.92	80.15	91.25	34.22
1	-200.00	-181.35	130.12	128.20	-235.92	-10.28	171.75	170.69	30.09
1.5	-80.00	-75.08	390.44	324.70	3.02	-6.55	620.03	532.47	104.02
2	50.19	56.28	571.05	456.40	168.15	10.82	914.65	710.95	198.78
2.5	130.93	121.29	690.38	535.20	278.02	-7.95	469.20	341.26	129.22
3	107.16	100.23	760.22	563.30	332.68	-6.92	658.47	462.01	231.92
3.5	87.56	80.11	770.21	540.40	334.41	-9.31	861.49	574.61	317.45
4	-90.00	-83.24	723.12	465.00	283.20	-8.12	968.68	658.60	440.20
4.5	-174.94	-160.60	614.18	332.30	172.73	-8.93	482.43	306.91	207.55
5	-472.74	-499.78	416.30	124.10	-16.10	5.41	183.30	124.83	96.78
5.5	-1000.00	-1060.61	186.48	-73.10	-223.32	5.71	117.58	93.11	78.94
6	-1907.11	-1788.61	-1581.02	-2447.10	-1965.90	-6.63	11.61	36.82	9.91
6.5	-782.54	-875.79	373.44	32.40	40.76	10.65	142.64	103.70	104.65
7	-381.40	-421.82	786.61	333.10	488.26	9.58	286.48	178.97	215.75
7.5	150.00	145.47	1170.54	640.50	901.99	-3.11	704.66	340.30	520.05
8	451.22	444.97	1442.23	866.10	1210.38	-1.41	224.12	94.64	172.01
8.5	590.48	650.89	1628.87	1025.60	1434.88	9.28	150.25	57.57	120.45
9	708.03	762.04	1728.32	1121.70	1592.49	7.09	126.80	47.20	108.98
9.5	789.13	880.07	1740.17	1154.30	1656.20	10.33	97.73	31.16	88.19
10	832.21	924.03	1657.62	1125.70	1612.46	9.94	79.39	21.83	74.50
10.5	801.45	897.40	1478.71	1044.00	1457.41	10.69	64.78	16.34	62.40
11	798.21	879.03	1188.45	939.10	1187.28	9.19	35.20	6.83	35.07
11.5	598.47	664.62	914.31	803.40	919.17	9.95	37.57	20.88	38.30
12	304.31	311.28	914.31	-342.80	-45.66	2.24	193.73	210.13	114.67